THE
PHYSICAL REVIEW
A journal of experimental and theoretical physics established by E. L. Nichols in 1893

SECOND SERIES, VOL. 68, NOS. 3 AND 4 AUGUST 1 AND 15, 1945

The Beta-Ray Spectra of Cu^{64} at Low Energies

JOHN BACKUS*
Radiation Laboratory, University of California, Berkeley, California
(Received June 2, 1945)

An electrostatic beta-ray spectrometer has been constructed utilizing the focusing action of the electric field between concentric cylindrical conductors. A Geiger tube counter using an argon-alcohol mixture was used; a technique for making windows for the counter was developed whereby electrons of energies as low as 5 kev could be counted. A source of radioactive Cu^{64} was mounted on a very thin collodion film in order to eliminate the effects of back scattering. The positron and electron spectrum of Cu^{64} was plotted with the apparatus in the region below 50 kev. It was found that the ratio of the number of positrons to the number of electrons in this region did not agree with the number predicted by the Fermi theory of beta-disintegration.

INTRODUCTION

THE continuous beta-ray spectrum has been the object of much investigation since its discovery. Many of the results have been discordant and are only lately beginning to show some agreement. Practically all the research has been confined to the upper region of the spectrum, the region below about 50 kev remaining completely unknown until quite recently. The object of the present research was the investigation of the electron and positron spectrum of Cu^{64} in the region below 50 kev.

Flammersfeld,[1] using RaE in a magnetic spectrometer, obtained the first reliable data in the low energy region. By comparing the curves obtained with sources mounted on supports of various materials and thicknesses, he was able to determine at what point the spectrum became distorted by the low energy electrons scattered back from the support. By using as a support a 0.1μ lacquer film, he obtained the spectrum down to 25 kev free from back-scattering. His work showed that in order to obtain the true spectrum at low energies, it is absolutely essential to use a very thin source and support. In fact, the work of Tyler[2] on the spectrum of Cu^{64} showed that the influence of back scattering was appreciable even at energies in the neighborhood of 200 kev; spectra obtained with thick sources showed a greater preponderance of electrons in the region below 400 kev than spectra obtained with thinner sources. Tyler did not attempt to measure the spectrum below about 60 kev.

For the present work it was decided to measure the two spectra of Cu^{64} in the extreme low energy region below 50 kev. Radioactive Cu^{64} was first investigated by Van Voorhis,[3] using a cloud chamber. The half-life is 12.8 hr.; it decays either by positron emission to Ni or by electron

*At University of Southern California, Los Angeles, California, after November 1, 1945.

[1] A. Flammersfeld, Zeits. f. Physik 112, 727 (1939).

[2] A. W. Tyler, Phys. Rev. 56, 125 (1939).

[3] S. N. Van Voorhis, Phys. Rev. 50, 895 (1936).

emission to Zn. The ratio of the number of electrons to the number of positrons is about 1.6:1. The upper limits given by Tyler[2] for the electrons and positrons are respectively 0.578 $\pm$0.003 Mev and 0.659$\pm$0.003 Mev.

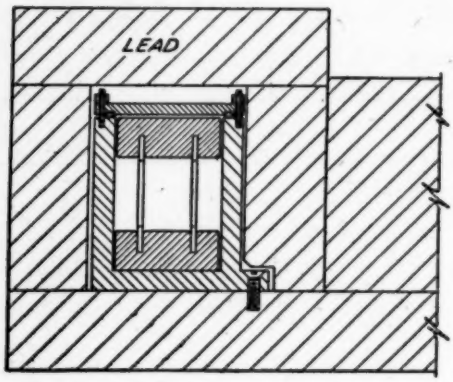

FIG. 1. Vertical section through spectrometer.

Since Cu^{64} emits both particles in nearly equal numbers, it is possible to plot both spectra under nearly identical conditions, using the same apparatus and the same source. From the formula given by Fermi[4] in his theory of beta-disintegration, the theoretical distributions and their ratio can be plotted and compared with the experimental curves.

APPARATUS

The apparatus used was an electric spectrometer originally constructed for work with recoil ions; it utilizes the focusing action of a cylindrical electric field, as discussed by Hughes and Rojansky.[5] Suppose two coaxial cylindrical electrodes of radii $\rho-\frac{1}{2}\Delta\rho$, $\rho+\frac{1}{2}\Delta\rho$ are maintained at a difference of potential ΔV. A charged particle of energy E will then travel along the median circle of radius ρ provided

$$\Delta V/E=2\log[(\rho+\tfrac{1}{2}\Delta\rho)(\rho-\tfrac{1}{2}\Delta\rho)]. \quad (1)$$

For any practical case

$$\Delta V/E=2\Delta\rho/\rho, \quad (2)$$

this expression being good to within 1 percent for $\Delta\rho<\frac{1}{3}\rho$. Suppose an entrance slit were located at the radius ρ; if now two particles enter the field through this slit with energy E and with their directions of motion making angles $+\alpha$, $-\alpha$ with the median circle, their paths will cross again at an angle

$$\theta=\pi/\sqrt{2}=127^\circ\,17' \quad (3)$$

measured from the entrance slit. The point of crossing will be displaced toward the center by an amount $\rho\alpha^2/3$. If an exit slit of width ds is placed at the focus, the spread in energy of the particles passing through it is given by

$$dE/E=ds/\rho. \quad (4)$$

If $\phi(E)$ is the number of particles passing through the slit obtained as a function of energy E with the spectrometer, the true energy distribution $f(E)$ will be given by

$$f(E)=\phi(E)/E. \quad (5)$$

The vacuum chamber for the spectrometer was a portion of a ring-shaped trough of brass subtending an angle of about 120 degrees. It was turned from a brass casting, and it was found necessary to coat the outside completely with solder to make it vacuum tight. The inside measured $1\frac{5}{16}''$ wide by 2″ deep. The deflecting grids were spaced 0.62″ apart by means of slotted hard rubber blocks which also served to fix the grids in the center of the trough. The radius to the midpoint between the grids was 6.0″. Plates at the two ends of the trough carried adjustable rectangular openings to serve as entrance and exit slits.

The radioactive source was mounted on a rod which entered the apparatus through a sylphon bellows so that the position of the source could be adjusted. It was placed $\frac{1}{2}''$ in front of the entrance slit which was about $\frac{5}{32}''$ wide. A small gate operated from the outside through a Wilson type vacuum seal allowed the source to be closed off from the system so that background readings could be taken.

A small box was soldered on the other end of the trough outside the exit slit; this box carried the thin-window counter. To count electrons, the counter was mounted on the end of the box directly opposite the exit slit. The apparatus could also be arranged to count positive ions. To do this, the counter was mounted on the side of the box, and an insulated metal plate was

[4] E. Fermi, Zeits. f. Physik **88**, 161 (1934).
[5] A. L. Hughes and V. Rojansky, Phys. Rev. **34**, 284 (1929).

placed in the box in line with the exit slit and facing the counter window. When this plate is given a potential of -5000 volts, positive ions coming through the slit are accelerated toward the plate, where they strike it and liberate secondary electrons; these electrons are accelerated away from the plate, and since they leave perpendicular to it, then enter the counter through the thin window.

A vertical section through the apparatus is shown in Fig. 1, a plan view in Fig. 2. The apparatus is surrounded with lead as shown in order to shield the counter from gamma-rays from the source. It is evacuated by means of a two-stage oil diffusion pump backed by a Cenco Hyvac mechanical pump.

The apparatus was first tested with lithium ions obtained from a filament coated with Li_2CO_3. The deflecting plates first used were solid copper plates spaced 1″ apart; with these plates, the curve of counts *vs.* voltage on deflecting plates was very broad. By using a very narrow entrance slit and mounting the Li ion source about three inches away so as to get a narrow beam, double peaks were obtained, indicating that the ions were being reflected from the plates so as to pass through the exit slit at deflecting voltages other than the proper value. The solid plates were therefore removed and replaced by grids made of 7-mil wire wound on metal frames with about 0.05″ spacing between turns. With these grids a sharp peak was obtained at the proper voltage, but in some cases as many as four additional peaks could be counted, all at voltages across the grids higher than the proper value. These peaks were due to ions passing through the inside grid into the region between the grid and the chamber where the field was in the direction to bend them back out. It was found that by placing defining mica slits between the grids and mica baffles between the walls of the chamber and the grids, the additional peaks were removed and the apparatus then worked as expected.

THE THIN WINDOW COUNTER

The counter used was made by drilling a $\frac{5}{8}$″ hole through a 1″ square copper block $2\frac{1}{4}$″ long. Glass plugs waxed into the hole at either end carried a 0.010″ tungsten wire. Brass angles hard soldered to the sides of the block allowed it to be fastened to the spectrometer. A hole in the side adjacent to the spectrometer carried the grid which supported the collodion windows; this grid contained a hexagonal array of 397 holes, 0.013″ diameter, spaced 0.020″ apart. Rubber gaskets between the grid and counter and between the grid and spectrometer formed the vacuum seals. Figure 2 shows the counter as mounted for counting electrons.

The collodion windows are prepared as follows: Flexible collodion (e.g., Merck) is diluted with an equal volume of amyl acetate. Two drops only of this solution are dropped in rapid succession from an ordinary medicine dropper into a pan of distilled water. The pan should be at least ten inches in diameter. The solution spreads out over a circle some eight inches in diameter and dries in a few seconds; it can then be cut into quarters by sawing a wire through it with a rapid up-and-down motion, starting at the center. The quarters are lifted out by means of a wire frame shaped like Fig. 3. The frame is

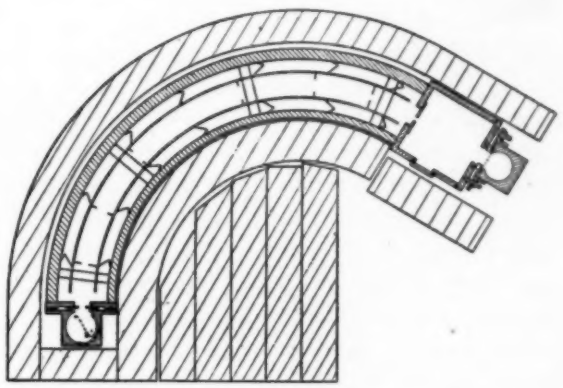

FIG. 2. Horizontal section through spectrometer.

placed under the center of the portion of film and lifted straight up so that the film drapes over the sides, thus forming a double layer. By this method breakage due to the surface tension of the water is minimized, as is also the occurrence of small pinholes. Interferometer measurements show that films formed in this way are about 0.08μ thick. Two such films placed in contact and observed in white light show a brilliant golden color.

The films when dry are given a very thin coat of silver by evaporation. A layer just visible as a

slight darkening is sufficient; such a layer is about 40 atoms thick. This silvering process is necessary to make the counter work properly. Counters used with unsilvered windows behaved in a very erratic manner. The grid upon which the film is mounted is dipped into acetone containing a few drops of collodion and dried. The film is then lowered on to it, silvered side up, and the wire frame cut away by means of a wire dipped in amyl acetate. The pressure of the gas in the counter is sufficient to seal the film vacuum-tight to the grid. No increase in pressure in the spectrometer could be noticed when the counter was filled. Figure 4 shows a curve of the transmission of the window for electrons plotted against the voltage of the electrons. It is seen that 4000 volts is sufficient for practically 100 percent penetration.

The counter is filled with a mixture of one volume ethyl alcohol vapor to about six volumes argon, the pressure used being 5 cm. The windows described above will stand about twice this pressure and will stand repeated fillings. The mixture should stand long enough for the two gases to mix thoroughly before the counter is used; filling the counter from a flask containing the mixture already prepared is the best way to accomplish this. The mixture will slowly diffuse through the counter-window, so a ballast flask is necessary to keep the pressure from falling too rapidly. The counter described was used with a ballast flask of 500 cc capacity, and one filling would last about eight hours, the counter voltage dropping about 200 volts during this time.

The counter was used with a high voltage supply of the type described by Gingrich[6] and the quenching circuit of Neher and Harper[7] feeding into a scale of 16 counting circuit. The counter used had a threshold of 800 volts when freshly filled and a plateau of 100 volts.

FIG. 3. Wire frame for lifting thin collodion films from the water surface.

[6] N. S. Gingrich, Rev. Sci. Inst. **7**, 207 (1936).
[7] H. V. Neher and W. W. Harper, Phys. Rev. **49**, 940 (1936).

PREPARATION OF THE SOURCE

The radioactive Cu^{64} for the source was obtained by bombarding zinc with deuterons from the 60″ cyclotron in the Crocker Radiation Laboratory, the reaction being $Zn^{68}(d, \alpha)Cu^{64}$. The copper was extracted by the electrolytic method described by Steigman.[8] The zinc is dissolved in HCl; 40 cc H_2SO_4 are added and the mixture boiled until SO_3 fumes are given off. This process is necessary to remove HCl from the solution, as copper does not plate well out of solutions containing it. The mixture is then diluted to about 300 cc and electrolyzed by use of a rotating cathode. The cathode used was a tungsten disk 2 cm in diameter, rotating 6000 r.p.m. Tests with solutions containing a known amount of copper showed that at a current of 10 ma, 2.9 v, two-thirds of the copper plated out in about three hours running. A drop of dilute nitric acid placed on the disk dissolved off the copper coating; the drop of solution was then picked up in a capillary tube and transferred to the collodion film support. This support was a 0.03μ film prepared as described above, using one drop of a more dilute collodion solution. A rectangular wire frame 1×3 cm carried the film. The drop of solution on its support was dried in a small vacuum chamber built for the purpose, then placed in the spectrometer. The effective width of the source was made small by tilting the film as shown in Fig. 2.

A voltage doubler circuit capable of giving 5000 volts above and below ground was used as the source of deflecting potential. From Eq. (2) above, $\Delta\rho/\rho=\frac{1}{10}$, $\Delta V=10{,}000$, so the highest energy beta-rays usable are 50 kev.

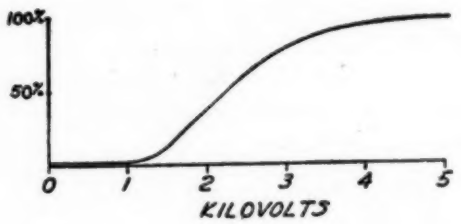

FIG. 4. Transmission of 0.1μ collodion counter window for electrons.

[8] J. Steigman, Phys. Rev. **53**, 771 (1938).

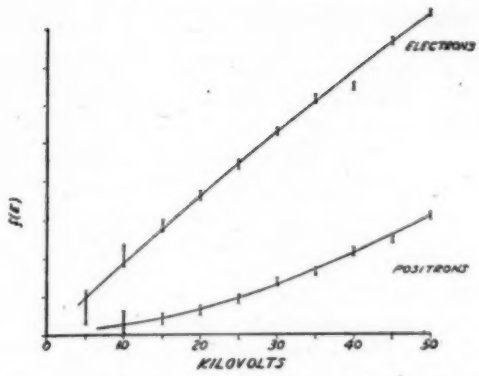

FIG. 5. Energy distribution of positrons and electrons from Cu^{64} below 50 kev.

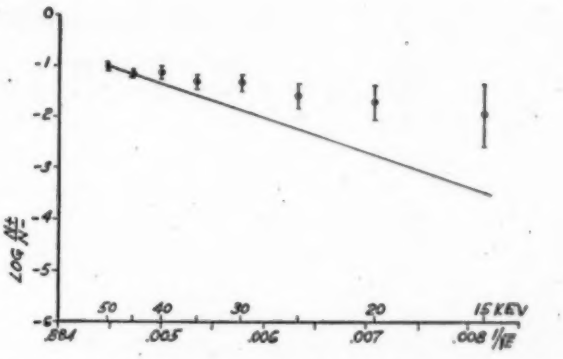

FIG. 6. Comparison of the theoretical and experimental ratio N_+/N_-.

RESULTS

Measurements were made on a source of about 15 mc. Background readings were taken periodically by closing the gate at the entrance slit. It was found that the background was independent of the voltage on the deflecting grids, being about 30 counts per minute. The highest counting rate measured was 1300 counts per minute, well within the capacity of the counter set. Counts were taken for two-minute periods and corrected for the decay of the source; the curves obtained plotted as a function of E were divided at each point by E to get the true distribution in energy of the positrons and electrons. The final curves obtained are shown in Fig. 5.

In 1934 Fermi[4] advanced a theory of beta-decay and gave a formula to represent the distribution of beta-rays in the continuous spectrum. From this formula the ratio of positrons to electrons in the Cu^{64} spectrum can be expressed as

$$N_+/N_-=A\ \exp\left[-2\pi\alpha Z((1+\eta^2)/\eta)^{\frac{1}{2}}\right], \quad (6)$$

where $\alpha=1/137$, Z the atomic number of the nucleus, and η the momentum of the particle in units of mc. A modification of the Fermi theory proposed by Konopinski and Uhlenbeck[9] gives the same expression for the ratio N_+/N_-. Using $Z=29$ and expressing η in terms of the energy E of the emitted particle in volts, one may for the region below 50 kev write Eq. (6) as follows:

$$\log N_+/N_-=k-670/(E)^{\frac{1}{2}}. \quad (7)$$

In Fig. 6 the straight line is the plot of Eq. (7), that is $\log N_+/N_-$ plotted against $1/(E)^{\frac{1}{2}}$. The circles represent the experimental values of $\log N_+/N_-$ taken from the original data. The constant in (7) has been determined so as to make the two curves coincide at 50 kev. The agreement is not good; the experiment shows a greater ratio of positrons to electrons at the low energy end of the spectrum than the theory predicts. This discrepancy cannot be ascribed to scattering due to the finite thickness of the source. This would change the form of the two curves of Fig. 5 but not their ratio, the positrons and electrons of a given energy being scattered equally.

In conclusion, I wish to thank Professor L. Alvarez for his interest and suggestions during the course of this work; Professor E. O. Lawrence for the use of the 60″ cyclotron in obtaining the radioactive copper used; Professor R. Oppenheimer and Dr. Philip Morrison for their theoretical contributions; and the entire staff of the Radiation Laboratory for their cooperation.

[9] E. J. Konopinski and G. E. Uhlenbeck, Phys. Rev. **48**, 7 (1935).

The Single Scattering of Electrons in Gases†

R. B. RANDELS,* K. T. CHAO,** AND H. R. CRANE
Harrison M. Randall Laboratory of Physics, University of Michigan, Ann Arbor, Michigan
(Received June 11, 1945)

The single scattering of electrons was measured by means of a cloud chamber. Electrons having energies from 0.9 to 12 Mev were used in air, argon, krypton, and xenon. A total of 2173 meters of track yielded 801 deflections between 15° and 90°. The projected angles of scattering were compared with the theoretical values obtained by making a plane projection of the Mott scattering distribution. The errors inherent in the cloud chamber method and the corrections to be applied were treated in detail. From a combination of the data for all the energies and gases, the ratio of the experimental to the theoretical scattering was found to be 1.02. The angle intervals 25°–35°, 35°–45°, and 45°–55°, taken individually, show a somewhat greater ratio: 1.20, 1.43, and 1.25, respectively. Throughout the data the variations of the scattering cross section with changes in atomic number, energy, and angle were as expected within the experimental accuracy. No support whatever was found for the large discrepancies reported by several other authors.

INTRODUCTION

IF cloud chamber measurements of the single scattering of electrons have been distinguished in any way, so far, it has been by the remarkable lack of agreement from one to another: variations of as much as a factor 40 have been reported for the same energy range and the same scattering gas. A review of all these experiments does not seem to be necessary at this point, since many of them are by now out of date as to apparatus and method, but in a later section of this paper a table of results will be given.

In setting out to do cloud chamber measurements, the experimenter is not at all free to choose any electron energy and any atomic number for the scattering gas he pleases, if he wishes to get usable data. A consideration of the scattering formula will assure him of this. The formula given by Mott[1] is

$$N(\theta)=\tfrac{1}{4}Nt\left(\frac{Ze^2}{mc^2\beta^2}\right)^2(1-\beta^2)$$
$$\times\left[\csc^4\frac{\theta}{2}-\beta^2\csc^2\frac{\theta}{2}+\pi\beta Z\alpha\cos^2\frac{\theta}{2}\csc^3\frac{\theta}{2}\right], \quad (1)$$

where $N(\theta)$ is the average number of deflections of angle θ, per unit solid angle, which an electron will suffer in a path length t in a gas, where N is the number of atoms per cc of the gas, and where the other symbols have their usual meaning. The coefficient of the angle term depends upon the atomic number and density of the gas in the cloud chamber, and the energy of the electrons. If conditions are chosen such that this coefficient is large, a good yield of large angle deflections will be obtained, but the measurement of angle and curvature of the tracks will be rendered uncertain by the great amount of small angle scattering along the tracks. Going to the other extreme will cure the trouble arising from the small angle scattering, but will make the results statistically bad because of the poor yield of large deflections. The range in which a compromise can be made is surprisingly narrow. Our experience has shown us that satisfactory working conditions are obtained by making the coefficient such that the number of deflections greater than 15 degrees is between 0.75 and 0.25 per meter of track length. It is interesting to note that if we were to keep the number of atoms per cc of gas constant and juggle the atomic number of the gas and the energy of the electrons in such a way that the frequency of scattering in a given angle interval remained constant, we would be doing the equivalent of keeping the classical distance of closest approach the same for all gases, at a given angle of scattering. In our experiments we almost

† The material in this paper formed the major part of a doctoral thesis submitted by the first author at the University of Michigan in 1940. A preliminary report was given at the meeting of the American Physical Society at Pittsburgh, Pennsylvania, June 20–22, 1940. (Phys. Rev. **58**, 201 (1940)).

* Now at the Corning Glass Works, Corning, New York.

** Now at National Central University, Chungking, China.

[1] N. F. Mott, Proc. Roy. Soc. **A124**, 425 (1929).

do this, and consequently, in terms of the classical distance of approach, our results are somewhat restricted. We mention this mainly because the classical distance of approach is of some significance in considering the relative importance of the three angle terms in the Mott formula.

Offsetting the limitation just mentioned, there are some important advantages in the cloud chamber method: 1. The energy of an electron can be determined, both before and after scattering, which shows whether or not the collision was elastic. 2. With extremely small chance of error, every deflection counted can be assumed to be a single deflection, without recourse to the Wentzel[2] criterion for single scattering. 3. The greatest source of worry in other methods of measurement is eliminated, namely the chance that a very small number of slow electrons (secondaries due to collisions at slit edges, secondaries from bremsstrahlung, and electrons that have simply bounced around the chamber several times) may account for a large portion of the intensity observed at large angles, because of the extremely large cross section for scattering which these slow electrons have.

EXPERIMENTAL METHOD

Apparatus

The cloud chamber used was fully automatic, 15 cm in diameter. The details have been published in another journal.[3] A special camera arrangement was set up for this experiment, consisting of one Sept 35-mm camera seeing the chamber from directly above and another seeing the chamber in a direction 20 degrees from the vertical. Since the source of electrons was an element emitting a continuous beta-ray spectrum, it was necessary to devise a means by which a desired band of energies could be selected. The selection was made outside the chamber, in order to avoid, as far as possible, having the photographs cluttered with tracks of undesired energies. This was accomplished conveniently by the use of adjustable slits in the external part of the magnetic field, as shown in Fig. 1. After negotiating the slit system, the electrons passed into the chamber through a slot 5 cm wide and 1 cm high, which was ground in the glass side wall of the chamber, and which was covered with an aluminum or a copper foil about 0.001 inch thick. To hold the foil so that it would withstand pressures inside the chamber from vacuum up to 2 atmospheres, it was necessary to mount the foil on a heavy brass shoe about 4 inches long, having the same curvature as the chamber wall, which was fastened to the glass with Picein. The light beam which illuminated the tracks was limited, by a system of slits, to a sheet of light 2 cm thick, extending an equal distance above and below the electron entrance slot.

Three different radioactive sources were used for the electrons. For those below 1.5 Mev radiophosphorus, P^{32} was used; for those from 1.5 to 2.5 Mev a thin-walled capsule containing about 0.5 mg of radium in equilibrium with its products was used; and for those from 2.5 to 12 Mev radiolithium, Li^8 was used. The Li^8 was made by bombarding a lithium target with deuterons for about 1 second just prior to each expansion of the cloud chamber by a technique that has been described in this journal.[4,5] All three of the sources gave copious supplies of electrons, making it possible to work with a rather large distance (50 to 100 cm) between the source and the defining slits. An advantage in

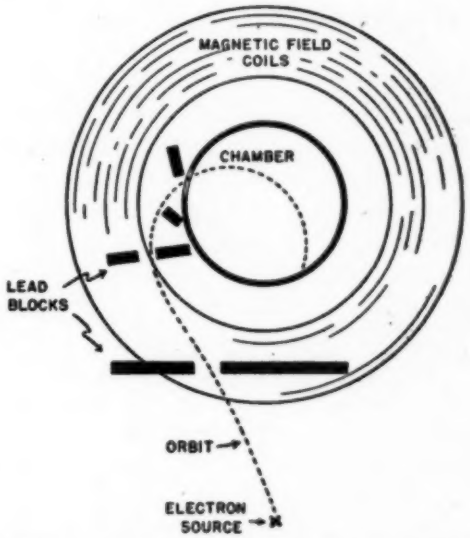

FIG. 1. System of slits used for selecting electrons within a narrow range of energy.

[2] G. Wentzel, Ann. d. Physik **69**, 333 (1922).
[3] H. R. Crane, Rev. Sci. Inst. **8**, 440 (1937).
[4] H. R. Crane, Phys. Rev. **52**, 11 (1937).
[5] D. S. Bayley and H. R. Crane, Phys. Rev. **52**, 604 (1937).

bending the electron paths in the external magnetic field, in addition to the selection of energies obtained, lay in the fact that large blocks of lead could be placed in the direct line between the source and the chamber to stop all gamma-radiation. This was of particular advantage when the radium source was used.

One liter each of xenon, krypton, and argon, 99 percent pure, were purchased for the experiments. An all glass system of "plumbing" was set up which made possible the evacuation of the chamber and the transfer of the gases back and forth between their bulbs and the chamber. An activated charcoal trap which could alternately be heated electrically and cooled with liquid air was used as a pump for transferring the gases. Each time the chamber was filled the pressure was read on a mercury barometer, and then a few cc of liquid alcohol were admitted through a needle valve. Upon transferring the rare gas back into the bulb the alcohol vapor was removed by a liquid air trap. The rare gases were transferred into the chamber and out again many times without mishap during the course of the experiments.

Selection and Measurement of Tracks

The selection of the tracks that are considered to be suitable for measurement is a matter that unavoidably involves some human judgement, with its attendant possibility of systematic error. The first requirement in combatting this is to design the mechanical set-up so that a relatively large percentage of all the tracks in the chamber are fit for measurement, and the second requirement is to make a system of rules such that the choice of tracks is as automatic as possible. The first of these requirements was met by using the slit system and pre-selection of energies already described. Confusion in the chamber was minimized by adjusting the electron intensity at all times so that an average of only three tracks appeared on each picture, and by adjusting the slits so that these had approximately the desired energy and were in the best part of the chamber. The second requirement was met by setting up the following rules of procedure for selection of the tracks for measurement.

1. The photograph taken from directly above the chamber is projected natural size onto a sheet of paper. On the paper is drawn a circle 11 cm in diameter, and this is centered in the image of the chamber, leaving a 2-cm border all around. Only the track length and only the scattering events lying within this circle are recorded. The purpose of the border is as follows: When a short piece of track lies inside the circle, the part in the border can be used as an aid in determining its curvature, but only the length inside the circle is included in the data. When a track is scattered just at the edge of the circle, the part in the border makes possible the determination of the angle of deflection. If such a circle were not used one would often meet the situation of being required to accept a scattering event just at the edge of the chamber, and of having no way of determining the angle of deflection.

2. Tracks accepted must fall within a range of curvature decided upon before beginning to measure the particular series of photographs. For each energy band used, the magnetic field is chosen so as to give the most readily measurable curvatures, usually centering around 10- or 15-cm radius. Typical limits for acceptance are 7 to 20 cm.

3. Tracks accepted must be sharp. A few old and fuzzy tracks were present in all the runs, but they amounted to only about 2 percent of the total in the usual run and perhaps 5 percent of the total in the worst runs. Most of these could have been eliminated by using a synchronized mechanical shutter in the path of the electrons, but instead we attempted to sweep out the early tracks by leaving the electrical field on until the completion of the expansion. This, we now know, was not entirely successful. Borderline cases were troublesome, in that they required a decision, and we regard these as a fertile source of error, for it is exceedingly difficult to form the same opinion of a partially fuzzy track when it has a 40-degree deflection in it as when it has no such deflection.

4. No minimum length is placed upon a track for acceptance. Any piece of track which begins at the entrance slot at the side of the chamber and which satisfies the other requirements must be accepted and its length added to the total. Most of the tracks extend across the entire chamber, but when one does not, it means that the electron passed out of the illuminated part of the chamber, which is a region 2 cm in height.

Scattering in the foil covering the entrance slot of the chamber, or, more often, one or more deflections in the gas of 5 or 10 degrees can cause the electron to pass out of the light beam when part way across the chamber.

After a track has been accepted, the procedure is to trace it with a sharp pencil, on the paper on which it is projected. This paper has the limiting circle on it, and in those cases in which it will be useful, the part of the track lying outside the circle is traced, as well as that lying inside. Only the photograph taken from directly above the chamber is projected and traced in this manner; the photograph taken from an angle is used when necessary to dispel confusion which arises when several tracks cross within a small area, when one track lies above another, etc.

The curvatures of the tracks are measured by fitting circles to them, a sheet of celluloid being used upon which is engraved a set of concentric arcs in steps of $\frac{1}{2}$-cm radius. The track length is measured with the help of a flexible rule, which is simply bent to fit each track. The angle of scattering is measured with a special pair of celluloid cards, as illustrated in an earlier publication.[6] Each of the cards has on it a set of concentric arcs, in steps of $\frac{1}{2}$-cm radius, and each has one edge which is a common radius of all the arcs. One card is right-handed and one is left-handed. In use one of the cards is placed so that one of the arcs coincides with the track and so that the radius edge cuts the track at the point of scattering. A pencil line is then drawn along the radius edge, which is perpendicular to the direction of the track at the point of scattering. The part of the track lying on the other side of the scattering point is treated the same way with the other card, and the angle between the two lines drawn along the radius edges is the angle of deflection of the electron. In a few cases the track obviously contains a minor deflection so that the segments must then be measured separately.

PROJECTION OF THE SCATTERING FORMULA

Most of the previous investigators have tried to have the conditions of measurement such that the results could be compared directly with the Mott formula, in its usual form. After some preliminary trials, we concluded that more accuracy could be obtained by measuring only the projected angle of deflection of the tracks and then projecting and integrating the scattering formula to conform to the experiment. No error is introduced by projecting the theoretical distribution, while one of the most dangerous sources of error is avoided by not having to measure the tracks and their deflections in three dimensions. As described in the section on the selection of tracks, the projected angles of deflection of all scattering events were included in the data, even those which were deflected sharply upward or downward. However, relatively little contribution is made to any given projected angle interval by tracks which have a large vertical component of scattering, because of the rapid fall-off in scattering cross section with increasing angle. Thus, for example, the number of electrons in the 35–45-degree interval in the projection is very largely composed of those actually scattered at 35–45 degrees, a point to be kept in mind when comparing the experimental and theoretical dependence of scattering cross section upon angle.

The projection of the Mott formula is not difficult, but is somewhat tedious, so only an outline of the method will be given here. By use of the substitution $mc^2\beta/e(1-\beta^2)^{\frac{1}{2}}=H\rho$ the Mott formula can be written

$$N(\theta)=\frac{NZ^2e^4}{4}\left(\frac{1}{H\rho}\right)^2\left[\frac{1}{\beta^2}\csc^4\frac{\theta}{2}-\csc^2\frac{\theta}{2}+\frac{\pi Z\alpha}{\beta}\csc^3\frac{\theta}{2}\cos^2\frac{\theta}{2}\right], \quad (2)$$

where $N(\theta)$ is the number of deflections per unit solid angle per cm track length, N is the number of atoms per cc in the gas, H is the magnetic field in gauss, and ρ is the radius of curvature of the track in cm. The coefficient in front of the bracket in (2) will be referred to as k. The resolution of the scattering angle θ into a horizontal angle ϕ and a vertical angle ψ is accomplished by the transformation $\cos\theta=\cos\phi\cos\psi$. Integrating over ψ from $-\pi/2$ to $+\pi/2$ we obtain the following result for the three terms

[6] N. L. Oleson, K. T. Chao, and H. R. Crane, Phys. Rev. 60, 378 (1941).

of (2).

$$\frac{8k}{\beta^2 \sin^2\phi}[1+(\pi-\phi)\cot\phi]d\phi=\frac{k}{\beta^2}f_1(\phi)d\phi,$$

$$-\frac{4k}{\cos\phi}\left[\frac{\pi-\phi}{\sin\phi}-\frac{\pi}{2}\right]d\phi=-kf_2(\phi)d\phi,$$

$$\frac{2^{\frac{1}{2}}\pi Z\alpha k}{\beta}\Big[1+\sum_{\text{even}}\frac{1\cdot3\cdots2n+1}{2\cdot4\cdots2n}\cdot\frac{2\cdot4\cdots n}{1\cdot3\cdots n+1}\times(4n+1)\cos^n\phi+\frac{\pi}{2}\sum_{\text{odd}}\frac{1\cdot3\cdots2n+1}{2\cdot4\cdots2n}\times\frac{1\cdot3\cdots n}{2\cdot4\cdots n+1}(4n+1)\cos^n\phi\Big]d\phi=\frac{Zk}{\beta}f_3(\phi)d\phi. \quad (3)$$

Since in our experiment deflections to the left and to the right are placed in a single group, the above formula must be multiplied by 2; it becomes

$$N(\phi)d\phi=2k\left[\frac{1}{\beta^2}f_1(\phi)-f_2(\phi)+\frac{Z}{\beta}f_3(\phi)\right]d\phi. \quad (4)$$

Numerical values of $f_1(\phi)$, $f_2(\phi)$, and $f_3(\phi)$, and their integrals over 10-degree intervals in ϕ, obtained by graphical integration, are given in Table I. In using the table to compute the value of (4) to compare with any group of experimental data it is necessary to determine $\langle 1/H\rho^2\rangle_{Av}$, because of the spread in $H\rho$ within the group of data. These values are readily available, however, because the data are classified in intervals of $H\rho$ in the beginning. $1/\beta$ and $1/\beta^2$ are taken to be unity.

TABLE I. Values of function in Eq. (4).

	$f_1(\phi)$	$f_2(\phi)$	$f_3(\phi)$
15°	1410.0	39.6	1.80
20	594.0	27.9	0.960
30	177.0	16.9	0.395
40	76.5	11.7	0.201
50	39.6	8.72	0.116
60	23.6	6.80	0.0725
70	15.4	5.52	0.0475
80	10.8	4.72	0.0327
90	8.00	4.15	0.0228
Integrated values, 10° interval			
15–25°	117.0	5.02	0.180
25–35	32.6	2.99	0.0709
35–45	13.6	2 07	0.0359
45–55	7.11	1.54	0.0206
55–65	4.22	1.20	0.0127
65–75	2.74	0.972	0.00795
75–85	1.91	0.830	0.00576
85–90(×2)	1.41	0.726	0.00401
Total 15–90	179.9	14.99	0.336

CORRECTIONS AND ESTIMATES OF ERRORS

If the tracks were perfect circles there would be practically no error of measurement except that brought about by the fact that the circles on the measuring card are drawn in steps of ½ cm. This error is ±2.5 percent at 10-cm radius. A more serious source of error is the fact that small angle multiple scattering distorts the tracks from true arcs of circles. This effect makes itself felt both in the measurement of the radius of curvature and in the measurement of the angle of scattering. We shall consider first the error introduced into the measurement of the radius of curvature by the multiple scattering. There are a number of ways the error can be estimated, all of them on somewhat uncertain ground, because in the problem of deciding which of the circles on the card best fits the track, the psychology of the measurer is involved to a considerable degree. One method of treating the problem is the following.

On a magnified scale the path of the electron in a gas is composed of n circular arcs of length $s_1, s_2, \cdots s_n$, all of the same radius of curvature ρ, which is determined by the magnetic field. The angles which the arcs make with each other at the $n-1$ intersection points are the small scattering angles and will be denoted by $\phi_1, \phi_2 \cdots \phi_{n-1}$. As a first approximation we may assume that the measurer judges the curvature by the total change in angle which the tangent makes with a fixed direction, divided by the total length $L=\sum_1^n s_i$ of the track. This gives

$$1/\rho_0=1/\rho+(\phi_1+\phi_2+\cdots\phi_{n-1})/L.$$

If $\rho_0=\rho+\Delta\rho$ this can be written approximately as

$$\Delta\rho/\rho=-\frac{\rho}{L}\sum_1^{n-1}\phi_i. \quad (5)$$

The probability distribution for scattering is

symmetric, so $\bar{\phi}=0$ and $\langle\Delta\rho\rangle_{Av}=0$. Further, since the different scattering acts are independent of each other,

$$\langle\Delta\rho^2\rangle_{Av}/\rho^2=(\rho^2/L^2)(n-1)\langle\phi^2\rangle_{Av}. \tag{6}$$

Finally it is necessary to average over all possible number of scattering acts and ways of dividing the total length L in pieces $s_1\cdots s_n$. Since according to (6) $\langle\Delta\rho^2\rangle_{Av}$ is simply proportional to the number of scattering acts and independent of the way in which the total length L is subdivided, this averaging process gives

$$\langle\Delta\rho^2\rangle_{Av(2)}/\rho^2=(\rho^2/L^2)\nu\langle\phi^2\rangle_{Av}, \tag{7}$$

where ν is the average number of scattering acts in the track length L.

The most direct way to evaluate (7) is to make use of the fact that $\nu\langle\phi^2\rangle_{Av}$ is just

$$\int_{\phi_{\min}}^{\phi_{\max}}\phi^2N(\phi)d\phi, \tag{8}$$

where $N(\phi)$ is that defined by (4). Since $\phi_{\max}$ is small, the first term only of (4) with $f_1(\phi)=8\pi/\phi^3$ will be sufficient. The result is

$$\langle\Delta\rho^2\rangle_{Av(2)}/\rho^2=(\rho^2/L^2)\cdot 16\pi k\log(\phi_{\max}/\phi_{\min}). \tag{9}$$

$\phi_{\min}$ is the lower limit imposed upon the angle of scattering by screening, and for this we use $\lambda/a=(1-\beta^2)^{\frac{1}{2}}/137\beta Z^{\frac{1}{3}}$, as is done by E. J. Williams.[7] $\phi_{\max}$ in our case is the angle at which the deflections begin to be clearly recognizable as single events and for this we have taken three degrees. The value of k can of course be computed directly from the atomic number and density of the gas and the energy of the electrons, but this involves making a weighted average over all energies and different gases used. A more direct method is to make use of the relation between k and the number of deflections greater than 15° observed per unit length of track. The integral of (4) between the limits 15° and 90° can be set equal to the number of deflections observed between those limits of angle, per cm of track length, which is 0.0036 for air, 0.0026 for argon, 0.0037 for krypton, and 0.0055 for xenon. The integral of the part inside the bracket can be read from the last line of Table I. We set $\beta=1$ where it occurs inside the bracket, and we must evaluate $\log\phi_{\max}/\phi_{\min}$, for each case. Tracks for which $\rho=L$ are taken as typical ones. For these, we obtain $\langle\Delta\rho^2\rangle_{Av}/\rho^2=0.0016$, 0.0013, 0.0017, and 0.0025 for air, argon, krypton, and xenon, respectively.

As a refinement in the argument one might attempt to introduce into (5) a weighting factor to take account of the fact that deflections near the center of the track will have a greater influence upon the measured curvature than will those near either end. Equation (5) then takes the more general form

$$\Delta\rho/\rho=-(\rho/L)\sum_{1}^{n-1}\phi_iF(x_i), \tag{10}$$

where $F(x)$ is some function which is zero at either end of the track and maximum at the center, and whose integral over the length of the track is unity. The parabola $F(x)=6(x/L)(1-x/L)$ is such a function. Using this we find that $\langle\Delta\rho^2\rangle_{Av}/\rho^2$ is about 20 percent greater than the result in the above paragraph.

Assuming that the error in ρ produced by the multiple scattering can be represented by the symmetrical Gauss error function, we find the effect of that error upon the single scattering results can be calculated approximately. The theoretical single scattering intensity, computed from the measured value of

$$\sum_{i=1}^{n}l_i/(H\rho)^2$$

(where $l_1\cdots l_n$ are all the pieces of track measured) will be too high by the factor

$$\frac{\int_{-3\alpha}^{3\alpha}(\rho+x)^{-2}\exp(-x^2/\alpha^2)dx}{\int_{-3\alpha}^{3\alpha}\rho^{-2}\exp(-x^2/\alpha^2)dx}, \tag{11}$$

where $\alpha^2=2\langle\Delta\rho^2\rangle_{Av}$. The limits of integration, $\pm3\alpha$, are arbitrarily chosen to give sufficient accuracy and to avoid the singularity at $-\rho$. Evaluating (11) for the values of $\langle\Delta\rho^2\rangle_{Av}$ just calculated, we find the correction factor to be 1.01, which is agreeably small.

The other way in which small angle scattering introduces an error into the final result is through

[7] E. J. Williams, Proc. Roy. Soc. **A169**, 531 (1939).

its effect upon the measurement of the large deflections. The large deflections are measured by determining the angle between the arcs which are fitted to the tracks, at their intersection. Because of the fact that the track is not circular, the actual direction of travel of the electron is not quite the same as the direction of the tangent to the fitted circle at the point at which the deflection occurs. The question we have to answer is, to what extent, in the various parts of the track, is the wandering in direction taken into account in the process of fitting the true arc to the track? Certainly the wandering in the last millimeter of path before the point of the large deflection will have but slight effect upon the fitting of the circle, so we can say that all of the multiple scattering in this last millimeter will enter as an error in the measurement of the direction of the track at the point of the large deflection. On the other hand, it can be seen clearly by sketching a few typical cases that wandering near the middle of the track will have a much reduced effect upon the measurement of the deflection, and that wandering near the far end will have practically no effect. The problem then reduces to that of deciding upon an arbitrary weighting function, to describe the effect of small scattering angles along the track as a function of their distance from the point of the large deflection. After drawing many hypothetical cases, and remembering our experience at measuring a great many tracks, we arrived at the following as reasonable: the full value of a small deflection which occurs close to the large deflection is added to the large deflection; those 1 cm from the large deflection are added with a weighting factor $\frac{1}{2}$, and so on, giving the weighting function $\exp -0.7x$ where x is the distance from the large deflection. The calculation with this function is straightforward. We set

$$\langle\Delta\phi^2\rangle_{Kr}=2\int_0^L\int_{\phi\min}^{\phi\max}[\phi e^{-0.7x}]^2N(\phi)d\phi dx, \quad (12)$$

and evaluate it as we evaluated (9). The factor 2 above enters because the same error is made in the determination of the direction on each side of the point of the large deflection. $\langle\Delta\phi^2\rangle_{Kr}$ comes out to be 0.0022, 0.0017, 0.0021, and 0.0035 radians^2 for air, argon, krypton, and xenon, respectively.

Assuming that $W(\Delta\phi)$ has the form of a symmetrical Gauss error function, we can easily make an approximate calculation of the amount by which the observed scattering intensity is too high. The factor is

$$F=\frac{\int_{-3\alpha}^{3\alpha}N(\phi+x)\exp(-x^2/\alpha^2)dx}{\int_{-3\alpha}^{3\alpha}N(\phi)\exp(-x^2/\alpha^2)dx}, \quad (13)$$

where $\alpha^2=2\langle\Delta\phi^2\rangle_{Kr}$, and where the integration is again cut off at $\pm3\alpha$, to avoid the singularity. We have done the integration graphically, and the results are given in Table II. In the smallest angle interval (15°–25°) the size of the correction factor is too great for comfort, in view of the fact that it rests upon a somewhat arbitrary assumption. Its sensitivity to the exponent in the weighting factor is indicated by experimentally doubling and halving the exponent in the typical case of krypton, 15°–25°. This gives correction factors of 1.73, 1.35, and 1.13 for exponents -2×0.7, -0.7, and $-\frac{1}{2}\times0.7$, respectively. Fortunately the correction factor has little importance for angles greater than 25°.

The error in the knowledge of the magnetic field strength is estimated to be about ±3 percent. Since this enters into the uncertainty in $H\rho$ in just the same way as the error in ρ does, it should be handled in the way we have already outlined for the error in ρ. $\langle\Delta H^2\rangle_{Kr}/H^2=0.0014$,

TABLE II. Correction factor, F [Eq. (13)].

	Air	Argon	Krypton	Xenon
15°	1.56	1.40	1.53	2.10
20	1.27	1.19	1.26	1.43
30	1.11	1.09	1.11	1.17
40	1.06	1.04	1.06	1.08
50	1 03	1.02	1.02	1.04
60	1.02	1.01	1.01	1.02
70	1.01		1.01	1.01
80				1.01
90				
15–25	1.37	1.27	1.35	1.61
25–35	1.16	1.12	1.15	1.27
35–45	1.07	1.05	1.07	1.12
45–55	1.03	1.02	1.03	1.06
55–65	1.02	1.01	1.02	1.03
65–75	1.01		1.01	1.02
75–85				1.01
85–90				

TABLE III. Comparison of theoretical and experimental results.

Gas	Energy range (Mev)	Effective energy (Mev)		15°–25°	25°–35°	35°–45°	45°–55°	55°–65°	65°–75°	75°–85°	85°–90° (×2)
Air	0.9–1.3	1.1	Theory	63.0	14.1	5.1	2.3	1.3	0.7	0.4	0.3
			Exp.	43.0	16.0	6.5	2.0	2.0	2.0	0	1.0
Air	1.3–1.6	1.4	Theory	66.0	14.7	5.3	2.4	1.4	0.8	0.5	0.3
			Exp.	45.5	22.0	6.0	2.5	2.0	0	0	0
Air	1.6–4.5	2.2	Theory	78.0	17.6	6.3	3.0	1.6	0.9	0.6	0.4
			Exp.	93.5	18.5	12.0	5.0	0.5	2.0	0	0
A	0.8–3.3	2.4	Theory	30.3	7.2	2.7	1.3	0.7	0.4	0.2	0.1
			Exp.	30.0	10.5	5.0	2.5	1.0	0	1.0	0
A	3.3–9.3	4.6	Theory	32.2	7.6	2.8	1.4	0.7	0.4	0.2	0.1
			Exp.	52.0	10.5	4.5	5.0	1.0	0	0	0
Kr	1.9–9.3	4.5	Theory	33.0	7.5	2.8	1.4	0.7	0.4	0.3	0.2
			Exp.	43.0	7.0	1.0	1.0	0	1.0	1.0	1.0
Xe	1.5–2.9	2.0	Theory	80.0	17.0	6.0	2.8	1.5	0.9	0.5	0.3
			Exp.	73.5	17.0	7.5	3.0	1.0	2.0	1.0	1.0
Xe	2.9–5.8	4.7	Theory	97.0	21.0	7.4	3.5	1.8	1.0	0.6	0.4
			Exp.	62.5	23.5	3.5	2.5	3.0	2.0	0	0
Xe	5.8–12.0	7.5	Theory	90.0	20.0	6.9	3.3	1.8	1.0	0.6	0.4
			Exp.	86.5	27.5	18.0	3.5	3.0	0	0	0
Total			Theory	569.5	126.7	45.3	21.6	11.5	6.5	3.9	2.5
			Exp.	529.5	152.5	64.0	27.0	13.5	9.0	3.0	3.0

which, when treated by an equation similar to (11), gives a correction to the scattering curve of about 1 percent.

The partial pressures of the gases in the chamber enter the calculation of the expected scattering in the first power, so any error in their measurement which has a symmetrical distribution will give zero correction, for a large number of runs. The only possible source of systematic error we know of in this connection is the following: In using the pressure of the gas in the expanded chamber for the calculation we assumed that all of the scattering occurred after the completion of the expansion. If some of the tracks were actually due to electrons which passed through the chamber before the completion of the expansion, then the above assumption is in error, and a correction will have to be made to the effective pressure of the gas. However, from the mobilities of the ions under the electric clearing field in the chamber it can easily be shown that the life of an ion track before condensation is sufficiently short (by a factor 10 to 100) to exclude the possibility that the tracks photographed were due to electrons which entered the chamber appreciably before the completion of the expansion. We seem to be safe in using the pressure of the fully expanded chamber in the calculation.

RESULTS AND CONCLUSIONS

Experimental Data

In all of the measurements a total of 2173 meters of track length was used and 801.5 deflections between 15° and 90° were found. Table III gives all of the data on scattering in collected form. The column labeled "effective energy" gives the energy corresponding to $(H\rho)_{eff}$ where $1/(H\rho)^2_{eff}=\langle 1/(H\rho)^2\rangle_{Av}$, that is, the energy which would give the same theoretical scattering as the group of tracks under consideration. Half-integers appear in the numbers of tracks observed, because cases which fell on the dividing line between two angle intervals were split between the two intervals.

All the data are collected in Table III. We find 801.5 scattering events observed in the angle range 15° to 90°, while theory predicts 787.5.

This apparent excellent agreement means little more, however, than that the scattering in the lowest angle group checks with theory, since a preponderance of the scattering events lies in that group. The data, when broken down into angle intervals (bottom row of Table III) show that the scattering in the intervals 25°–35°, 35°–45°, and 45°–55° runs in excess of the theoretical by 20 percent, 43 percent, and 25 percent, respectively. For these intervals the statistical accuracy is not bad, so this evidence for an excess over the theoretical value is considered to be strong, though not conclusive. The data in Table III are further subdivided according to the gas used and the energy range of the electrons. None of these groups shows a behavior which is strikingly different, or perhaps even significantly different, from any other group. The statistical accuracy is still good enough to show this when the data are so subdivided, and we believe that this result is in itself important, because there is much contradictory material in the literature on this point.

The attempt was made to learn the frequency of occurrence of large energy losses, but the number of cases was found to be too small to permit a statistical study. For example, two cases showing more than 50 percent energy loss were found in all of the xenon pictures; theory predicted eight cases.

Other Experimental Work

Before asking the reader to consider any final conclusions we wish to present a summary of other work which has been done on the same problem. Table IV contains results of experiments in which individual scattering events were examined in the cloud chamber, by much the same method as our own. The total length of track and number of deflections measured are given not only to indicate the statistical accuracy, but to indicate the extent to which small angle scattering may have influenced the results.

In addition to the material given in Table IV mention should be made of the following experiments, most of which were done by methods other than the cloud chamber method. Chadwick and Mercier[8] measured the scattering of Ra E beta-rays in Al, Cu, Ag, and Au foils, using the annular ring method. Their results, obtained in the angle range 20°–40°, gave good agreement with theory. Henderson[9] later made an experiment with similar geometry and electron energy, but used gases instead of foils. The ratios of his experimental results to the theoretical predictions were 1.8, 1.4, 1.2, 1.2, and 1 for H_2, He, N_2, air, and A, respectively. Neher[10] measured the single scattering of cathode rays (145 kv) in Al, Ag, and Au foils at angles between 95° and 173°. He found that the scattering in Al was 1.32 times that predicted by the Mott theory. He did not commit himself as to whether there was agreement with theory or not in the cases of Ag and Au, because of the poorer accuracy of the theory for these elements and energies. Saunderson and Duffendack[11] studied both the single and multiple scattering of 0.2 and 1.1 Mev (Ra E) beta-rays in Al, Cu, Ag, and Au foils. They found no evidence for a large discrepancy between theory and experiment. Gautier[12] measured the scattering of 0.2 to 1.2 Mev (Ra E) beta-rays in hydrogen, air, and

TABLE IV. Comparison of results.

Element	Energy, Mev	Angle, deg.	Track length, meters	No. of deflections	Ratio exp. to theor.	Author
N	0.4–1.1	20–180	875	201	0.85	1
N	1.5–3.0	20–180	180	212	10 to 100	2
N	0.2–1.1	20–180	82	113	1.7	3
N	1.5–3.0	20–180	116	92	12	3
N	0.3–2.5	20–180	294	47	0.7	4
N	0.2–3.0	15–180	515	42	1.3	5
N	0.2–3.1	15–180	367	41	1.5	6
F	0.2–3.0	15–180	910	113	1.2	5
A	1.7–2.4	30–180	350	48	0.75	7
A	0.2–1.1	20–150	103	308	1.0	8
A	1.5–3.0	20–150	130	84	2.5	8
A	0.2–3.0	20–180	708	153	1.5	5
Kr	0.5–2.6	40–180	140	10	0.16	9
I	0.7–1.2	20–180			0.4	10
I	0.8–3.2	15–180	459	249	1.0	11
Xe	0.5–2.6	40–180	240	51	0.2	9
Xe	2.1	20–180	64	161	0.85	12
Xe	2.1	40–180	172	101	0.85	12
Hg	0.5–1.1	20–180	350	152	0.15	13

[1] F. C. Champion, Proc. Roy. Soc. **A146**, 83 (1934).
[2] D. Skobeltzyn and E. Stepanowa, Nature **137**, 456 (1936).
[3] E. Stepanowa, Physik. Zeits. Sowjetunion **12**, 550 (1937).
[4] M. D. Borisov, V. P. Brailovski, and A. I. Leipunski, Comptes Rendus (Doklady) de l'Acad. des Sciences d l'U.S.S.R. **26**, 142 (1940).
[5] E. Bleuler, P. Scherrer, and W. Zünti, Phys. Rev. **61**, 95 (1942).
[6] E. Bleuler, Helv. Phys. Acta **15**, 613 (1942).
[7] K. Zuber, Helv. Phys. Acta **11**, 370 (1938).
[8] E. Stepanowa, J. Phys. U.S.S.R. **1**, 204 (1939).
[9] H. Klarmann and W. Bothe, Zeits. f. Physik **101**, 489 (1936).
[10] A. Barber and F. C. Champion, Phys. Rev. **55**, 111 (1939).
[11] W. Segrist, Helv. Phys. Acta **16**, 471 (1943).
[12] R. L. Sen Gupta, Proc. Phys. Soc. London **51**, 355 (1939).
[13] A. Barber and F. C. Champion, Proc. Roy. Soc. **A168**, 159 (1938).

[8] J. Chadwick and P. H. Mercier, Phil. Mag. **50**, 208 (1925).

[9] M. C. Henderson, Phil. Mag. **8**, 847 (1929).
[10] H. V. Neher, Phys. Rev. **38**, 1321 (1931).
[11] J. S. Saunderson and O. S. Duffendack, Phys. Rev. **60**, 190 (1941).
[12] T. N. Gautier, Phys. Rev. **63**, 456 (1943).

argon, between angles of 10° and 30°. He found that the scattering varied in the expected way with atomic number, but did not determine the absolute scattering cross section.

Conclusions

After seeing Table IV one might be discouraged from attempting any concluding remarks as to whether the scattering is too high or too low. It is an author's privilege, however, to have more faith in his own results than in those of others, so on that basis the following conclusions will be drawn.

1. The highly anomalous results obtained by several other authors, and which have led them to postulate new kinds of interactions between electrons and nuclei, have not been substantiated by our experiments.

2. One of the stated objectives in most single scattering experiments has been to determine whether the experimental results show better agreement with the Mott formula, which is obtained by taking into account the spin of the electron, or with a formula derived without the spin interaction. The latter is given by the first term only of the Mott formula. It is our opinion that the combination of the inaccuracies in the cloud chamber measurements made to date (including our own) and the uncertainties due to the approximations made in the theory places such a decision just outside the range of possibility. Our own results, taken at their face value, are more favorable to the "non-spin" formula than to the "spin" formula, as one can easily see by comparing $f_1(\phi)$ in Table I with $f_1(\phi)-f_2(\phi)+Zf_3(\phi)$, but no significance is to be attached to that fact, because there are more reasonable directions in which to look for the explanation of the discrepancy.

3. The results in Table III run consistently higher than the theoretical values, by an amount which we believe to be outside our experimental error. At least part of the discrepancy may disappear when the following refinements are made in the theory: (a) In the derivation of the Mott formula the radiative force is not taken into account. Mott[13] has shown that when this is included the theoretical value of the scattering is raised by a few percent. (b) The Mott theory involves an approximation which becomes bad at large Z. Bartlett and Watson[14] have made a numerical calculation for the scattering in mercury, and the corrections to be applied to the Mott values turn out to be large: for 1.67-Mev electrons (the highest energy they give) the factor is maximum for 90 degree scattering and is 1.89. On this basis many of the results in Table IV are subject to serious revision, and our own data, for xenon at least, should be modified appreciably. (c) Bartlett and Welton[15] have treated the effect of screening in mercury, and while this correction can be neglected in our data, it should be applied to some of the values in Table IV, particularly those of Barber and Champion on mercury.

4. A point that is perhaps a secondary one is that our results show the expected behavior with variation in atomic number, angle of scattering and electron energy. A fact which was discussed in the introduction should be called to mind again, namely that the energy and atomic number were of necessity varied in such a way that the classical distance of closest approach of the electron to the nucleus remained about constant for a given angle of scattering. This may detract somewhat from the generality of the result.

ACKNOWLEDGMENTS

The authors wish to acknowledge with thanks the valuable help obtained through discussions with Professor S. A. Goudsmit and Professor G. E. Uhlenbeck. The work was made possible, financially, through a grant from the Horace H. Rackham Fund.

[13] N. F. Mott, Proc. Camb. Phil. Soc. **27**, 255 (1930–1931).
[14] J. H. Bartlett and R. E. Watson, Phys. Rev. **56**, 612 (1939).
[15] J. H. Bartlett and T. A. Welton, Phys. Rev. **59**, 281 (1941).

PHYSICAL REVIEW VOLUME 68, NUMBERS 3 AND 4 AUGUST 1 AND 15, 1945

The Intensity of Cosmic-Ray Electrons Relative to Mesotrons at Sea Level

B. LOMBARDO, JR.* AND W. E. HAZEN
University of California, Berkeley, California
(Received May 17, 1945)

A cloud-chamber analysis of the electronic component of cosmic rays at sea level has been carried out with no distorting magnetic field. Electrons were identified by their behavior while passing through lead absorbers, and their energies were determined from the ranges, for low energies, and from the shower sizes, for high energies. The processes of mesotron collision and decay in air account for all of the observed electrons. The results are in agreement with the hypothesis that the mesotron decays into one electron and one neutrino.

INTRODUCTION

RECENT experiments and calculations have shown that all of the electrons observed at low altitudes can be accounted for in terms of mesotron collisions and decay processes.[1-3] Greisen's experimental results,[1] however, indicated a deficiency of electrons as far as the usual picture of mesotron decay is concerned, and he consequently suggested the possibility of a three-particle decay (two neutrinos and one electron).

Counter experiments involve so many important corrections and auxiliary experiments when it is desired to separate electron and mesotron initiated phenomena that there is considerable uncertainty in the results. Some of the corrections and, in some cases, the primary observations themselves are based on theoretical calculations that have never been adequately verified in the realm of cosmic-ray energies. For example, figures for the penetration of electron showers in lead are based on types of analysis that have never claimed accuracy of better than 20 percent insofar as approximations in the calculations themselves are concerned,[4] to say nothing of the lack of quantitative experimental verification of the radiation probabilities at high energies.

In view of the difficulties in the analysis of counter data, a preliminary experiment has been performed with a direct observation technique (Wilson Cloud chamber) that eliminates all of the aforementioned difficulties. Direct observations of the absorption of individual rays were made, and these observations, together with simultaneous confirmatory observations of scattering, ionization, change in ionization, and shower production, leave virtually no uncertainty in interpretation. The critical question of lower energy limits for the lower energy electrons involves collision loss, which has been well verified, and only a small amount of radiation loss. Since there was no magnetic field, the lower energy end of the spectrum was undistorted.

EXPERIMENTAL ARRANGEMENT

The cloud chamber was in the form of a cylinder of 30-cm diameter and 30-cm length. Six lead plates in the chamber, the upper three of 2-mm and the lower three of 7-mm thickness, acted as absorbers and aided in the identification of individual cosmic rays. The plates were faced with aluminum-foil reflectors so thin that their absorption was negligible. It was found that the thermally-dependent characteristics of cloud-chamber operation were very uniform throughout the chamber when the lead plates terminated an inch or two in front of the black velvet. The illumination was provided by argon flash tubes, as in previous work, but the high voltage of the power source (17 microfarads charged to 10,000 volts) necessitated the use of an "ignitron" switch in series with the flash tubes. The operation of the cloud chamber was initiated by three counter tubes placed above the chamber. The counters defined a volume that was in the observed region and that was completely intercepted by the lead plates. The counter cathodes were thin films of colloidal graphite painted directly on the glass walls. A hinged door in the

* Now at Universidad Nacional, Panama.
[1] K. Greisen, Phys. Rev. **63**, 323 (1943).
[2] H. E. Stanton, Phys. Rev. **66**, 48 (1944).
[3] D. B. Hall, Phys. Rev. **66**, 321 (1944).
[4] H. J. Bhabha and S. K. Chakrabarty, Proc. Roy. Soc. **A181**, 267 (1943).

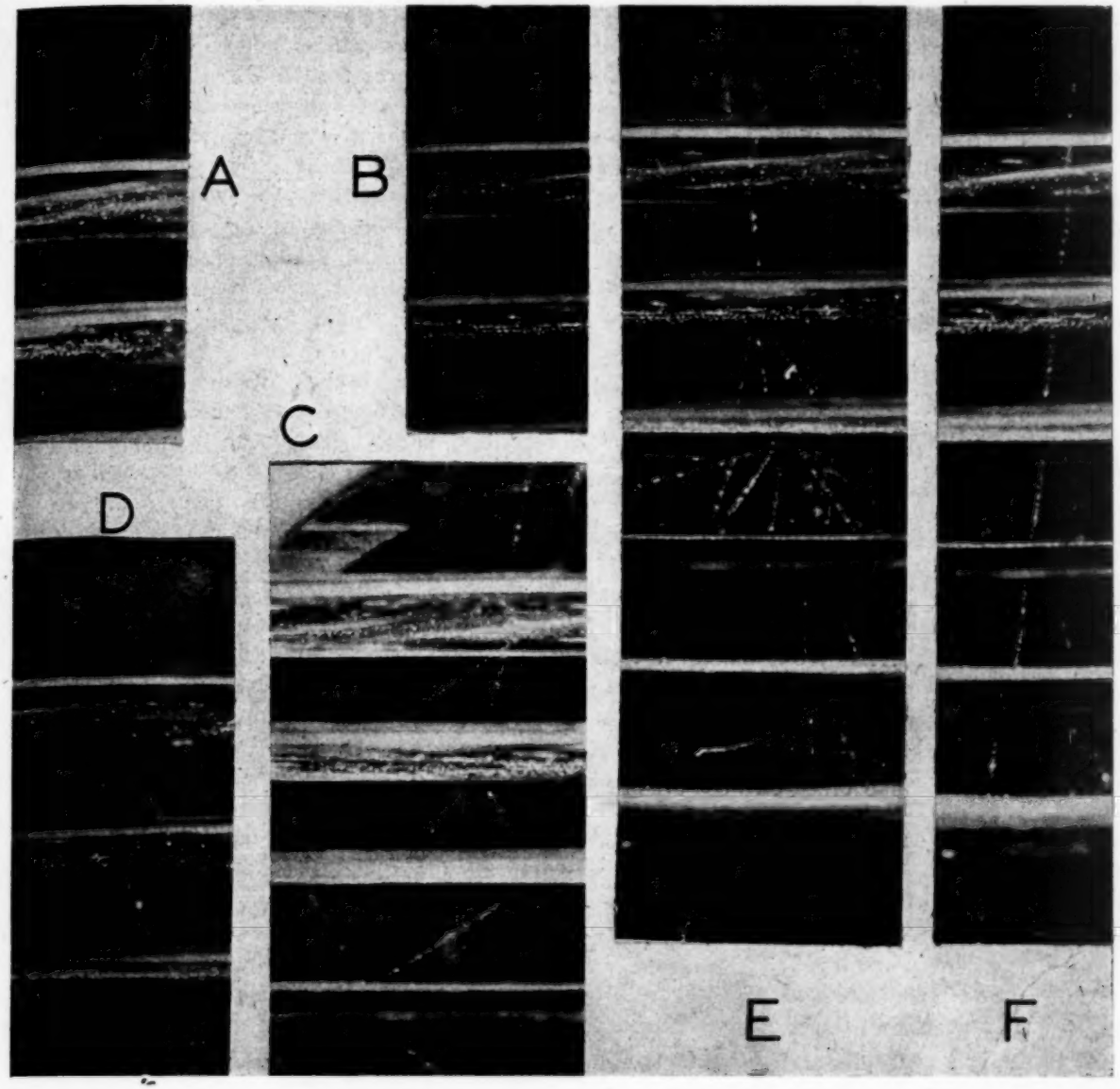

FIG. 1. Photographs illustrating various classifications of particles. (*A*) An electron with $6.6<E<10$ Mev. (*B*) An electron with $10<E<14.5$ Mev. (*C*) An electron with $21.5<E<83$ Mev. (*D*) An electron with $14.5<E<21.5$ Mev. (*E*) An electron with $250<E<500$ Mev. (*F*) A mesotron with $p>1.3\times10^8$ ev/*c*.

sheet-metal roof allowed the elimination, during favorable weather, of all absorber above the apparatus. Stereoscopic photographs were taken with 13.5-cm lenses and 35-mm film.

METHOD OF ANALYSIS

The minimum electron energies required for penetration of the various absorbers were calculated by numerical integrations of the curves for the rate of energy loss as a function of energy. The rate of energy loss due to electron collisions was obtained from Richtmyer and Kennard.[5] In the case of glass, an average value for A/Z and A was determined from the relative abundance of the constituents. This procedure is justified by the facts that A/Z is nearly $\frac{1}{2}$ for all the constituents, and Z enters only in a logarithm term.

[5] Richtmyer and Kennard, *Introduction to Modern Physics* (McGraw-Hill Book Company, Inc., New York, 1942), p. 682.

The rate of energy loss due to radiative collisions was obtained from curves interpolated between those of Heitler[6] for H_2O, Cu, and Pb. The equivalent radiation unit of length, which is used in the calculations of the asymptotic radiation probability for high energy and in the calculation of the energy loss from the radiation probabilities, was obtained by use of Eq. (1.29a) of Rossi and Greisen.[7]

The lowest energy rays that could be observed in the chamber were those that had penetrated 1.52 cm of glass. A numerical integration of the energy loss *versus* energy curve for glass indicates a minimum energy of 6.6 Mev for an electron to reach the interior of the cloud chamber. Some of the photographs were taken with an iron door of 1.0-mm thickness above the counters, and in this case the lower energy limit was 7.7 Mev. The remaining photographs were obtained with two sheets of iron and a layer of insulation board above the apparatus with a consequent raising of the lower energy limit to 9.6 Mev. In passing through the iron the energy loss of these low energy electrons is approximately one-third radiation loss. The resulting uncertainty in energy of individual rays arising from the large fluctuations in radiation loss involves only one-tenth of the total energy loss and therefore is not important. With the glass as the only absorber, radiation loss is negligible.

TABLE I. Observed numbers of electrons.

Absorber	E limit	No. of electrons	Electrons per mesotron
1.52 cm glass	6.6 Mev	52	38 percent
+2 mm Pb	10	38	28
+4 mm Pb	14.5	31	23
+6 mm Pb	21.5	27	20
+13 mm Pb	83	19	14
(showers)	100	10	7.3
	250	0	0
	500	0	0
Mesotrons		136	
1.52 cm glass and 1 mm Fe	8.1	71	31.5
+2 mm Pb	11.5	57	25
+4 mm Pb	16.5	44	19.5
+6 mm Pb	24	29	13
+13 mm Pb	90	19	8.5
(showers)	100	15	6.7
	250	6	2.7
	500	3	1.3
Mesotrons		225	
1.52 cm glass, 1.55 cm Celotex, and 1.4 mm Fe	9.6	70	31
+2 mm Pb	13.5	55	24.5
+4 mm Pb	18.5	43	19
+6 mm Pb	28	31	14
+13 mm Pb	93	22	10
(showers)	100	17	7.5
	250	3	1.3
	500	0	0
Mesotrons		225	
(showers)*	100	16	6.0
	250	9	3.4
	500	3	1.2
Mesotrons		267	

* The last four lines are from data of S. Nassar.

The second group of electrons, those that penetrated the first 2-mm lead plate but stopped in the second, would have larger fluctuations in energy loss since a larger fraction of the energy is dissipated in radiation, but the fluctuations would still be small. In the case of electrons that penetrated three or more lead plates, the radiation losses become comparable with collision losses, and the fluctuations in energy loss begin to limit the usefulness of data consisting of small samples in the determination of an energy spectrum at high energies. Electrons that penetrated any of the thicker lead plates nearly always gave rise to showers, and their energies could be estimated from the size of the shower.

Slow mesotrons that stopped in the chamber could be distinguished by the lack of multiplication, by the small scattering, and by the increased ionization in the last air space traversed. Actually there was only one such particle, and it was a post-expansion traversal. Illustrative photographs are shown in Fig. 1.

Only counter tripping particles were considered. These were identified from the track widths as far as time of occurrence was concerned and from the parallax in the stereoscopic photographs as far as position was concerned. These criteria were critical only in identifying the few cases where more than one particle passed through the counters simultaneously, particles that were separate before striking the apparatus. There

[6] W. Heitler, *Quantum Theory of Radiation* (The Clarendon Press, Oxford, 1936), p. 173.
[7] B. Rossi and K. Greisen, Rev. Mod. Phys. **13**, 240 (1941).

were only a few such cases, such as air showers and mesotrons accompanied by electron secondaries that had been produced in air. These few cases were not important when considering total numbers of particles.

RESULTS AND CONCLUSIONS

The results are summarized in Table I in terms of actual numbers of observed rays, and, in the last column, the observations are reduced to numbers of electrons relative to the numbers of mesotrons with $H\rho > 4.2 \times 10^5$ gauss-cm or p (Rossi units) $> 1.3 \times 10^8$ ev/c. The counter system defined a solid angle that restricted the rays essentially to the vertical. Rossi and Klapman[8] have calculated the number of electrons with $E > 10^7$ ev to be expected as a result of both the collisions and also the decay of mesotrons. Greisen[1] has made calculations for other lower energy limits that involve averaging over-all zenith angles. Since his average is not significantly different from the results of Rossi and Klapman for lower energy limit 10^7 ev, the results will be used as they stand for comparison with the experimental data. The theoretical values of Greisen for decay electrons have, however, been multiplied by 100/68 in order to reduce the figures to number of electrons per mesotron with $p > 1.3 \times 10^8$ ev/c. The results are given for a mesotron mass of 180 and lifetime of 2.2 microseconds. Greisen's figures for collision electrons have likewise been multiplied by 64/68 to reduce the values to number of electrons per mesotron with $p > 1.3 \times 10^8$ ev/c.

A comparison of the calculated and the measured values is made in the graph of Fig. 2. It is seen that the agreement is tolerable; i.e., it is probably within the uncertainties of the calculations and measurements. The scatter of the experimental points indicates the magnitude of the statistical uncertainties. As far as systematic errors in the data are concerned, it is believed that the points for the lowest three energies may be relatively too low since there existed some possibility of not detecting a ray that stopped in the first lead plate. As mentioned earlier, the

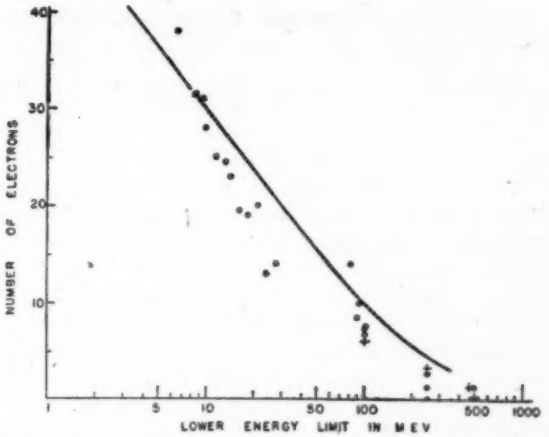

FIG. 2. Integral spectrum for electrons at sea level. The curve is from calculations of Greisen. (See reference 1.) The number of electrons is relative to the number of mesotrons with $p > 1.3 \times 10^8$ ev/c and is expressed in percent. The points indicated by + are from data obtained by S. Nassar in connection with another experiment.

points in the vicinity of energies 20–30 Mev and greater depend significantly on radiation theory which has not been carefully verified at these high energies. The points at energies greater than 70 Mev involve shower theory which also has not been quantitatively verified. But the estimates of energies are based on detailed observations of the showers and therefore are more reliable than counter observations which depend on a rather specific property in many cases.

Scattering in the absorbers and the variation in the traversed thickness of counter walls, both of which increase the energy loss, have been neglected. The latter increases the average energy loss only a few percent. The former is most important in lead and, if taken into account, would shift the points between 10 and 50 Mev to the right in Fig. 2.

In all of the above, it has been assumed that the mesotron decay products are one electron and one neutrino. Thus we can conclude that there is no need for the hypothesis of decay into one electron and two neutrinos unless evidence for another source of cosmic-ray electrons is uncovered.

We are much indebted to Mr. Robert Brown who assembled the original apparatus and obtained some preliminary photographs and to Miss Salwa Nassar who furnished data on the frequency of occurrence of electron showers.

[8] B. Rossi and S. J. Klapman, Phys. Rev. 61, 414 (1942).

PHYSICAL REVIEW VOLUME 68, NUMBERS 3 AND 4 AUGUST 1 AND 15, 1945

General Theory of Pressure Broadening of Spectral Lines

ALEXANDER JABŁOŃSKI
Department of Physics, Polish School of Medicine, Edinburgh, Scotland

(Received November 6, 1944)

A new, more consistent, shape has been given to the theory of pressure broadening of spectral lines recently published by the author. In contradistinction to other theories, the present theory constitutes a very close analogy to the theory of intensity distribution in molecular spectra. There is no doubt that both phenomena are due to the same cause, i.e., to the relative movements of atomic nuclei. Thus, the theoretical treatment of both must be identical as far as possible. The method used by James and Coolidge for the calculations of intensity distribution in H_2 and D_2 continuous spectra can be adapted to the calculations of the profiles of broadened lines. In this case, presumably, it will not be possible to represent the intensity distribution in a closed form. In order to obtain a closed form, Condon's method (the quantum mechanical form of the Franck-Condon principle) is applied, and the Wentzel-Kramers-Brillouin approximate eigenfunctions are used for nuclear motions. The limitations of applicability of this approximation are discussed (the same limitations apply *a fortiori* to the applicability of every theory based on the classical description of nuclear motions). Because of the above simplifications, the resulting intensity distribution formula must be considered as an asymptotic one only, valid in a restricted region of frequencies of the broadened line and only in the case of heavy atoms and high temperatures (it certainly fails in the case of broadening by light gases such as He and H_2 or electrons), though it still constitutes a better approximation than that previously published. Apart from a correction which is in most cases insignificant, it is identical with Kuhn's intensity distribution obtained on the basis of the primitive form of the Franck-Condon principle. The present paper is drafted so as to be comprehensible to the reader without knowledge of the preceding papers of the author, the main results of which are being included here.

I. INTRODUCTION

SINCE 1937 I have developed in several papers[1] a theory of pressure broadening of spectral lines differing from other theories inasmuch as it constitutes a close analogy to the quantum-mechanical treatment of intensity distribution of molecular spectra. The causes which induced me to publish one more paper on this subject are these: a new, more consistent, and, I hope, more digestible form is given to the theory; a better approximation is reached in the approximate final formula; the limitations of its applicability are discussed (these limitations apply *a fortiori* to all other theories published hitherto); and the way to still better approximations is indicated. Besides, it seemed necessary to emphasize once more the close analogy between the mechanism of pressure broadening and of the production of molecular spectra. This analogy is overlooked in most of the papers published recently. There is a predominating tendency to keep as close as possible to the classical collision damping theories.[2] These theories, although their aesthetic value must not be underestimated, cannot give better information about pressure broadening of spectral lines than does the classical treatment of molecular spectra[3] (consisting of Fourier analysis of electronic frequencies modulated by nuclear vibrations) about intensity distribution in molecular spectra. Since the quantum-mechanical procedure, in which the nuclear motions are described by eigenfunctions, leads to very satisfactory results in the case of molecular spectra,[4] one can reasonably expect that the same procedure applied to pressure broadening of spectral lines will give good results as well. After all, both phenomena are due to the same cause, that is, to the relative move-

[1] A. Jabłoński, Acta Phys. Pol. **6**, 371 (1937) (henceforth designated by J.1); Acta Phys. Pol. **7**, 196 (1938) (J.2); Physica **8**, 541 (1940) (J.3). One more paper published in Acta Phys. Pol. is not accessible and will not be quoted here.

[2] H. A. Lorentz, Proc. Amst. Acad. **8**, 591 (1906); W. Lenz, Zeits. f. Physik **25**, 299 (1924); **80**, 423 (1933); **83**, 139 (1933); V. Weisskopf, Zeits. f. Physik **75**, 287 (1932) and Physik. Zeits. **34**, 1 (1933) (henceforth designated by W.1 and W.2 respectively).

[3] W. Lenz, Zeits. f. Physik **25**, 299 (1924); H. Sponer and E. Teller, Rev. Mod. Phys. **13**, 75 (1941), (henceforth quoted as S.T.).

[4] S. W. Brown, Zeits. f. Physik **82**, 768 (1933); A. S. Coolidge, H. M. James and R. D. Present, J. Chem. Phys. **4**, 193 (1936); H. M. James and A. S. Coolidge, Phys. Rev. **55**, 184 (1939); A. S. Coolidge, Phys. Rev. **65**, 236 (1944). (The last three papers will be quoted henceforth by C.J.P., J.C. and C. respectively).

ments of nuclei. It is expedient to recall briefly the main outlines of molecular theory,[5] which can have direct application to the pressure broadening theory.

According to Born and Oppenheimer,[6] an eigenfunction ψ_{rel}, which arises from the relative movement of all constituents (electrons and nuclei) of a molecule can in most cases be written approximately as

$$\psi_{rel}=\psi_{el}\psi_{nucl}, \tag{1}$$

where ψ_{el} denotes the electronic eigenfunction, depending upon electronic and nuclear positions, and ψ_{nucl} is the vibrational eigenfunction, depending upon the relative positions of nuclei only. The total eigenfunction of a molecule can be obtained by multiplying ψ_{rel} by the rotational eigenfunction ψ_{rot} (for restrictions cf. S.T.). Since the last function is unimportant in our problem,[7] we shall omit it in further considerations. The energy corresponding to ψ_{rel} is approximately equal to the sum of electronic energy, E_{el}, and translational energy of the nuclei E_{nucl}:

$$E_{rel}=E_{el}+E_{nucl}. \tag{2}$$

The transition probabilities are proportional to D^2 (square of matrix elements); D being given by:

$$\begin{aligned} D&=\int\int \psi'^{*}_{rel} M \psi''_{rel} d\tau_{el} d\tau_{nucl} \\ &=\int\int \psi'^{*}_{el}\psi'^{*}_{nucl} M \psi''_{el}\psi''_{nucl} d\tau_{el} d\tau_{nucl} \\ &=\int \mathfrak{M}\psi'^{*}_{nucl}\psi''_{nucl} d\tau_{nucl}, \end{aligned} \tag{3}$$

where M is the variable part of electric moment of the molecule.

Further simplification is obtained by expanding $\mathfrak{M}$ (depending on normal coordinates ξ_i) in power series

$$\mathfrak{M}=\mathfrak{M}_0+\sum_i \mathfrak{M}_i\xi_i+\sum_{kl}\mathfrak{M}_{kl}\xi_k\xi_l+\cdots, \tag{4}$$

and neglecting all the terms but, say, the first two. If only the first term $\mathfrak{M}_0$ is taken into account, there results Condon's approximation (the quantum-mechanical form of the Franck-Condon principle); the integral (3) becomes:

$$D=\mathfrak{M}_0\int \psi'^{*}_{nucl}\psi''_{nucl} d\tau_{nucl}=\mathfrak{M}_0 A, \tag{5}$$

where

$$A=A_{v'v''}=\int \psi'^{*}_{nucl}\psi''_{nucl} d\tau_{nucl}, \tag{6}$$

$A^2_{v'v''}$ being the probability of a change of the vibrational state, say from v'' to v', accompanying the electronic transition in the molecule.[8]

For qualitative estimations of $A^2_{v'v''}$ the classical form of the Franck-Condon principle (F.C.P.) can be very useful. It can be formulated as follows:[9]

If there occurs an electronic transition in a system of N atoms (as in an N-atomic molecule), no one of the N nuclei makes any considerable instantaneous change in its position or momentum while the transition occurs. There is an instantaneous change of mutual potential energy only, the last being dependent on the electronic state of the system (or its constituents).

If rotational energy is omitted, the emitted or absorbed energy quantum is (in each of the above approximations)

$$\hbar\omega=E'_{rel}-E''_{rel}=E'_{el}-E''_{el}+E'_{nucl}-E''_{nucl}. \tag{7}$$

Each of the above approximations can be adapted to the theory of pressure broadening of spectral lines, but, so far, only the primitive form of the F.C.P.[10] and its quantum-mechanical form[11] have actually been used.

---

[5] Cf. S. T., reference 3.

[6] M. Born and R. Oppenheimer, Ann. d. Physik **84**, 457 (1927); Cf. S.T., reference 3.

[7] Cf. J.1.

[8] E. U. Condon, Phys. Rev. **32**, 825 (1928). It can be easily shown that $\sum_{v'} A^2_{v'v''}=1$, if summation is carried out over all the existing states v'. Eventually, integration over continuous states has to be carried out. The same relation holds for transitions from one particular state v' to all existing states v'': $\sum_{v''} A^2_{v'v''}=1$. (Cf. A. Jabłoński, Acta Phys. Pol. **6**, 360 (1937).)

[9] A. Jabłoński, Zeits. f. Physik **73**, 281 (1931).

[10] A. Jabłoński, Zeits. f. Physik **70**, 723 (1931); H. Margenau, Phys. Rev. **40**, 387 (1932); M. Kulp, Zeits. f. Physik **79**, 495 (1932); H. Kuhn, Phil. Mag. **18**, 987 (1934) and Proc. Roy. Soc. A158 and 212 (1937). (The last paper will be henceforth designated by K.) For further literature see H. Margenau and W. W. Watson, Rev. Mod. Phys. **8**, 22 (1937).

[11] W.1 and W.2, reference 2; J.1, J.2, and J.3, reference 1.

If the law of conservation of energy is taken into account, the primitive F.C.P. leads to

$$E'_{\text{nucl}}-E''_{\text{nucl}}=V'(\xi)-V''(\xi), \qquad (8)$$

(the difference of potential energies in two electronic states, in relative positions of the nuclei occupied during the electronic transition) and (7) becomes

$$h\omega=E_{\text{el}}'-E_{\text{el}}''+V'(\xi)-V''(\xi). \qquad (9)$$

Equation (9) constitutes the starting point of pressure broadening theories, based on the classical F.C.P. (statistical or potential theories).

The classical theories[2] are based on the assumption that atoms or molecules emit a wave train of variable frequency (the frequency being dependent on the positions of moving nuclei). The intensity distribution is calculated by means of Fourier analysis of variable frequency (and eventually of variable amplitude too). The classical theories of intensity distribution in molecular spectra as well as those of pressure broadening of spectral lines cannot claim to describe the phenomena adequately (unless it is rigorously demonstrated). The same applies to theories, which, though based on Dirac's theory of radiation, describe the nuclear motion classically by considering merely the electronic energy levels as functions of time (their variability being assumed caused by the nuclear movements).[12]

An attempt to bridge the gulf between the classical and quantum-mechanical treatment of the problem has been made by Weisskopf.[2] Because of excessive simplifications his demonstration cannot be considered as convincing. Actually he has shown that, for the case of rectilinear motion of a radiating or absorbing atom in a potential field, the integral (6) can be transformed into an integral of the Fourier type, if Wentzel-Kramers-Brillouin (W.K.B.) eigenfunctions are used. The Fourier integral is then identical with that constituting the starting point of the classical pressure broadening theories. The assumption of rectilinear motion is incompatible with the fact that the atomic collision problem is a central force problem. The difficulty arising from the failure of W.K.B. approximation in the region of the point of closest approach of the colliding atoms (classical turning point) is not surmounted by Weisskopf's treatment, but merely completely camouflaged. As will be shown further, this difficulty is quite a serious one. In addition, Weisskopf treats the continuous translational energy spectrum as a discrete one should be treated, thus omitting an important factor in the final intensity distribution formula.[13] Moreover, there is no justification in the case of a gas consisting, say, of n atoms for replacing the nuclear eigenfunction, which can be approximately written as a product of eigenfunctions of the particular nuclei

$$\psi=\prod_i^n \psi_i$$

merely by means of a single eigenfunction describing the rectilinear motion of the absorbing (or emitting) atom in a fixed potential field. Further simplifications have been introduced by Weisskopf in order to obtain the classical collision damping formula. Weisskopf neglects all the collisions with impact parameters ρ larger than a certain optical collision radius ρ_0, the effect produced by those with $\rho<\rho_0$ being assumed independent of ρ. Thus, Weisskopf's theory cannot possibly describe the phenomena adequately.

A theory concerning the particular case of broadening of resonance lines by intrinsic pressure was developed by Houston.[14] There is no reason, however, to suppose that the present theory cannot embrace this particular case too.

But the last word belongs, of course, to experiment. This word, however, seems not yet to have been pronounced. One of the causes is

[12] H. Margenau and W. W. Watson, reference 10; L. Spitzer, Jr., Phys. Rev. **55**, 699 (1939); **56**, 39 (1939); and **58**, 348 (1940). I do not share the opinion expressed by L. Spitzer that a formula obtained in this way would represent the "true" intensity distribution.

[13] In the case of continuous eigenvalues, eigendifferentials instead of eigenfunctions must be used. If, by using a limited space, the continuous spectrum is transformed into a discrete one, a factor, denoting the density of energy levels, appears in the intensity distribution formula. This factor being omitted in Weisskopf's considerations, an incorrect dependence of the width of the line on energy of collision (i.e., of the temperature of the gas) is obtained.

[14] W. V. Houston, Phys. Rev. **54**, 884 (1938). In this theory too, the nuclear motion is treated classically. The papers of Furssow and Wlasow, mentioned by Houston, were not accessible to the writer. The same applies to the paper by E. Lindholm (Ark. Math. Astr. Fys. **28B**, 1, No. 3 (1943)).

the lack of knowledge of the exact form of potential curves,[15] which prevents theoretical results sufficiently accurate for experimental distinction between different competing theories from being obtained. Experimental difficulties and the difficulties of exact numerical computations constitute the other causes. Yet, one can assert that the primitive form of Lorentz-Weisskopf-Lenz collision damping theory is certainly incompatible with experimental results. Except in the case of broadening by dipole interaction (observed by Rompe and Schulz), the intensity distribution does not result from the above theory. But even the case of dipole interaction cannot be considered as a proof of the collision damping theory, because in this particular case the observed dispersion intensity distribution results not only from the above theory but also from the statistical ones.[16]

According to Unsöld[17] the variation of equivalent breadths throughout the Mg series 3^1P-n^1D in the solar spectrum agrees well with collision damping theory if it is assumed that the lines are broadened by the Stark effect caused by electrons and ions. However, the theoretical values used by Unsöld in his calculations do not agree at all with the later experimental results of Eckarth.[18] If the experimental values of Stark effect constants are put into Unsöld's formulae, the agreement disappears entirely. Thus, Unsöld's results too by no means confirm the Lorentz-Weisskopf-Lenz theory.

As shown by Kuhn,[19] Minkowski,[20] and Rühmkorf[21] the intensity distribution in a certain range of frequencies within the broadened lines agrees well with that predicted by statistical theories. The same distribution (apart from a factor, constituting as a rule only an insignificant correction) results from the present theory for the asymptotic case of heavy atoms having large kinetic energy.[20] The limitations of its applicability are discussed in IX. These experiments thus support the present theory as well. The experiments of Horodniczy and the writer,[21] though perhaps not very precise ones, show that any influence of the temperature, that is, of the number of collisions per second, is much less pronounced than was to be expected according to Weisskopf and can also be considered as supporting rather the statistical theories (and thus the present theory as well).

Although below merely an asymptotic distribution is obtained (mainly because of the difficulties of more exact calculations of integral (6)), the way is still open to more precise calculations. The most suitable way seems to be the use of a differential analyser for calculations of eigenfunctions describing the nuclear movements and the integrals (6) or eventually, if necessary, (3). This method was used very successfully by Coolidge, James, and Present[22] for calculations of intensity distribution in H_2 and D_2 continuous spectra.

II. ON THE PROBABILITY DISTRIBUTION OF A QUANTITY COMPOSED OF A SUM OF QUANTITIES WITH PROBABILITY DISTRIBUTIONS OF A PARTICULAR FORM INDEPENDENT OF ONE ANOTHER

The problem we shall consider here has a direct application to the theory of pressure broadening. Although it does not constitute a characteristic feature of this particular theory, nevertheless its solution is essential for estimation of the conditions in which the single transits of atoms past each other are so predominant that the multiple transits can be neglected. Moreover, this makes it possible eventually to take into account also the multiple transits.

The problem is: The probability distributions $P_1(x_1)$, $P_2(x_2)$, $\cdots P_n(x_n)$ of certain quantities x_1, x_2, $\cdots x_n$ being given, calculate the probability distribution $P(X)$ of

$$X=\sum_{i=1}^{n} x_i$$

on the assumption that the $P_i(x_i)$ are independent of one another.

The general case, when $P_i(x_i)$ are not specified,

[15] Cf. e.g., L. Gropper, Phys. Rev. **55**, 1095 (1939).
[16] K, reference 10.
[17] A. Unsöld, Zeits. f. Astrophys. **12**, 56 (1936).
[18] H. Eckarth, Zeits. f. Physik **107**, 182 (1937).
[19] K. reference 9; R. Minkowski, Zeits. f. Physik **93**, 731 (1935) and H. A. Rühmkorf, Ann. d. Physik [5] **33**, 21 (1938).
[20] The distribution obtained in J.3 (reference 1) differs by a factor 2 from the statistical distribution of Kuhn. The present formula constitutes a better approximation.
[21] H. Horodniczy and A. Jabłoński, Nature **142**, 1122 (1938) and **144**, 594 (1939).
[22] C.J.P.; J.C., reference 4.

is of little interest and is trivial. When the probability distribution

$$P_{1,2,\cdots(n-1)}\left(\sum_{i=1}^{n-1} x_i\right)$$

of an algebraic sum of $n-1$ quantities is known, one obtains the probability distribution $P(X)$ of

$$X=\sum_{i=1}^{n} x_i=\sum_{i=1}^{n-1} x_i+x_n$$

by forming a product of probabilities

$$P_{1,2,\cdots n-1}(X-x_n)P_n(x_n)$$

and integrating[23] over the whole range of variability of x_n, say, from $-\infty$ to $+\infty$:

$$P(X)=\int_{-\infty}^{+\infty} P_{1,2\cdots(n-1)}(X-x_n)\cdot P_n(x_n)dx_n. \quad (10)$$

By means of this procedure, one can calculate the probability distribution of a sum of any number of quantities by calculating successively the probability distribution of a sum of two quantities, then that of three, and so on, until all the quantities are taken into account.

The particular form of probability distribution we shall consider here is that of

$$\int_{\Delta x_i} P_i(x_i)dx_i=\int_{\Delta x_i}[(1-\epsilon)\delta(x_i)+W(x_i)]dx_i, \quad (11)$$

where Δx_i can be arbitrarily small. Thus, we assume that the probability of $x_i=0$ is $1-\epsilon$ and for $x_i\neq 0$ the probability of x_i being within Δx_i is

$$\int_{\Delta x_i} W(x_i)dx_i\approx W(x_i)\Delta x_i.$$

For our purposes it will suffice to consider the simplest case, when $P_1(x_1)=P_2(x_2)=\cdots P_n(x_n)$ for $x_1=x_2=\cdots x_n$.[24] Since

$$\int_{-\infty}^{+\infty} P_i(x_i)dx_i = \int_{-\infty}^{+\infty}[(1-\epsilon)\delta(x_i)+W(x_i)]dx_i=1, \quad (12)$$

ϵ must be given by

$$\epsilon=\int_{-\infty}^{+\infty} W(x_i)dx_i. \quad (13)$$

Here, ϵ denotes the probability of $x_i\neq 0$.

Now we shall show that if all $P_i(x_i)$ are identical and of the type (11), the probability distribution

$$\int_{\Delta X} P(X)dX \text{ of } X=\sum_{i=1}^{n} x_i$$

is:

$$\int_{\Delta X} P(X)dX=\int_{\Delta X}\Big[\delta(X)(1-\epsilon)^n + \sum_{\nu=1}^{n}\binom{n}{\nu} W^{(\nu)}(X)(1-\epsilon)^{n-\nu}\Big]dX, \quad (14)$$

where $W^{(1)}(X)$ is identical with $W(x_i)$ in (11). The integral $\int_{\Delta X} W^{(\nu)}(X)dX$ denotes the probability that the sum of ν quantities, none of which vanish, lies between X and $X+\Delta X$. $W^{(\nu)}(X)$ is obtained from $W^{(\nu-1)}(X)$ by a procedure analogous to that given by (10):

$$W^{(\nu)}(X)=\int_{-\infty}^{+\infty} W^{(\nu-1)}(X-x_i)W^{(1)}(x_i)dx_i.^{25} \quad (15)$$

For $n=2$ (14) can be verified immediately by means of (10) and (15):

$$\begin{aligned}\int_{\Delta X}\int_{-\infty}^{+\infty}&[\delta(X-x_j)(1-\epsilon)+W^{(1)}(X-x_j)]\\ &\times[\delta(x_j)(1-\epsilon)+W^{(1)}(x_j)]dXdx_j\\ =\int_{\Delta X}\int_{-\infty}^{+\infty}&[\delta(X-x_j)\delta(x_j)(1-\epsilon)^2\\ &+W^{(1)}(X-x_j)\delta(x_j)(1-\epsilon)\\ &+\delta(X-x_j)(1-\epsilon)W^{(1)}(x_j)\\ &+W^{(1)}(X-x_j)W^{(1)}(x_j)]dXdx_j\\ =\int_{\Delta X}\Big[&\delta(X)(1-\epsilon)^2\\ &+\binom{2}{1}W^{(1)}(X)(1-\epsilon)+W^{(2)}(X)\Big]dX, \quad (16)\end{aligned}$$

[23] We assume that the x_i are continuous.

[24] The more general case of $P_1(x_1)\neq P_2(x_2)\neq\cdots P_n(x_n)$ for $x_1=x_2=x_3=\cdots x_n$ is treated in J.1, reference 1.

[25] For example,

$$W^{(2)}(X)=\int_{-\infty}^{+\infty} W^{(1)}(X-x_i)W^{(1)}(x_i)dx_i, \text{ where } X=x_i+x_j.$$

which is identical with (14) for $n=2$

$$\left(W^{(2)}(X)=\int_{-\infty}^{+\infty}W^{(1)}(X-x_j)W^{(1)}(x_j)dx_j\right).^{25}$$

In order to prove the expression (14), we need now show merely that if it is admitted to be true for n quantities, it will prove to be true for $n+1$ quantities as well. This can be done by applying the procedure (10) to (14) and taking into account (15):

$$\int_{\Delta X}\int_{-\infty}^{+\infty}\left[\delta(X-x_{n+1})(1-\epsilon)^n+\sum_{\nu=1}^{n}\binom{n}{\nu}W^{(\nu)}(X-x_{n+1})(1-\epsilon)^{n-\nu}\right]\left[\delta(x_{n+1})(1-\epsilon)+W^{(1)}(x_{n+1})\right]dXdx_{n+1}$$

$$=\int_{\Delta X}\left[\delta(X)(1-\epsilon)^{n+1}+\sum_{\nu=1}^{n}\binom{n}{\nu}W^{(\nu)}(X)(1-\epsilon)^{n+1-\nu}+W^{(1)}(X)(1-\epsilon)^n+\sum_{\nu=1}^{n}\binom{n}{\nu}W^{(\nu+1)}(X)(1-\epsilon)^{n-\nu}\right]dX$$

$$=\int_{\Delta X}\left[\delta(X)(1-\epsilon)^{n+1}+\sum_{\nu=1}^{n}\binom{n}{\nu}W^{(\nu)}(X)(1-\epsilon)^{n+1-\nu}\right.$$

$$\left.+W^{(1)}(X)(1-\epsilon)^n+\sum_{\nu=2}^{n+1}\binom{n}{\nu-1}W^{(\nu)}(X)(1-\epsilon)^{n+1-\nu}\right]dX$$

$$=\int_{\Delta X}\left[\delta(X)(1-\epsilon)^{n+1}+\sum_{\nu=1}^{n+1}\binom{n+1}{\nu}W^{(\nu)}(X)(1-\epsilon)^{n+1-\nu}\right]dX, \tag{17}$$

since

$$\binom{n}{\nu}+\binom{n}{\nu-1}=\binom{n+1}{\nu}.$$

Equation (17) being of the same form as (14) and (14) being proved true for $n=2$ (by Eq. (16)), the expression (14) is thus established.

In the limiting case of $\epsilon=1$ all the terms in (14) except the last one vanish. For $\epsilon\ll 1$ Eq. (14) can be written as:

$$\int_{\Delta X}P(X)dX=\int_{\Delta X}\left[\delta(X)e^{-\epsilon n}+\sum_{\nu=1}^{n}\binom{n}{\nu}W^{(\nu)}(X)e^{-\epsilon(n-\nu)}\right]dX. \tag{14a}$$

Equation (14) or (14a) can be immediately applied to the pressure broadening of spectral lines[26] if changes of translational energy of the particular perturbers (perturbing atoms or molecules) due to an electronic transition in the radiator (radiating or absorbing atom) can be considered as independent of one another. The mutual collisions of perturbers with one another are practically irrelevant. In this case $\int_{\Delta X}P(X)dX$ is the probability distribution of the changes X of the total translational energy of the whole gas (n perturbers+radiator), $\int_{\Delta X_i}W^{(1)}(x_i)dx_i$—the probability that the translational energy of a particular nucleus changes its value by an amount x_i and $1-\epsilon$ the probability that this energy remains unchanged.

X is related directly to the frequency actually absorbed or emitted by the radiator. The absorbed frequency ω is

$$\omega=\omega_0+X/\hbar, \tag{18}$$

and the emitted frequency

$$\omega=\omega_0-X/\hbar, \tag{18a}$$

where ω_0 denotes the frequency of the unperturbed line. Obviously X can be both positive (increase of translational energy) and negative (decrease of translational energy). Thus, the intensity distribution is directly given by probability distribution (14).

It is now clear that if the independence of nuclear movements is assumed,[27] it is sufficient to know $W^{(1)}(X)$ (which can be considered as intensity distribution in the case when only one radiator and one perturber are present in the container), in order to calculate successively $W^{(2)}(X)$, $W^{(3)}(X)$, $\cdots W^{(n)}(X)$, and thus the

[26] The same considerations could be applied with slight modifications to a system of atoms (e.g., molecule) with nuclear movements described by means of normal coordinates.

[27] This assumption may, however, not always correspond to the real conditions.

total intensity distribution $P(X)$ resulting from the action of n perturbers present in the container. The first term of (14) then denotes that part of the intensity which survives from the original intensity of the unperturbed line in its exact position ω_0 (the line being assumed for the sake of simplicity as infinitely narrow). The term containing $W^{(1)}(X)$ gives the contribution of single transits, $W^{(2)}(X)$ of double, $W^{(3)}(X)$ of triple; $\cdots W^{(\nu)}(X)$ of ν fold transits to the intensity in ω given by (18).

Because of the assumption of infinite narrowness of original spectral line and additivity of the effects produced by separate perturbers, formula (14) must be considered as an approximate one.

$$\epsilon=\int_{-\infty}^{+\infty}W^{(1)}(X)dX$$

cannot be calculated without exact knowledge of $W^{(1)}(X)$ in the whole range of X, and its computation may prove a hard task. Nevertheless, if one assumes that the effect produced by the transits with impact parameters ρ larger than a certain $\rho_{\max}$ can be practically neglected;[28] i.e., if one assumes a finite sphere of action of interatomic forces, ϵ can be estimated roughly even without relying on the quantum-mechanical theory developed below. It is of the order of magnitude of $(\rho_{\max}/R)^3$, where R denotes the radius of the container (which we suppose for the sake of simplicity to be spherical). Thus, e.g., for $\rho_{\max}=10^{-7}$ cm and $R=1$ cm, $\epsilon\sim10^{-21}$. For $n\epsilon\ll1$, $(1-\epsilon)^{n-\nu}\approx e^{-\epsilon(n-\nu)}\approx1$, and the factors $(1-\epsilon)^{n-\nu}$ can be omitted in (14). In the above case of $\rho_{\max}=10^{-7}$ cm and $R=1$ cm, this can be done if $n\ll10^{21}$.

As was shown (J.1, reference 1),

$$\int_{-\infty}^{+\infty}W^{(1)}(X)dX:\int_{-\infty}^{+\infty}W^{(2)}(X)dX:\cdots\int_{-\infty}^{+\infty}W^{(\nu)}(X)dX=\epsilon:\epsilon^2:\cdots\epsilon^\nu,$$

i.e.,

$$\epsilon\int_{-\infty}^{+\infty}W^{(\nu)}(X)dX=\int_{-\infty}^{+\infty}W^{(\nu+1)}(X)dX.$$

Since the $W^{(\nu)}(X)$ are essentially positive, there must always exist a region of X in which $W^{(\nu+1)}(X)/W^{(\nu)}(X)$ is of the order of magnitude of ϵ.[29] Thus, the ratio of any two neighboring terms in (14), say, of that containing $W^{(\nu+1)}(X)$ to that containing $W^{(\nu)}(X)$,

$$\frac{n-\nu}{\nu+1}\frac{W^{(\nu+1)}(X)}{W^{(\nu)}(X)}\frac{1}{1-\epsilon}$$

is, in this region, of the order of $[(n-\nu)/(\nu+1)]\times[\epsilon/(1-\epsilon)]$. If

$$\frac{n-\nu}{\nu+1}\frac{\epsilon}{1-\epsilon}\ll1,$$

only single transits are relevant and all the terms in (14) but the first two can be neglected. The importance of further terms becomes appreciable at higher densities of gas. The higher the density of the gas, the farther away from the beginning of the sum (14) does the most important term of the sum lie.

III. GENERAL FORM OF $W^{(1)}(X)$

Now we have to proceed to calculate $W^{(1)}(X)$.

The assumption of independence of the movements of the nuclei of a gaseous system consisting of a radiator and n perturbers is equivalent to the assumption that the total eigenfunction of the system ψ_{nucl} can be represented as a product of eigenfunctions $\psi_{\text{nucl }i}$ representing the movements of separate nuclei

$$\psi_{\text{nucl}}=\prod_i^n\psi_{\text{nucl }i},$$

and the corresponding total translational energy E_t as the sum of translational energies E_i of separate nuclei

$$E_t=\sum_{i=1}^n E_i.$$

In this case (14) can be applied to the calculation of intensity distribution within a broadened line if $W^{(1)}(X)$ is calculated first for a single couple of

[28] Strictly speaking this is never the case, the interatomic forces being in principle of infinite range.

[29] It is, however, not generally true that, if the $W^{(\nu)}(X)$ are decreasing functions of $|X|$, $W^{(\nu+1)}(X)$ must decrease more rapidly than $W^{(\nu)}(X)$ does (as sometimes assumed). So, e.g., if $W^{(1)}(X)$ has the form of a dispersion curve (and thus all the $W^{(\nu)}(X)$ have the same form as well but with half width ν times the half width of $W^{(1)}(X)$), $W^{(\nu+1)}(X)/W^{(\nu)}(X)$ is an *increasing* function of $|X|$.

atoms consisting of a radiator and a perturber.[30] In order to make possible the application to our problem of molecular theory as described in paragraph I, we suppose the above couple of atoms to be enclosed in a container of finite volume thus forcing the states of nuclear motion to become discrete and, in addition, making it easier to normalize the corresponding eigenfunctions. Thus (3) or (5) and (6) can be immediately used, the role of vibrational eigenfunctions now being played by nuclear eigenfunctions. These eigenfunctions are solutions of Schrödinger's equation for the two-body problem in relative coordinates r, which result when the motion of the mass center is separated. They are discrete if boundary conditions $\psi_{\text{nucl}}(R)=0$ are imposed at the walls of the container (which it is convenient to regard as a sphere of radius R with radiator at its center). Thus we obtain two sets of nuclear eigenfunctions for two combining electronic states as functions of r. Only the radial eigenfunctions are relevant in our problem (cf. J.1). The shape of this function depends not only upon relative kinetic energy and mutual potential energy of the couple, but upon its angular momentum as well. Let v' and v'' be the radial quantum numbers (the number of nodes of the radial eigenfunction), and l' and l'' the angular momentum (rotational) quantum numbers of the states of nuclear motion in both electronic states respectively. The radial eigenfunctions $\psi_{v'l'}$ and $\psi_{v''l''}$ corresponding to the states with quantum numbers v' and l' (upper electronic state of the radiator) and v'' and l'' (lower electronic state of the radiator) respectively are solutions of Schrödinger equations:

$$\frac{d\psi_{v'l'}}{dr}+\frac{2\mu}{\hbar^2}\left(E_{v'l'}-V'(r)-\hbar^2\frac{l'(l'+1)}{2\mu r^2}\right)\psi_{v'l'}=0 \quad (19)$$

and

$$\frac{d\psi_{v''l''}}{dr}+\frac{2\mu}{\hbar^2}\left(E_{v''l''}-V''(r)-\hbar^2\frac{l''(l''+1)}{2\mu r^2}\right)\psi_{v''l''}=0 \quad (19a)$$

respectively, where μ denotes the reduced mass of the couple, $V'(r)$ and $V''(r)$ the mutual potential energy of the couple of atoms corresponding to the upper and lower electronic state, $E_{v'l'}$ and $E_{v''l''}$ the relative energy values of nuclear motion in quantum states v', l' and v'', l'' which may be found by taking into account the boundary conditions. We need not treat in detail the rotational eigenfunctions, the only effect of which is that in our approximation, only transitions between nuclear motion states $v', l' \leftrightarrow v'', l''$ with unchanged angular momentum $l'=l''$ are allowed. This follows from the orthogonality of rotational eigenfunctions. If instead of the radial eigenfunctions, we substitute the total nuclear eigenfunctions; i.e., $\psi_{vl}\psi_{\text{rot}}$ in the integrals (3) or (6) and integrate over the whole range of variability of respective angles, only those integrals do not vanish for which $l'=l''$.[31] Apart from this "selection rule," the angular momentum comes to light in the centrifugal potential $\hbar^2 l(l+1)/2\mu r^2$ in Eqs. (19) and (19a) and thus in the radial eigenfunctions. The centrifugal potential induces the dependence on l of the matrix elements $D_{v'v''l}$ (cf. (3), (5) and (6)). For very large l's, the eigenfunctions of both sets become practically identical and thus orthogonal. Hence, practically no transitions $v' \leftrightarrow v''$ with $v' \neq v''$ will occur between states with sufficiently large l's. For smaller values of l, the dependence of $D_{v'v''l}$ on l becomes very marked. Classically speaking, the effect on spectral lines produced by collisions depends very markedly on impact parameter. Thus, it is by no means justifiable to assume that all the collisions with impact parameters smaller than a certain "optical collision radius" ρ_0 are equally effective, and those with larger impact parameter are entirely ineffective.

Let us now assume that the couple is in a state v'', l'' (lower electronic state) and consider all the possible transitions from this state v'',

[30] Cf. J.1, reference 1. The applicability of this procedure to the calculations involving multiple collisions is limited to the cases when the mutual potential energy of the radiator and all the perturbers can be represented as a sum of the mutual potential energies of separate perturbers and the radiator. This generally seems to be at best only very roughly the case; the different orientations of angular momenta of the atoms relative to the axis joining the nuclei of the couple lead to different potential curves; these orientations may be disturbed by the presence of additional perturbers.

[31] Cf. J.1, reference 1.

$l''\to v'$, l' (absorption line). In order to obtain the relative intensity distribution in energy scale, we have to multiply $D^2_{v'v''l}$ by the density of nuclear motion energy levels in the upper electronic state $dv'/dE_{v'}$. For sufficiently large R, the energy states are dense enough to be treated v' as a continuous function of $E_{v'}$. The resulting intensity (or frequency) scale is proportional to $D^2_{v'v''l}(dv'/dE_{v'})$, except, however, for $D^2_{v'v''l}$ with $v'=v''$, i.e., for the position ω_0 of the original unperturbed line. In this position there will be always a discontinuity because, obviously, $D_{v'v''l}$ with $v'=v''$ is very much larger than any matrix element with $v'\neq v''$. The chance of an electronic transition without change of translational energy of the nuclei of the couple is very much larger than that with any change; this follows both from the above estimate of ϵ and from considerations on the product of nuclear eigenfunctions in the integral (3). This situation remains practically unchanged by the fact that, strictly speaking, $E_{v'}$ is not quite exactly equal to $E_{v''}$ for $v'=v''$, $E_{v'}$ and $E_{v''}$ being dependent slightly on mutual potential energy of the atoms different in two electronic states under consideration.

We may, instead of considering the case of a particular fixed l, allow the l's to be distributed at random according to a certain partition law $Q(l)$. $Q(l)$, denoting the probability of occurence of a rotational quantum number l, has to be calculated later. That is, if we consider the transitions from the levels with a certain fixed v'' and the l's distributed according to $Q(l)$ to all existing levels v'' with unchanged l's (except that one with $v'=v''$), the probability distribution of the changes of the nuclear motion energy of the couple (in energy scale) becomes:

$$W^{(1)}(X)=W^{(1)}(E_{v'}-E_{v''})$$

$$=\sum_{l=0}^{l_{\max}} Q(l)\frac{D^2_{v'v''l}}{\sum_{v'=1}^{\infty} D^2_{v'v''l}}\frac{dv'}{dE_{v'}}$$

$$\approx\int_0^{l_{\max}} Q(l)\frac{D^2_{v'v''l}}{S}\frac{dv'}{dE_{v'}}dl \quad (20)$$

and correspondingly, for the case of an emission line:

$$W^{(1)}(X)=W^{(1)}(E_{v'}-E_{v''})$$

$$=\sum_{l=0}^{l_{\max}} Q(l)\frac{D^2_{v'v''l}}{S}\frac{dv}{dE}$$

$$\approx\int_0^{l_{\max}} Q(l)\frac{D^2_{v'v''l}}{S}\frac{dv''}{dE_{v''}}dl. \quad (21)$$

The upper limit $l_{\max}$ denotes the largest l occurring in $Q(l)$ or eventually the largest l relevant in our calculations. For very large $l_{\max}$ the sums can be approximately replaced by integrals. The strength

$$S=\sum_{v'=1}^{\infty} D^2_{v'v''l}=\sum_{v''=1}^{\infty} D^2_{v'v''l}$$

of the electronic transition under consideration is put in the denominators of (20) and (21) to secure proper normalization of $W^{(1)}(X)$ as expressing the probability of occurrence of $X=E_{v'}-E_{v''}$. Expressions (20) or (21) substituted in (14) (or (14a)) lead to the intensity distribution normalized so as to give the total intensity of the line equal to unity. Thus, the absolute intensity of $\omega=\omega_0+(X/\hbar)$ will be equal to that given by (14) multiplied by the total intensity of the unperturbed line. For the sake of simplicity we have supposed that the width of the unperturbed line is infinitely small. To obtain the true intensity distribution with full accuracy, we should impose on that calculated in the above way the natural and Doppler distributions. Generally the corrections for these effects can be neglected in the wings of the broadened line. The expressions (20) and (21) may be used for the most exact calculations. They become much simpler if Condon's approximation is considered sufficient (presumably, this will usually be so). Since in this case

$$S=\mathfrak{M}_0^2=\sum_{v'=1}^{\infty} D^2_{v'v''l}=\sum_{v''=1}^{\infty} D^2_{v'v''l}$$

and $D_{v'v''l}=\mathfrak{M}_0 A_{v'v''l}$ [cf. (5) and (6)], (20) and (21) become:

$$W^{(1)}(X)\approx\int_0^{l_{\max}} Q(l)A^2_{v'v''l}\frac{dv'}{dE_{v'}}dl$$

(absorption line), (20a)

and

$$W^{(1)}(X) \approx \int_0^{l_{\max}} Q(l) A^2_{v'v''} \left| \frac{dv''}{dE_{v''}} \right| dl \quad \text{(emission line).} \quad (21a)$$

The calculations of $W^{(1)}(X)$ can be carried out conveniently by the aid of a differential analyzer.[32]

Usually there is more than a single potential curve in each electronic state. Instead of the above simple $W^{(1)}(X)$ one must use then

$$W^{(1)}(X) = a_1 W_1^{(1)}(X) + a_2 W_2^{(1)}(X) + \cdots = \sum_i a_i W_i^{(1)}(X). \quad (22)$$

Here, a_i denotes the relative abundance of transitions between two particular potential curves. a_i must fulfill the condition $\sum_i a_i = 1$. Each $W_i^{(1)}(X)$ must be calculated separately, $D_{v'v''l}$ or $A_{v'v''l}$ being dependent on the shape of different potential curves in both electronic states. The multiplicity of potential curves causes a serious difficulty if multiple encounters come into play, i.e., at higher densities of gas. Equation (22) must not be forgotten while calculations for a particular line and gas mixture are carried out.

For the case $n\epsilon \ll 1$ the intensity distribution far enough from the unperturbed frequency ω_0 of the line, and, in any case, outside the half value width of the natural and Doppler intensity distribution is according to (14) and (22) simply:

$$I(\omega) = nh \sum_i a_i W_i^{(1)}(X) = nh \sum_i a_i W_i^{(1)}(h(\omega_0 - \omega)) = (4/3)\pi R^3 hN \sum_i a_i W_i^{(1)}(h\Delta\omega), \quad (23)$$

with $W_i''(X)$ calculated as indicated above. $Q(l)$ and dv/dE can be calculated easily with sufficient accuracy. Because of difficulties of exact calculation of $D_{v'v''l}$ or even $A_{v'v''l}$, we shall restrict ourselves to calculation of the asymptotic expressions of $A_{v'v''l}$ valid in the case of heavy nuclei with large kinetic energies in a limited spectral region of the broadened line and even then only approximately.

[32] Cf. C.J.P. and J.C., reference 4; the writer had no opportunity of using this method.

IV. CALCULATION OF $Q(l)$

In our case $Q(l)$ is simply proportional to the statistical weight $2l+1$ of the state l:

$$Q(l) = g \cdot (2l+1). \quad (24)$$

The factor g may be evaluated by comparison of (24) with the classical probability distribution of the impact parameters for large l's. The classical value of the impact parameter corresponding to the angular momentum $\hbar[l(l+1)]^{\frac{1}{2}}$ is:

$$\rho = \hbar[l(l+1)/2\mu E]^{\frac{1}{2}}, \quad (25)$$

where μ is the reduced mass of the couple and E its relative translational energy. For large l's, $Q(l)dl \approx Q'(\rho)d\rho$, i.e., is equal to the chance of the occurrence of impact parameter within the limits ρ and $\rho+d\rho$. For the case of a spherical container with radius R the classical calculation gives:

$$Q'(\rho)d\rho = \frac{3}{R^3}(R^2-\rho^2)^{\frac{1}{2}}\rho d\rho,$$

or for the only important case $\rho \ll R$

$$Q'(\rho)d\rho = \frac{3}{R^2}\rho d\rho = \frac{3}{2R^2}d\rho^2. \quad (26)$$

From (25) and (26) we obtain

$$Q'(\rho)d\rho = \frac{3\hbar^2}{4R^2\mu E}(2l+1)dl. \quad (27)$$

Thus[33]

$$Q(l) = \frac{3\hbar^2}{4R^2\mu E}(2l+1). \quad (28)$$

V. THE DENSITY OF TRANSLATIONAL ENERGY LEVELS[34]

The asymptotic solutions of Schrödinger Eqs. (19) and (20) for $r \to \infty$ (i.e., for $V(r) \to 0$ and $\hbar^2 l(l+1)/2\mu r^2 \to 0$) have the form

$$\psi^{(A)}_{\text{nucl } vl}(r) = (2/R)^{\frac{1}{2}} \cos\left[(2\mu E_v)^{\frac{1}{2}} r/\hbar + \delta\right], \quad (29)$$

where $(2/R)^{\frac{1}{2}}$ is the normalization factor securing the condition

$$\int_0^R \psi^{(A)2}_{\text{nucl } vl}(r)dr = 1$$

[33] In the previous papers the angular momentum was treated classically.

[34] Cf. J.1, reference 1.

and δ a phase constant. Imposing the boundary condition $\psi^{(A)}_{\text{nucl } vl}(R)=0$ on (29) we have:

$$\frac{(2\mu E_v)^{\frac{1}{2}}}{\hbar}R+\delta=\frac{2v+1}{2}\pi, \tag{30}$$

(v integral) and hence the density of translational energy levels is given by

$$\frac{dv}{dE_v}=\frac{\mu^{\frac{1}{2}}R}{\pi\hbar(2E_v)^{\frac{1}{2}}}=\frac{\mu R}{\pi\hbar p_v(\infty)}, \tag{31}$$

where $p_v(\infty)=p_{v\,r=\infty}(r)$ is the value of the radial component of the relative momentum of the couple for $r\to\infty$.

VI. APPROXIMATE CALCULATION OF $A_{v'v''l}$ BY MEANS OF WENTZEL-KRAMERS-BRILLOUIN EIGENFUNCTIONS

In order to calculate approximately the integral (6), we shall apply the solutions of Schrödinger's Eqs. (19) and (19a) in the form of the Wentzel-Kramers-Brillouin approximation. They can be written as follows:

$$\psi_{vl}=\left(\frac{2}{R}\right)^{\frac{1}{2}}\left[\frac{2\mu E_{vl}}{2\mu(E_{vl}-V(r))-\hbar^2\frac{l(l+1)}{r^2}}\right]^{\frac{1}{4}}$$

$$\times\cos\left\{\frac{1}{\hbar}\int_{r_0}^{r}\left[2\mu(E_{v_i}-V(r))-\hbar^2\frac{l(l+1)}{r^2}\right]^{\frac{1}{2}}dr+\delta\right\}=\left(\frac{2p(\infty)}{Rp(r)}\right)^{\frac{1}{2}}\cos\left[\frac{1}{\hbar}\int_{r_0}^{r}p(r)dr+\delta\right], \tag{32}$$

where $p(r)=[2\mu(E_{vl}-V(r))-\hbar^2l(l+1)/r^2]^{\frac{1}{2}}$ is the radial component of relative momentum of the couple with reduced mass μ and angular momentum $\hbar[l(l+1)]^{\frac{1}{2}}$. The normalization factor $(2p(\infty)/R)^{\frac{1}{2}}$ follows from the asymptotic form (29) of the solution. Equation (32) is valid only for $r>r_t$ (r_t the distance of closest approach or classical turning point has to be found from the equation $p(r_t)=0$) and fails in the region of r_t. We refrain temporarily from discussion of the phase constant δ (δ depends on the lower limit of the integral involved in (32) for which we have put r_t).

The integral (6) with eigenfunctions (32) becomes:

$$A_{v'v''l}\approx\frac{2}{R}\int_0^R\left\{\left(\frac{p'(\infty)}{p'(r)}\right)^{\frac{1}{2}}\cos\left[\int_{r_t}^{r}\frac{p'(r)}{\hbar}dr+\delta'\right]\left(\frac{p''(\infty)}{p''(r)}\right)^{\frac{1}{2}}\cos\left[\int_{r_t}^{r}\frac{p''(r)}{\hbar}dr+\delta''\right]\right\}dr$$

$$=\frac{1}{R}\int_{r_t}^{R}\left(\frac{p'(\infty)p''(\infty)}{p'(r)p''(r)}\right)^{\frac{1}{2}}\left[\cos\left(\int_{r_t}^{r}\frac{p'(r)-p''(r)}{\hbar}dr+\delta'-\delta''\right)\right.$$

$$\left.+\cos\left(\int_{r_t}^{r}\frac{p'(r)+p''(r)}{\hbar}dr+\delta'+\delta''\right)\right]dr. \tag{33}$$

The second cosine term is a very rapidly oscillating function of r and thus its contribution to the value of the integral (33) can be neglected. As to the first cosine term, the most important region of r is that in the neighborhood of $r=r_c$ for which $p'(r)=p''(r)$. It contributes most to the value of the integral (33) because the oscillation of the first cosine term becomes slowest there (apart, presumably, from the region of the classical turning point, which, however, we are compelled to omit here). r_c is just that distance in which, according to the classical form of F.C.P., the transition $p'(r_c)\leftrightarrow p''(r_c)$ takes place. Hence, the correspondence between the classical and quantum-mechanical form of F.C.P. becomes apparent. The square of the integral (33) ($A^2_{v'v''l}$) is the probability of change of translational energy by $X=E_{v'}-E_{v''}$ equal to that resulting from the classical F.C.P. for the transition in r_c:

$$X=V'(r_c)-V''(r_c)=\hbar(\omega_0-\omega)=\hbar\Delta\omega. \tag{34}$$

Neglecting the second term in (33) and developing the integrand involved in the first term in series

in the neighborhood of r_c we obtain:

$$A_{v'v''l}=\frac{1}{R}\int_{r_l}^{R}\left[\frac{p'(\infty)p''(\infty)}{p'(r)p''(r)}\right]^{\frac{1}{2}}\cos\left\{\frac{1}{\hbar}\int_{r_l}^{r_c}(p'(r)-p''(r))dr+\delta'-\delta''\right.$$
$$\left.+\frac{1}{\hbar}\int_{r_c}^{r}\left[p'(r_c)-p''(r_c)+\left[\frac{d}{dr}(p'(r)-p''(r))\right]_{r=r_c}(r-r_c)+\cdots\right]dr\right\}dr. \quad (35)$$

Putting $r-r_c=\xi$ and neglecting all the terms of the series but the two first, we obtain instead of (35) (if the equality $p'(r_c)=p''(r_c)=p(r_c)$ is taken into account and the factor of the cosine term brought before the sign of integration and its value at $r=r_c$ attributed to it):[35]

$$A_{v'v''l}=\frac{(p'(\infty)p''(\infty))^{\frac{1}{2}}}{Rp(r_c)}\int_{-\infty}^{+\infty}\cos(\alpha\pm\beta\xi^2)d\xi=\frac{(p'(\infty)p''(\infty))^{\frac{1}{2}}}{Rp(r_c)}\left(\frac{\pi}{|\beta|}\right)^{\frac{1}{2}}\cos\left(\alpha\pm\frac{\pi}{4}\right), \quad (36)$$

where

$$\alpha=\frac{1}{\hbar}\int_{r_0}^{r_c}(p'(r)-p''(r))dr+\delta'-\delta''$$

and

$$\beta=\frac{1}{2\hbar}\left[\frac{d}{dr}(p'(r)-p''(r))\right]_{r=r_c}=\frac{1}{2\hbar}\left[\frac{-\mu\dfrac{dV'(r)}{dr}}{\left[2\mu(E_{v'l}-V'(r))-\hbar^2\dfrac{l(l+1)}{r^2}\right]^{\frac{1}{2}}}\right.$$
$$\left.-\frac{-\mu\dfrac{dV''(r)}{dr}}{\left[2\mu(E_{v''l}-V''(r))-\hbar^2\dfrac{l(l+1)}{r^2}\right]^{\frac{1}{2}}}\right]_{r=r_t}=-\frac{1}{2\hbar}\frac{\mu\left(\dfrac{dU(r)}{dr}\right)_{r=r_c}}{p(r_c)}, \quad (37)$$

with $U(r)=X=V'(r)-V''(r)$ (cf. Eq. (34)). (The restrictions of applicability of (37), mentioned in J.3, are groundless). Thus (34) becomes:

$$A_{v'v''l}=A_X=\frac{1}{R}\left(\frac{p'(\infty)p''(\infty)2\pi\hbar}{p(r_c)\mu|dU/dr|_{r=r_c}}\right)^{\frac{1}{2}}\cos\left(\alpha\pm\frac{\pi}{4}\right)=\frac{1}{R}\left(\frac{p'(\infty)p''(\infty)2\pi\hbar}{p(r_c)\mu|dX/dr|_{r=r_c}}\right)^{\frac{1}{2}}\cos\left(\alpha\pm\frac{\pi}{4}\right). \quad (38)$$

The limitations of applicability of this approximate formula will be discussed in paragraph IX.

VII. ASYMPTOTIC INTENSITY DISTRIBUTION DUE TO THE SINGLE ENCOUNTERS

We now proceed to calculate the $W^{(1)}(X)$. From (20a), (28), (31) and (38) we obtain for the case of an absorption line:

$$W^{(1)}(X)=\int_0^{l_1}\frac{3}{4}\frac{\hbar^2}{\mu E_{v''}R^2}(2l+1)\frac{\mu Rp'(\infty)p''(\infty)}{\pi\hbar p'(\infty)R^2p(r_c)}\frac{2\pi\hbar}{\mu|dX/dr|_{r=r_c}}\cos^2\left(\alpha\pm\frac{\pi}{4}\right)dl+\zeta(X,l_t)$$
$$=\frac{3}{4}\frac{\hbar^2}{\mu E_{v''}R^3|dX/dr|_{r=r_c}}\int_0^{l_1}\frac{(2l+1)2\cos^2\left(\alpha\pm\frac{\pi}{4}\right)}{\left(1-\dfrac{V''(r_c)}{E_{v''l}}-\hbar^2\dfrac{l(l+1)}{2\mu E_{v''l}r_c^2}\right)^{\frac{1}{2}}}dl+\zeta(X,l_t)$$
$$=\frac{3}{2}\frac{r_c^2\left(1-\dfrac{V''(r_c)}{E_{v''l}}\right)^{\frac{1}{2}}}{l_t(l_t+1)R^3|dX/dr|_{r=r_c}}\int_0^{l_1}\frac{(2l+1)2\cos^2\left(\alpha\pm\frac{\pi}{4}\right)}{\left(1-\dfrac{l(l+1)}{l_t(l_t+1)}\right)^{\frac{1}{2}}}dl+\zeta(X,l_t), \quad (39)$$

[35] The treatment of $p'(r)$ and $p''(r)$ in the factor of the cosine term as constants equal $p(r_c)$, i.e., equal to their value in the most important region of integration, constitutes a crude approximation which must not be used if r_c does not lie sufficiently far away from the turning point r_t.

where l_t has to be found from

$$2\mu(E_{v''l}-V''(r_c))-\hbar^2\frac{l_t(l_t+1)}{r^2}=p''^2(r_c)=0;$$

thus $l=l_t$ is the value of l for which $r_c=r_t$, i.e., the classical turning point. For the upper limit of integration we have put a provisionally unspecified l_1. One could conjecture that the integration should be extended at least over all $l\leqq l_t$ corresponding to all collisions with impact parameters ρ smaller than r_c (i.e., smaller than the distance in which according to classical F.C.P. the transition actually takes place) thus neglecting the region of r outside the classical range of motion. Because of the failure of W.K.B. approximation in the region of $l=l_t$ it is safer to put $l_1<l_t$ as the upper limit of integration and add a correction term $\zeta(X, l_t)$ (depending on X and l_t) which order of magnitude we shall estimate very roughly later. The more accurate calculations involving eigenfunctions valid in the regions of turning points and outside the classical range of motion would be very tedious unless carried out by the aid of the differential analyzer.

A further simplification arises if $\cos(\alpha\pm\pi/4)$ is a sufficiently rapidly oscillating function[36] of l. Apart from l, α depends on $E_{v'}$ and $E_{v''}$. In this case $\cos^2(\alpha\pm\pi/4)$ can be replaced by its average value $\langle\cos^2(\alpha\pm\pi/4)\rangle_{Av}=\frac{1}{2}$. Equation (39) becomes then:

$$W^{(1)}(X)=\frac{3}{2}\frac{r_c^2\left(1-\frac{V''(r_c)}{E_{v''}}\right)^{\frac{1}{2}}}{l_t(l_t+1)R^3|dX/dr|_{r=r_c}}\int_0^{l_1}\frac{2l+1}{\left[1-\frac{l(l+1)}{l_t(l_t+1)}\right]^{\frac{1}{2}}}dl+\zeta(X,l_t)$$

$$=\frac{3r^2}{R^3|dX/dr|_{r=r_c}}\left(1-\frac{V''(r_c)}{E_{v''}}\right)^{\frac{1}{2}}\left[1-\left(1-\frac{l_1(l_1+1)}{l_t(l_t+1)}\right)^{\frac{1}{2}}\right]+\zeta(X,l_t), \quad (40)$$

and correspondingly for the case of an emission line

$$W^{(1)}(X)=\frac{3r_c^2}{R^3|dX/dr|_{r=r_c}}\left(1-\frac{V'(r_c)}{E_{v'}}\right)^{\frac{1}{2}}\left[1-\left(1-\frac{l_1(l_1+1)}{l_t(l_t+1)}\right)^{\frac{1}{2}}\right]+\zeta(X,l_t). \quad (40a)$$

The asymptotic forms $W_A^{(1)}(X)$ of $W^{(1)}(X)$ are

$$W_A^{(1)}(X)=\frac{3r_c^2(1-V''(r_c)/E_{v''})^{\frac{1}{2}}}{R^3|dX/dr|_{r=r_c}}\ \text{(absorption line)}, \quad (41)$$

and

$$W_A^{(1)}(X)=\frac{3r_c^2(1-V'(r_c)/E_{v'})^{\frac{1}{2}}}{R^3|dX/dr|_{r=r_c}}\ \text{(emission line)}. \quad (41a)$$

Before we proceed to discuss (40) and (40a), we shall show that (41) and (41a) lead in the case of $V(r_c)/E_v\ll 1$ to Kuhn's intensity distribution derived from the classical form of F.C.P.

VIII. THE ASYMPTOTIC INTENSITY DISTRIBUTION

According to (34)

$$X=V'(r_c)-V''(r_c)=\hbar(\omega-\omega_0)=\hbar\Delta\omega,$$

where ω is the frequency resulting from the classical F.C.P. Hence, one can get immediately the asymptotic form of the intensity distribution. Since $\Delta\omega$ is a function of r_c, r_c can be represented as a function of $\Delta\omega$, say $r_c=f(\Delta\omega)$. Substituting $X=\hbar(\Delta\omega)$ and $r_c=f(\Delta\omega)$ in (41) or (41a), and $n=(4/3)\pi R^3N$, where N denotes the number of perturbers per 1 cm³, in (23), we obtain from (23) and (41) or (41a):

$$I_A(\omega)=\sum_i a_i 4\pi N f^2(\Delta\omega)\frac{\left(1-\frac{V''(r_c)}{E_{v''}}\right)^{\frac{1}{2}}}{|d\Delta\omega/dr_c|}$$

(absorption line) (42)

[36] The necessary condition is, that $|X|=|E_{v'}-E_{v''}|$ is sufficiently large, or, in other words, the region of frequencies under consideration far enough from the center of the unperturbed line.

TABLE I. Values of l_t and $\varkappa$ corresponding to $r_c=3.3$ AU for Hg+A and Hg+He.

Perturber \ T	1000°K		300°K	
	l_t	$\varkappa$	l_t	$\varkappa$
A	158	2.7	86	2.3
He	25	1.5	14	1.2

and

$$I_A(\omega)=\sum_i a_i 4\pi N f^2(\Delta\omega)\frac{\left(1-\dfrac{V''(r_c)}{E_{v''}}\right)^{\frac{1}{2}}}{|d\Delta\omega/dr_c|} \quad \text{(emission line).} \quad (42a)$$

$I_A(\omega)$ should be, strictly speaking, averaged over all E occurring in the gas under consideration, but since usually the factor in brackets constitutes a small correction only (at least in a certain range of frequencies), we shall put simply $E=\frac{3}{2}kT$. $I_A(\omega)$ depends on the temperature only through this factor and the dependence is usually only very slight. This dependence may, however, become much more prominent in the region of the line arising from transitions in the repulsive branches of potential curves and particularly at the points at which $V\approx E$. Apart from the above factor, (42) and (42a) are identical with the equation constituting the starting point of the statistical theories.

For the case of two single potential curves of the form

$$V'(r_c)=-C'/r_c^{\eta} \quad \text{and} \quad V''(r_c)=-C''/r_c^{\eta} \quad (43)$$

we have

$$\Delta\omega=\frac{1}{\hbar}\frac{C'-C''}{r_c^{\eta}}=\frac{K}{r_c^{\eta}}, \quad r_c=f(\Delta\omega)=\left(\frac{K}{\Delta\omega}\right)^{1/\eta}$$

and

$$V''(r_c)=\frac{C''}{K}\Delta\omega;$$

thus (42) becomes:

$$I_A(\omega)=\frac{4\pi NK^{3/\eta}}{\eta(\Delta\omega)^{(\eta+3)/\eta}}\left(1+\frac{2C''\Delta\omega}{3KkT}\right)^{\frac{1}{2}}, \quad (44)$$

which is identical with Kuhn's[37] distribution for $2c''\Delta\omega/3KkT\ll 1$.

[37] The intensity distribution derived in J.3 (reference 1) differs from Kuhn's formula by a factor two; it constitutes, however, a worse approximation than the present one.

Thus, the intensity distribution resulting from the primitive form of F.C.P. has found its justification on the basis of the quantum-mechanical theory.

IX. LIMITATIONS OF THE APPLICABILITY OF THE ASYMPTOTIC INTENSITY DISTRIBUTION

The main cause of inaccuracy of the asymptotic intensity distribution is the failure of the W.K.B. approximation in the region of the upper limit of the integration with respect to l in (40) and (40a). The condition of validity of the W.K.B. approximation is:

$$dp(r)/dr\ll p^2(r)/\hbar, \quad (45)$$

or

$$\hbar^2\frac{l(l+1)}{r^3}-\mu\frac{dV}{dr}\ll\frac{1}{\hbar}\left[2\mu(E-V)-\hbar^2\frac{l(l+1)}{r^2}\right]^{\frac{1}{2}}. \quad (46)$$

Let us consider the case

$$|\hbar^2 l(l+1)/r^3|\gg|\mu(dV/dr)|.$$

Instead of (46) we have then:

$$\hbar^2[l(l+1)]^{\frac{1}{2}}\ll 2\mu(E-V)r^2-\hbar^2 l(l+1). \quad (47)$$

Obviously (47) can be satisfied only by $l<l_t$, since the right side vanishes for $l=l_t$ and the left side is always positive. Considering $r=r_c$ as fixed, let us develop the right side of (47) in series in the neighborhood of l_t. Putting $l_t-l=\Delta l$ and neglecting all the terms but the first two, we have

$$\hbar^2[l(l+1)]^{\frac{1}{2}}\ll(2l_t+1)\Delta l, \quad (48)$$

since the first term of the series vanishes for $l=l_t$. Hence,

$$\Delta l\gg\frac{[l_t(l_t+1)]^{\frac{1}{2}}}{2l_t+1}=\varkappa(l_t). \quad (49)$$

Since (39)–(41a) are derived by use of W.K.B. approximation, the extension of integration involved there beyond the limit $l_1=l_t-\Delta l$ appears unjustified. Unfortunately, (49) gives no information how much larger Δl must be than $\varkappa(l_t)$ in order to obtain the desired accuracy and how large is the error committed. Should we assume that $\Delta l=10\varkappa(l_t)$ secures a sufficient margin of

The second term in brackets is positive if the initial state corresponds to an attraction potential curve; otherwise it is negative.

safety, Δl would become 18 for $l_t=100$ and 11 for $l_t=10$. Table I is given to illustrate the conditions in the case of Hg.

Thus it is clear that the asymptotic distribution (42) cannot be applied to the cases of light perturbers (or radiators or both) such as H_2 or He (and still more in the case of electrons as perturbers). Its application to the heavy atoms still involves a considerable amount of uncertainty, which may be very roughly estimated.

Presumably, $W_A^{(1)}(X)$ is always larger than would be the true $W^{(1)}(X)$, since $W_A^{(1)}(X)$ is obtained by extension of the integration involved in (41) or (41a) up to the region of $l=l_t$, where the W.K.B. eigenfunctions and thus $A^2_{v'v''l}$ become infinite. This could never be the case if exact eigenfunctions, which must be finite everywhere, were used; moreover, obviously, the true value of $A^2_{v'v''l}$ can never exceed unity and for $X\neq 0$ must be actually $A^2_{v'v''l}\ll 1$. In order to get an idea, if not of the error itself involved in $I_A(\omega)$ but, at least, of the order of magnitude of the proportion of $I_A(\omega)$ which may be reasonably considered as uncertain we may proceed as follows. We assume that we can obtain the right order of magnitude of $\zeta(X, l_t)$ (cf. (40)) if we suppose that in the region $l_1 \leqq l \leqq l_t$ the value of $A^2_{v'v''l}$ remains constant and equal to that at l_1. That is, l in the denominator of the integrand in (40) may have the value $l=l_1$ in this whole region. We now carry out the integration involved in the first term between the above limits (l_1, l_t) under this assumption. This procedure may lead to a value of $W_A^{(1)}(X)$ which is too small since the true $W^{(1)}(X)$ grows probably when l increases from l_1 to l_t. We thus obtain:

$$\zeta(X, l_t)=O\left[\tfrac{1}{2}W_A^{(1)}(X)\left(1-\frac{l_1(l_1+1)}{l_t(l_t+1)}\right)^{\frac{1}{2}}\right]. \quad (50)$$

Now

$$\frac{l_1(l_1+1)}{l_t(l_t+1)}=\frac{(l_t-\Delta l)(l_t-\Delta l+1)}{l_t(l_t+1)} \approx 1-\frac{(2l_t+1)\Delta l}{l_t(l_t+1)}. \quad (51)$$

Putting $\Delta l=b\kappa(l_t)$, where the factor $b>1$ may be chosen large enough to give a sufficient margin of safety, we obtain from (40), (49)–(51)

$$W^{(1)}(X)=W_A^{(1)}(X)\left[1-O\left(\frac{1}{2}\frac{b}{[l_t(l_t+1)]^{\frac{1}{2}}}\right)\right], \quad (52)$$

and thus

$$I(\omega)=I_A(\omega)\left[1-O\left(\frac{1}{2}\frac{b}{[l_t(l_t+1)]^{\frac{1}{2}}}\right)\right]. \quad (53)$$

The term $b/2[l_t(l_t+1)]^{\frac{1}{2}}$ represents the presumed order of magnitude of the proportion of $I_A(\omega)$ which may be considered as uncertain. Its dependence on l_t is rather slight, and thus it does not influence considerably the *slope* of the intensity curve. It vanishes for $l_t\to\infty$, and thus the asymptotic distribution becomes equal to the true one for $l_t=\infty$; nevertheless, even for Hg+A at 1000°K (large l's) it reaches 0.4 for $r_c=3.3$A if value $b=10$ is assumed. Possibly our estimate is overpessimistic (as the experimental results seem to indicate), but until more exact calculations are carried out, there is no reason to be more optimistic. Certainly a still larger degree of uncertainty is involved in the results of all theories describing the nuclear movements classically.

The second source of error which may be discussed here is the approximate computation of integral (36). We therefore extended the limits of integration from $-\infty$ up to $+\infty$ (instead of O and R). This may be justified only in the case when the phase of $\cos(\alpha+\beta\xi)$ grows rapidly enough with ξ; in any case it is necessary that the phase should increase by at least π while ξ grows from 0 to r_c. Thus, the necessary condition for the applicability of the above procedure is that $|\beta r_c^2|>\pi$ or

$$r_c>\left(\frac{2\pi hp(r_c)}{\mu|dX/dr|_{r=r_c}}\right)^{\frac{1}{2}}. \quad (54)$$

For $|X|=hK/r^\eta$, this becomes

$$r_c<\left(\frac{\eta K\mu}{2\pi p(r_c)}\right)^{1/(\eta-1)}. \quad (55)$$

Expression (55) shows that our approximation ceases to be valid for large r_c, i.e., for the region of the center of the line. In the case of Hg+A and $T=1000$°K, (55) leads to the restriction of the asymptotic distribution to the frequencies corresponding to the transitions in $r_c<6.4\times10^{-8}$ cm in agreement with experimental results of

Kuhn.[38] For $Hg+H_2$ at the same temperature $r_c<2.1\times10^{-8}$ cm.

One could suppose that for very large r_c (large l's) the perturbation theory could be successfully applied[39] in order to obtain the intensity distribution of the central part of the broadened line, but, presumably, sufficiently accurate calculations by this method would be as tedious as those carried out by means of (20) and (21) or (20a) and (21a) and certainly less accurate.

[38] K., reference 10.
[39] J.2, reference 1.

The shift of the maximum of the intensity is not considered here. It would result from (14) for high densities of perturbers if calculations of particular cases involving the effect of multiple encounters were carried out. Apart from this, a shift may also be caused by the displacement of translational motion energy levels due to the perturbations of these levels by mutual potential energy of the radiator and the perturbers. The last effect, however, is not included in our approximation.

PHYSICAL REVIEW VOLUME 68, NUMBERS 3 AND 4 AUGUST 1 AND 15, 1945

A Generalization of the Dielectric Ellipsoid Problem

R. CLARK JONES
Polaroid Corporation, Cambridge, Massachusetts

(Received June 18, 1945)

The classical problem of the dielectric ellipsoid involves the determination of the field within a homogeneous, isotropic, dielectric ellipsoid when it is placed in a uniform electric field. In the present generalization, both the ellipsoid and the medium in which it is placed, although still homogeneous, are anisotropic and also possess conductivities which are anisotropic. The principal axes of the ellipsoid, of the two dielectric tensors, and of the two conductivity tensors, may all be differently oriented. The external field, although uniform in space, varies sinusoidally with time. The condition specified in the last sentence is consistent with the electromagnetic field equations only in a region whose maximum dimension is small compared with $\lambda/2\pi$ where λ is the wave-length which corresponds to the frequency in question. Thus the solution given here is restricted by the condition that the maximum dimension of the ellipsoid must be small compared with $\lambda/2\pi$.

INTRODUCTION

IN the application to practical problems of Wiener's general theory[1] of the electrical and optical properties of heterogeneous materials, the writer has found it desirable to have the solution of a generalization of the dielectric ellipsoid problem. The solution of this generalized problem is presented in this paper.

The classical problem of the dielectric ellipsoid[2] involves finding the field within a homogeneous, isotropic, dielectric ellipsoid when the ellipsoid is placed in a uniform electric field. In the present generalization, the ellipsoid is anisotropic and has a finite electric conductivity, and the medium in which it is imbedded is likewise anisotropic and conducting. Furthermore, the electric field, which is uniform except for the disturbance produced by the presence of the ellipsoid, varies sinusoidally with time. The conditions that the electric field be uniform in space and that it vary sinusoidally with time are evidently inconsistent with the electromagnetic field equations, but the conditions may be satisfied to any desired degree of approximation by making the dimensions of the ellipsoid sufficiently small compared with the wave-length which corresponds to the frequency in question. Accordingly, the solution obtained here holds only for the case in which the maximum dimension of the ellipsoid is small compared with c/ω where c is the velocity

[1] Otto Wiener, Abhandl. d. Sächs. Ges. d. Wiss. **32**, 509–604 (1912).
[2] J. A. Stratton, *Electromagnetic Theory* (McGraw-Hill Book Company, Inc., New York, 1941), pp. 211–213.

of light, and ω is the angular frequency of the electric field.

A solution which does not involve the limitation described in the last sentence has been obtained[3] for the scattering of plane waves by a dielectric sphere which is isotropic and which has a finite conductivity.

STATEMENT OF THE PROBLEM

The problem to be solved is as follows: In a universe filled with a homogeneous material described by a dielectric tensor[4] ϵ_2 and a conductivity tensor σ_2, there exists a uniform electric field $\mathbf{E}_2 e^{i\omega t}$ which varies sinusoidally with time at the radian frequency ω. Now suppose that an ellipsoidal cavity be cut from the material, and that the cavity be filled with a second homogeneous material whose dielectric tensor is ϵ_1 and whose conductivity tensor is σ_1. The principal axes of ϵ_1, ϵ_2, σ_1, σ_2 and of the ellipsoid may all be differently oriented.

The problem is the determination of the electric field within the ellipsoid as a function of the frequency, of the shape and orientation of the ellipsoid, and of the constitutive tensors ϵ_1, ϵ_2, σ_1, and σ_2.

METHOD OF SOLUTION

A solution will first be obtained for the simpler case in which the external medium is a vacuum. The solution for the more general case may then be obtained by an extension of the principle that any solution of an electrostatic problem depends only on the ratios of the dielectric constants and not on their absolute values.

The solution of the simpler problem involves the provisional assumption that the field within the ellipsoid is uniform, and the subsequent proof that this assumption leads to a consistent solution of the problem.

The assumed uniform field produces a polarization which is in phase with the field, as a consequence of the dielectric polarizability of the material. Another type of polarization which lags ninety degrees behind the field is also produced, as the result of the accumulation of free charge on the surface of the ellipsoid; the transport of free charge to the surface is due to the electrical conductivity of the material. The electric field caused by these polarizations may be calculated from the classical solution for the gravitational potential within a homogeneous ellipsoid. The total electric field within the ellipsoid is then the sum of the fields caused by the two separate kinds of polarization and the external field. Taken together with the constitutive relations, the relation stated in the last sentence leads directly to the solution of the problem when the external medium is a vacuum.

The following section contains a brief derivation of the electric field produced by a uniformly polarized ellipsoid. The result of this derivation is needed in the solution of the main problem, which is contained in the section which follows the next one.

ELECTRIC FIELD PRODUCED BY A UNIFORMLY POLARIZED ELLIPSOID

The gravitational or electrostatic potential Ω at an inner point of an ellipsoid of uniform mass or charge density ρ was shown by Dirichlet[5] to be given by:

$$\Omega = -\rho(A_x x^2 + A_y y^2 + A_z z^2), \tag{1}$$

where

$$A_x = \pi abc \int_0^\infty \frac{d\theta}{(a^2+\theta)\Delta}, \tag{2}$$

$$A_y = \pi abc \int_0^\infty \frac{d\theta}{(b^2+\theta)\Delta}, \tag{3}$$

$$A_z = \pi abc \int_0^\infty \frac{d\theta}{(c^2+\theta)\Delta}, \tag{4}$$

$$\Delta = \{(a^2+\theta)(b^2+\theta)(c^2+\theta)\}^{\frac{1}{2}}. \tag{5}$$

The origin of coordinates lies at the center of the ellipsoid, and the semi-axes a, b, and c lie along the x, y, and z coordinate axes, respectively. The relations (1)–(5) are derived by Kellogg[6] with the use of ellipsoidal coordinates and are derived by Meyer[7] by straightforward integration, using ordinary Cartesian coordinates.

[3] M. Born, *Die Optik* (Verlagsbuchhandlung Julius Springer, Berlin, 1933), pp. 274–285.
[4] Reference 2, p. 11.
[5] P. G. Dirichlet, J. f. Math. **32**, 80 (1846); *Werke*, Vol. 2, p. 11.
[6] O. D. Kellogg, *Potential Theory*, (Verlagsbuchhandlung Julius Springer, Berlin, 1929), pp. 192–194.
[7] G. F. Meyer, *Theorie der Bestimmten Integralle* (B. G. Teubner, Leipzig 1871), pp. 521–525, 531–547.

It follows directly from the definitions of A_x, A_y, and A_z that

$$A_x+A_y+A_z=2\pi. \tag{6}$$

When the semi-axes a, b, and c are all different, the quantities A_x, A_y, and A_z may be expressed in terms of incomplete elliptic integrals of the first and second kinds.[8] If, however, two of the axes are equal, so that the ellipsoid becomes a prolate or oblate spheroid, then these quantities may be expressed in terms of elementary functions.[9]

The following cases are of special interest:
Long thin circular rod ($a\gg b=c$):

$$A_x=0, \quad A_y=A_z=\pi.$$

Sphere ($a=b=c$):

$$A_x=A_y=A_z=2\pi/3.$$

Thin circular disk ($a\ll b=c$):

$$A_x=2\pi, \quad A_y=A_z=0.$$

Equation (1) represents the potential at an inner point of an ellipsoid which is uniformly charged throughout its volume. The potential at an inner point of a uniformly polarized ellipsoid may be obtained by taking two similar and parallel ellipsoids of exactly opposite charge densities, letting them interpenetrate so that the distance between their centers is small compared with the dimensions of the ellipsoid, and then taking the limit as the distance of separation vanishes and the charge density ρ of the positive ellipsoid becomes infinite, the product remaining finite. If $\mathbf{r}$ is the displacement of the positively charged ellipsoid from the negatively charged one, one finds, holding $\mathbf{P}=\rho\mathbf{r}$ constant and letting $\mathbf{r}$ approach zero, the following expression for the potential Ω_P at an inner point of an ellipsoid with a uniform polarization $\mathbf{P}$:

$$\begin{aligned}\Omega_P&=-\mathbf{r}\cdot\operatorname{grad}\Omega\\&=2xA_xP_x+2yA_yP_y+2zA_zP_z.\end{aligned} \tag{7}$$

The electric field at an inner point of a uniformly polarized ellipsoid may now be obtained by differentiation:

$$\begin{aligned}\mathbf{E}_P&=-\operatorname{grad}\Omega_P,\\E_{Px}&=-2A_xP_x,\\E_{Py}&=-2A_yP_y,\\E_{Pz}&=-2A_zP_z.\end{aligned} \tag{8}$$

Or, more generally in any Cartesian coordinate system,

$$\mathbf{E}_P=-2A\mathbf{P}, \tag{9}$$

where A is the tensor which has the form

$$A\equiv\begin{pmatrix}A_x & 0 & 0\\0 & A_y & 0\\0 & 0 & A_z\end{pmatrix}, \tag{10}$$

when the coordinate axes are parallel with the axes of the ellipsoid.

In the following development, it is more convenient to use the tensor B, which is equal to A divided by 2π:

$$B\equiv A/2\pi. \tag{11}$$

Equation (9) thus becomes

$$\mathbf{E}_P=-4\pi B\mathbf{P}. \tag{12}$$

With the assistance of this last equation, the solution of the main problem will now be resumed.

DETAILED SOLUTION WHEN THE EXTERNAL MEDIUM IS A VACUUM

Let us assume provisionally that the field within the ellipsoid is uniform and is given by the expression $\mathbf{E}_1e^{i\omega t}$. The exponential time factor $e^{i\omega t}$ will be omitted in the following expressions. The electric field $\mathbf{E}_1$ will produce a polarization of the ellipsoid which is given by

$$\mathbf{P}_\epsilon=\frac{\epsilon_1-1}{4\pi}\mathbf{E}_1. \tag{13}$$

The electric field will also produce an electric current density given by

$$\mathbf{i}=\sigma_1\mathbf{E}_1. \tag{14}$$

This current will bring about a transport of electric charge to the surface of the ellipsoid at the time rate $|\mathbf{i}|$ units of charge per second per unit area perpendicular to the vector $\mathbf{i}$. The actual amount of charge present at any time is thus given by $\int|\mathbf{i}|dt$, in units of charge per unit area perpendicular to $\mathbf{i}$. But by a well-

[8] Reference 6, p. 196; Reference 7, pp. 540–543.
[9] Reference 2, p. 214.

known theorem[10] of electrostatics, this charge distribution is equivalent to a polarization of the ellipsoid given by

$$\mathbf{P}_\sigma = \int i dt = \sigma_1 \mathbf{E}_1 / i\omega. \tag{15}$$

The total polarization of the ellipsoid is thus

$$\mathbf{P} = \mathbf{P}_\varepsilon + \mathbf{P}_\sigma = \frac{\varepsilon_1 - 1}{4\pi} \mathbf{E}_1, \tag{16}$$

where

$$\varepsilon \equiv \varepsilon + \frac{4\pi\sigma}{i\omega}. \tag{17}$$

The tensor ε is the complex dielectric tensor as usually defined.

By Eq. (12) of the last section, the electric field which is produced by this polarization is

$$\mathbf{E}_P = -4\pi \boldsymbol{B}\mathbf{P} = -\boldsymbol{B}(\varepsilon_1 - 1)\mathbf{E}_1. \tag{18}$$

The total field $\mathbf{E}_1$ within the ellipsoid is equal to the sum of the field $\mathbf{E}_P$ which is due to the polarization of the ellipsoid and the uniform external field $\mathbf{E}_2$. Thus,

$$\begin{aligned} \mathbf{E}_1 &= \mathbf{E}_2 + \mathbf{E}_P \\ &= \mathbf{E}_2 - \boldsymbol{B}(\varepsilon_1 - 1)\mathbf{E}_1, \end{aligned} \tag{19}$$

or

$$\mathbf{E}_2 = [1 + \boldsymbol{B}(\varepsilon_1 - 1)]\mathbf{E}_1. \tag{20}$$

This is the desired relation between the field $\mathbf{E}_1$ within the ellipsoid and the uniform external field $\mathbf{E}_2$.

It will be noted that the provisional assumption of a uniform electric field within the ellipsoid led to a total polarization, the electric field of which was uniform. The combination of the polarization field and the external uniform field is, therefore, also uniform, and the provisional assumption is thereby confirmed.

A homogeneous ellipsoid is the most general homogeneous solid which becomes uniformly polarized when it is placed in a uniform field.

DETAILED SOLUTION FOR AN ARBITRARY EXTERNAL MEDIUM

The solution just obtained satisfies the conditions that

$$\nabla \cdot \varepsilon_1 \mathbf{E} = 0 \tag{21a}$$

hold within the ellipsoid, that

$$\nabla \cdot \mathbf{E} = 0 \tag{22a}$$

hold in the region outside the ellipsoid, and that the normal component of $\varepsilon\mathbf{E}$ be continuous through the surface of the ellipsoid:

$$(\varepsilon_1 \mathbf{E})_{n1} = (\mathbf{E})_{n2}. \tag{23a}$$

In the more general problem, these relations are replaced by

$$\nabla \cdot \varepsilon_1' \mathbf{E} = 0, \tag{21b}$$

$$\nabla \cdot \varepsilon_2' \mathbf{E} = 0, \tag{22b}$$

and

$$(\varepsilon_1' \mathbf{E})_{n1} = (\varepsilon_2' \mathbf{E})_{n2}. \tag{23b}$$

Note now that if in the second set of relations, the tensor $\varepsilon_1' \varepsilon_2'^{-1}$ be written as $\boldsymbol{\alpha}$:

$$\boldsymbol{\alpha} \equiv \varepsilon_1' \varepsilon_2'^{-1}, \tag{24}$$

then the second set of relations may be written

$$\nabla \cdot \boldsymbol{\alpha}(\varepsilon_2' \mathbf{E}) = 0, \tag{21c}$$

$$\nabla \cdot \varepsilon_2' \mathbf{E} = 0; \tag{22c}$$

and

$$[\boldsymbol{\alpha}(\varepsilon_2' \mathbf{E})]_{n1} = [\varepsilon_2' \mathbf{E}]_{n2}. \tag{23c}$$

Comparison of this set of relations with the first set shows that the general problem is equivalent to the simpler problem in which the external medium is a vacuum, provided that in the more general problem, the expressions $\varepsilon_1' \varepsilon_2'^{-1}$ and $\varepsilon_2' \mathbf{E}$ are identified with the expressions ε_1 and $\mathbf{E}$ of the simpler problem. Accordingly, the solution (20) for the simpler case becomes:

$$\varepsilon_2 \mathbf{E}_2 = [1 + \boldsymbol{B}(\varepsilon_1 \varepsilon_2^{-1} - 1)]\varepsilon_2 \mathbf{E}_1, \tag{25}$$

or

$$\mathbf{E}_2 = [1 + \varepsilon_2^{-1} \boldsymbol{B}(\varepsilon_2 - \varepsilon_1)]\mathbf{E}_1, \tag{26}$$

where the primes have been omitted because they are no longer needed.

In order to obtain $\mathbf{E}_1$ as an explicit function of $\mathbf{E}_2$, it is necessary to determine the tensor which is reciprocal to the tensor $\boldsymbol{T}$:

$$\boldsymbol{T} \equiv 1 + \varepsilon_2^{-1} \boldsymbol{B}(\varepsilon_2 - \varepsilon_1), \tag{27}$$

whence the expression for $\mathbf{E}_1$ is

$$\mathbf{E}_1 = \boldsymbol{T}^{-1} \mathbf{E}_2. \tag{28}$$

The solution of the generalized problem stated at the beginning of this paper is given by the last three equations with Eqs. (2)–(5), (10), (11), and (17) serving to define the quantities which appear therein.

[10] M. Abraham and R. Becker, *Electricity and Magnetism* (Blackie and Son Limited, London, 1932), pp. 72, 73.

Proceedings of the American Physical Society

MEETING AT COLUMBUS, JUNE 15 AND 16, 1945

THE 266th meeting of the American Physical Society was held at Columbus (Ohio) in the Mendenhall Physics Laboratory of the Ohio State University on Friday and Saturday, June 15 and 16, 1945. This was our first experience with a meeting under the regime of limited attendance prescribed by the Office of Defense Transportation. The applicants for authorization to come to the meeting from outside of Columbus were fewer than fifty, so that none had to be denied; fewer than forty-five came. Attendance from Columbus raised the total to about seventy at the dinner and to nearly one hundred at the most largely attended scientific session. The meeting was accordingly akin to the small congenial meetings of "the old days," and the limitation on discussion could be loose as the limitation on attendance was strict. The Local Committee was headed by Dean Alpheus W. Smith, to whom and to whose colleagues the gratitude of the Society is due and is expressed.

Early plans for a large **Symposium on Biophysics,** intended to stimulate interest and to encourage the formation of a group in this field, were severely reduced in scope when the limitation on attendance became certain; but as a token of the interest of the Society in this field, D. W. Bronk was asked to arrange a half-day symposium, and responded by procuring four notable invited papers of which his own could unfortunately not be given. The actual speakers and titles were:

E. NEWTON HARVEY, *Princeton University:* **Bubble Formation in Blood and Tissues.**

ALEXANDER HOLLAENDER, *National Institute of Health:* **Studies of the Mechanism of the Effect of Ultraviolet Radiation on Microorganisms.**

K. S. COLE, *Columbia University:* **Electrical Properties of Nerve.**

The Division of Electron and Ion Optics held its second annual meeting, under the chairmanships of L. Marton and L. P. Smith. There were three contributed papers of which the abstracts are appended under the denotations **B1, B2, B3,** and five invited papers which were the following:

LLOYD P. SMITH, *RCA Laboratories:* **Quantum Effects in High Frequency Control of Electron Beams.**

FRANK GRAY, *Bell Telephone Laboratories:* **The General Solution for an Electron Stream in a Parallel Plane Diode.**

J. HILLIER AND R. F. BAKER, *RCA Laboratories:* **High Resolution Electron Diffraction.**

EUGENE FEENBERG, *Sperry Gyroscope Company:* **The Theory of Cascade Bunching.**

A. F. PREBUS AND IGNACE ZLOTOWSKI, *Ohio State University:* **The Accuracy of Electrolytic Trough Measurements.**

The abstracts of twenty-one contributed papers on the general programmes of the Society are appended hereinafter.

The dinner of the Society was held at the Deshler-Wallick Hotel on the evening of Friday, June 15, Harvey Fletcher presiding. Brief addresses were made by Alpheus W. Smith; by C. C. Williams of the Battelle Memorial Institute, on metallurgy in wartime; by A. R. Olpin of the Ohio State University Research Foundation, on research foundations generally; by E. U. Condon; and by the President.

The Council of the American Physical Society had met previously at New York in order to minimize travel for the majority of its members; the meeting occurred on May 5. Three candidates were elected to fellowship and seventy-four to membership. By delegation of power to the Secretary the Council assured the election to membership of candidates whose nominations should be received not later than June 30. Thirty-eight candidates were elected to membership under this delegation.

Lost through death: (as reported through June 30): H. C. Richards (*University of Pennsylvania*, F), E. C. Wiersma (*University of Delft*, M), P. I. Wold (*Union College*, F), R. C. Young (*William and Mary*, M).

Elected to Fellowship: P. Y. Chou, K. A. Norton, Dorothy Wrinch.

Elected to Membership: John Backus, Fred W. Billmeyer, Jr., David Bohm, John Wallace Carlson, George C. Dacey, Adrian Hilman Dahl, Philip J. Donald, Robert Bayard Edmonson,

Spofford G. English, Harold K. Farr, E. F. George, Leon R. Grove, George L. Jenkins, Eleanor Karasak, Richard Latter, John Seth Laughlin, Gordon M. Lee, Alan Roland Liss, Frederick P. Longwell, Gene McDaniel, Ralph O. McIntosh, Ernest Mayer, Arild J. Miller, Salwa C. Nassar, Nathan Grier Parke, III, Joseph Pierson, David Pomeroy, Merrill Rassweiler, Dexter H. Reynolds, Albert M. Rubenstein, W. Lewis Shetler, Bernard A. Shoor, Frank Milton Sparks, Ralph T. Squier, Charles W. Tope, Ferd Elton Williams, George W. Wood, John Lamar Worzel.

KARL K. DARROW, *Secretary*,
American Physical Society,
Columbia University, New York 27, New York

ABSTRACTS OF CONTRIBUTED PAPERS

B1. The Paths of Ions and Electrons in Crossed, Non-Uniform Electric and Magnetic Fields. NORMAN D. COGGESHALL, *Gulf Research and Development Company.*—The integration of the force equations for charged particles moving in certain types of non-uniform magnetic fields has been reported earlier.[1] It has been found that the force equations for a charged particle moving in the presence of particular types of crossed, non-uniform electric and magnetic fields may be integrated by a generalization of the same method. The cases which admit of the integration are those such that the electric and magnetic fields are crossed and are both functions of the same coordinate, either Cartesian or cylindrical. The integration may be done numerically by a direct method if the field variations are too complicated for analytical evaluation or if the fields are known only experimentally. Using this approach the calculations for some of the known types of crossed field mass spectrographs and beta-ray spectrographs are shown to be special cases of the general method. From the functions involved in the quadratures it is possible to deduce certain properties of the orbits such as periodicity, spatial extension, dependence on initial conditions, etc. The dependence of the calculated orbits upon initial energies, field strengths, particle masses, and starting direction will be shown and discussed for a number of physically interesting cases.

[1] N. D. Coggeshall and M. Muskat, Phys. Rev. **66**, 187 (1944).

B2. Anomalies in the Electron Diffraction Pattern of Magnesium Oxide. J. HILLIER AND R. F. BAKER, *RCA Laboratories.*—Magnesium oxide smoke and magnesium oxide reagent were examined by a transmission electron diffraction camera possessing a resolving power at least an order of magnitude higher than used previously. Under these conditions a number of the rings become multiple indicating that magnesium oxide does not have an accurately cubic structure. The (111) ring appears as a doublet with $d(111)=2.451$A and 2.398A. The (200) line appears single and sharp. The 220 had an unusual contour on the ring patterns but was resolved into five rings by studying single crystal reflections. The spacing corresponding to the five rings are as follows: 1.468, 1.477, 1.485, 1.493, 1.502. (222), (224), (226), and (333) rings were also observed as doubled. No structure has been found which explains satisfactorily all the observed rings and single crystal reflection patterns.

B3. The Electron Optics of Mass Spectrographs and Velocity Focusing Devices. R. G. E. HUTTER, *Stanford University.**—The well known results of the theory of mass spectrometers and velocity focusing devices are derived again by a different method which is simpler than the ones previously used. This method brings out more clearly the electron optical nature of the deflecting and focusing properties of the fields employed in the mentioned types of instruments.

* Now with Sylvania Electric Products, Inc.

C1. Effect of Excitation Frequency on Spectrum of Gaseous Discharges. KEITH J. HAYES, J. GIBSON WINANS, AND WARREN CULP, *University of Wisconsin.*—It has been observed by radio experimenters that commercial neon bulbs show a purple tinge when excited at frequencies above 10 megacycles. Spectroscopic studies of this effect were made with frequencies .29, .34, .75, 1.5, 8, 16, 32, 64, 130, 390, and 600 mc as well as 60 c and d.c. The purple glow appears at about 10 megacycles and increases in intensity up to 600 mc. The purple color is due to the excitation of the violet lines of argon which is present in small quantity in the tubes. The change occurred at the electrode as well as in the gas. A tube containing pure neon gave no noticeable change in spectrum with change in excitation frequency. A similar effect was observed with commercial argon filled bulbs. The spectrum at 60 cycles consisted almost entirely of the violet second positive bands of nitrogen. At frequencies above 10 mc, however, the orange first positive bands of nitrogen were obtained with high intensity, and the color of the discharge was orange instead of violet. Tubes containing pure nitrogen did not show this effect. These results show that in gas mixtures which show these effects, the spectra requiring the smaller excitation energy gain in intensity with increase in excitation frequency.

C2. Raman Spectra of Spiropentane and 1,1-Dimethylcyclopropane. FORREST F. CLEVELAND AND M. J. MURRAY, *Illinois Institute of Technology.*—Murray and Stevenson[1] synthesized a C_5H_8 hydrocarbon by the debromination of pentaerythrityl bromide with zinc dust and assigned to it the spiropentane structure (symmetry D_{2d}) on the basis of its Raman spectrum, chemical properties, and method of preparation. This structure has recently been confirmed by an electron diffraction investigation.[2] In the

present work, the depolarization factors of the Raman lines of spiropentane have been obtained by use of the method previously described.[3] Raman frequencies, estimated relative intensities, and qualitative depolarization factors have also been obtained for 1,1-dimethylcyclopropane. The spectra of the two compounds, each of which has at least one three-membered ring, are compared and discussed in the light of the group theory selection rules.

[1] M. J. Murray and E. H. Stevenson, J. Am. Chem. Soc. **66**, 812 (1944).
[2] J. Donohue, G. L. Humphrey, and V. Schomaker, J. Am. Chem. Soc. **67**, 332 (1945).
[3] Forrest F. Cleveland, J. Chem. Phys. **13**, 101 (1945).

C3. The Infra-Red Spectra of Chloroform and Bromoform. GEORGE L. JENKINS AND JOSEPH W. STRALEY. *University of North Carolina.*—The infra-red spectra of $CHCl_3$ and $CHBr_3$ has been observed in both the liquid and vapor states in the region from 2–15μ. A number of overtone and combination bands have been observed. The contour of several fundamental bands has been well enough established to warrant an approximate calculation of the moments of inertia and other molecular magnitudes. The frequencies in cm^{-1} of the fundamental bands which lie in the region examined are:

	$CHCl_3$		$CHBr_3$	
	Liquid	Vapor	Liquid	Vapor
δ_2	762.2	771.0	—	—
δ_5	3018.4	3034.4	3012.0	3049.2
δ_4	1216.5	1218.9	1142.4	1147.7

C4. Further Measurements on ω_1 and ω_2 of CD_3Cl in the Infra-Red. HARALD H. NIELSEN AND ALVIN H. NIELSEN,* *The Ohio State University, Columbus, Ohio.*—Of the vibration-rotation bands of CD_3Cl reported on at an earlier meeting,** ω_1 and ω_2 have been completely remapped in the first order of a 7200 line-per-inch Wood replica grating instead of in second order of an 800 line-per-inch grating. The parallel vibration ω_1 has been so well resolved, that a good knowledge of the rotational spacing is now available. This spacing, averaged over the whole band, is about 0.7 cm^{-1} instead of 1.01 cm^{-1} as previously reported. The value 0.7 cm^{-1} is in good agreement with the $\Delta\nu$ observed for the other parallel bands ω_3 and ω_4. The moment of inertia I_A calculated from this spacing is 80.1×10^{-40} g cm^2. Complete resolution of the Q branches in the perpendicular vibration ω_2 is also effected. It is believed that the positions of the rotation lines in both bands is known to ±0.07 cm^{-1}.

* The University of Tennessee, Knoxville, Tennessee.
** Chicago, December, 1944.

C5. Some New Measurements on ω_3 of $C^{12}O^{16}_2$ and $C^{13}O^{16}_2$. ALVIN H. NIELSEN* AND Y. T. YAO,** *The Ohio State University, Columbus, Ohio.*—The vibration designated ω_3 for the molecules[1,2] $C^{13}O^{16}_2$ and $C^{12}O^{16}_2$ with band centers at 2350 cm^{-1} and 2284 cm^{-1} have been completely remapped with a prism-grating spectrometer employing a 7200 line-per-inch Wood replica grating. In all portions of the bands where no overlapping occurs, the resolution of the rotation lines is complete. In the region where the P branch of the $C^{13}O^{16}_2$ overlaps with the R branch of the $C^{12}O^{16}_2$, though not complete, the resolution is sufficiently good to permit the identification of the lines of both bands. The grating was calibrated with a mercury arc, and it is believed that the rotation lines are now known to ±0.07 cm^{-1}. In mapping these bands galvanometer deflections were read at intervals of 0.07 cm^{-1} and plotted *versus* frequencies in cm^{-1}. The slits were set to include a frequency interval of 0.3 cm^{-1}. The data is being analyzed with a view to recalculating some of the constants relating to ω_3 and the convergence of the rotation lines.

* The University of Tennessee, Knoxville, Tennessee.
** The National University of Peking, Kunming, China.
[1] P. E. Martin and E. F. Barker, Phys. Rev. **41**, 291 (1932); D. Cameron and H. H. Nielsen, Phys. Rev. **53**, 246 (1938).
[2] Alvin H. Nielsen, Phys. Rev. **53**, 983 (1938).

C6. Absorption Bands in the Spectrum of Butadiene. Y. T. YAO, *National University of Peking, Kunming, China* (at present at *Ohio State University, Columbus, Ohio*). (*Introduced by H. H. Nielsen.*)—The absorption region in the spectrum of butadiene near 3.2μ has been examined using an echellette grating at intervals corresponding to 0.29 cm^{-1}. The slits subtend an interval of approximately 0.4 cm^{-1}. It was revealed that this region consists of at least two bands, one with its center at 3.21μ and the other with its center at 3.3μ. Some indication of rotational structure is found. The bands at 9.86μ and 11.01μ have been observed with a grating ruled with 800 lines per inch at intervals corresponding to 0.29 cm^{-1} and 0.214 cm^{-1}, respectively. A rotational separation of about 1.9 cm^{-1} is observed. This structure is better defined in the 11.01μ band than in the 9.86μ band.

D1. Width of Nuclear Levels. M. GOLDHABER, *University of Illinois.*—An extension of the analysis of the width of the known RaC′ levels, based on the data of Rutherford, Ellis, Lewis, and their co-workers, supports the view, recently expressed,[1] that the maximum gamma-ray width has been considerably underestimated in the past. Among the states of 2–3 Mev excitation energy, there appear to be several with a width of the order of a few ev, in contrast to the sharp states previously analyzed, which have widths of the order of 10^{-3} ev.[2] This suggests the possibility that some slow neutron groups of large total width, hitherto ascribed to an agglomeration of a large number of sharp compound nucleus states[2] may be due to wide compound nucleus states (see following abstract). The larger values for the radiation width bring the Bohr theory of nuclear reactions into better agreement with experiment in several other respects (e.g., probability of fast neutron capture, level density). A number of difficulties arise, however, if one tries to account for the sharp neutron groups (width $\lesssim$0.1 ev).

[1] M. Goldhaber, Phys. Rev. **67**, 59 (1945).
[2] See H. A. Bethe, Rev. Mod. Phys. **9**, 69 (1937).

D2. Evidence of Wide Neutron Groups. A. A. YALOW AND M. GOLDHABER, *University of Illinois.*—We have carried out a systematic search for wide neutron groups using various methods of investigation (self-absorption, absorption in boron, overlapping of levels; and combinations of these methods). Among the known groups of large

total width the Ag (22 sec.) B group and the Br (18 min. and 4.4 hr.) group have been studied in some detail and appear to be due to single wide levels. The B group was investigated by isolating it with a "double filter" of Cd+Au which removes *C* and *A* neutrons. A number of new cases of overlapping of neutron resonance levels of different elements have been observed. Evidence for fairly wide levels in Re and Ir has been obtained. With these elements as absorbers a considerable reduction is found in the activity produced by *R* neutrons in the following detectors: Mn (2.59 hr.), As (26.8 hr.), Br (18 min.), Pd (13.0 hr.),[1] Ag (22 sec. (B) and 2.3 min.), I (25 min.), W (24.1 hr.).

[1] See H. Feeny and F. Rasetti, Can. J. Research **A23**, 12 (1945).

D3. Search for (n, α)-Reaction in Rare Earth Elements with Slow Neutrons. H. D. ARNETT, GERTRUDE SCHARFF-GOLDHABER, AND G. S. KLAIBER,* *University of Illinois.*—The (n, α)-reaction can be expected to be exothermic in the rare earth region. If the ratio r of α-particles emitted per slow neutron captured, as well as the energy E released, were kyown, the width of the compound nucleus level could be calculated and compared with the directly measurable width of the neutron resonance level. Such measurements would yield valuable information about the nature of the sharp neutron resonance levels found for the rare earths. As a first step, we have renewed the attempt to detect α-emission from Sm under the action of slow neutrons,[1] and extended the work to a number of neighboring elements. Some improvements in technique were made and the arrangement calibrated with the $B^{10}(n, \alpha)$-reaction. No α-emission could be detected for C neutrons within the limits attainable in our experiment. For Sm and Gd we can deduce $r < 10^{-4}$. If the sharp levels were compound nucleus levels with a width ≤ 0.1 ev[2] and if we assume $E \geqslant 8$ Mev we obtain a theoretical estimate $r \gtrsim 10^{-3}$.

* Now at General Electric Research Laboratory, Schenectady, New York.
[1] J. Chadwick and M. Goldhaber, Proc. Cam. Phil. Soc. **31**, 612 (1935).
[2] H. H. Goldsmith and F. Rasetti, Phys. Rev. **50**, 328 (1936).

F1. Accelerational-Velocital Magnetic Forces. F. W. WARBURTON, *University of Kentucky.*—Magnetic potential energy as a function of relative position, velocity and acceleration of two electrical charges, when used in the generalized Lagrangian equations of motion and extended to include terms in $1/c^3$, provides expressions for the mutual force of one charge on the other containing the product of the velocity of one charge and the acceleration of the other. When averaged over a circular orbit oriented at random, one such term gives a net force due to electrons accelerated in starting or stopping a longitudinal conduction current in a bar of magnetic material, which appears sufficient to account for the shock effect studied by Perkins and Doolittle.

F2. Scattering of Electrons by Matter. GEORGE WINCHESTER, *Rutgers University.*—The scattering of electrons within an absorber is probably due to the non-uniform force fields within the material. The amount of matter (thickness or g cm^{-2}) necessary to absorb one-half of a certain intensity, let us say, of beta radiation from a radioactive material depends upon the force fields existing between the atoms of that particular absorber. If the force fields of any particular absorber (or scatterer) are changed then the one-half thickness value will also change, regardless of the number of atoms involved in the scattering. The scattering of beta particles of RaE by hard rolled and by annealed aluminum is definitely different (up to 17 percent, depending on the method of annealing) and can readily be shown experimentally. Also, the scattering of beta particles by a sheet of aluminum before and after prolonged gentle tapping is definitely different, the tapped condition causing the largest scattering. This may be due to an increase in the number of crystals per mm^2. It would thus appear that the coefficient of absorption of beta particles by a certain absorbing material depends upon its state of aggregation.

F3. Composition and Diffraction Effects in X-ray Microradiographs. J. M. HURD, C. M. LUCHT AND R. SMOLUCHOWSKI, *General Electric Research Laboratory.*—X-ray microradiographs provide a convenient method for the study of various phenomena in metals. A fine grain photographic emulsion allows the use of medium high magnifications (100 to 200). Variation of composition between various constituents can be detected and what is particularly interesting concentration gradients within a solid solution can be observed. These gradients are well nigh not detectable by other methods. Depending upon the orientation of a grain, various sets of crystallographic planes diffract the radiation and affect the transmitted intensity. Along grain boundaries dark and light lines and shadows are observed which are also explicable as a diffraction effect. In certain cases these shadows make an interpretation of concentration effects difficult.

F4. Magnetic Behavior of Molecularily Dispersed Iron. GEORGE ANTONOFF, *Fordham University.*—If an iron salt is electrolyzed with a mercury cathode, some of the iron penetrates into mercury forming an amalgam, and some of it settles on the surface in form of small dendrites of metallic iron. A test tube was taken of the size just to fit into the gap between the poles of an electromagnet. Some mercury was inserted into it to act as a cathode. The test tube was filled with a saturated solution of ferrous sulphate. An anode of soft iron was inserted into the upper part of the test tube. A current of about 1 amp. was passed through. After a certain time one could observe the formation of an amalgam near the surface. Then application of magnetic force caused sinking of the amalgam and reappearance of the free surface of mercury. Looking on the surface of mercury one also observed deposits of small particles of iron near the two poles. The reversal of poles produced no visible effect. This behavior was different from that described by Reynolds who worked with a colloidal solution of ferric hydroxide which deposited only on north pole. In this case the ferrous sulphate solution was apparently in a molecularily dispersed state in the initial stages, and the effect was dipolar.

F5. Flow of Fluids with Non-Uniform Viscosity in Tubes with Distensible Walls: Blood Flow. ALLEN L. KING, *Dartmouth College.*—Three important factors influence the rate of blood flow through a blood vessel: the non-uniformity of plasmal viscosity, the elasticity of the vessel wall, and the presence of erythrocytes and other corpuscles. If the viscosity η of an incompressible fluid depends on speed v and gradient dv/dr in a cylindrical tube, then at any cross-section of radius r the volume flowing by per unit time is $Q=\pi r^3\int_0^{v'}v\eta dv/\int_0^{v'}\eta dv$. The speed at the tube wall is assumed to vanish and that at the center v' to be a function of r. The denominator equals $-1/4(d(pr^2)/dx)$, where r and pressure p are functions of distance x along the tube axis. If the wall material consists of randomly distributed and twisted long chains of molecules, then by methods developed for the analysis of rubber, a relation between p and r may be found and used in the equation for Q. Often the presence of particles, such as erythrocytes in blood, is assumed to affect η; thus the term viscosity becomes less well-defined. In general, the rate of blood flow is not proportional to the difference in pressure between the ends of a blood vessel.

F6. A Correction of G. M. Counter Data. HENRY B. MANN AND J. D. KURBATOV, *Ohio State University.*—Two models have been offered for the correction of G.M. counter data, due to the finite resolving time τ. In the first it is assumed that in order for a counter to register a particle, that particle must be preceded by an interval τ during which no particle arrives at the counter.[1] In the second model it is assumed that any number of particles may arrive during this interval provided no discharge is produced during this time.[2] In the present work it is shown that, according to the second model, the mean number $B(T)$ of discharges during any time T is given by

$$B(T)=\int_0^T[1-p(t)]a(t)dt, \qquad (1)$$

where $a(t)$ is the total density of radiation penetrating the tube at the time t and $p(t)$ is the solution of the integral equation:

$$p(t)=\int_{t-\tau}^{t}[1-p(x)]a(x)dx, \qquad (2)$$

for $t>\tau$ and $p(t)=1-e^{-at}$ for $0\leq t\leq\tau$. $B(t)$ is explicitly obtained for the case that $a(t)$ is constant. In this case it is also shown that

$$aT=\frac{B(T)-\eta}{1-[B(T)-\eta]\frac{\tau}{T}}, \quad |\eta|\leq\frac{(a\tau)^2}{1-(a\tau)^2} \quad \text{for} \quad a\tau<1.$$

[1] L. I. Schiff, Phys. Rev. **50**, 88 (1936).
[2] B. V. Gnedenko, J. Exper. Phys. U.S.S.R. **11**, 101 (1941).

F7. An Ionization Gauge of Simple Construction. CHARLES FOGEL, *National Union Research Laboratories.*—A new ionization gauge is described for measuring pressures from 10^{-4} to less than 10^{-8} mm of mercury. Except for a multiplying factor of 10, it gives a direct reading of residual air pressure. The gauge employs two plates, as the electron and ion collector respectively. They are located on opposite sides of the filament, but equidistant from it. This allows easy outgassing of parts, either by electron bombardment or by r.f. heating. A protective shield in front of the ion collector aids in reducing the electrical leakage to that element. Danger of filament burn-out due to vacuum leaks has been removed by the choice of an oxide-coated filament.

F8. An Adsorption Isotherm of Radon. BENJAMIN P. BURTT AND J. D. KURBATOV, *Ohio State University.*—A procedure has been developed for obtaining an adsorption isotherm of minute quantities of radon from an air-radon mixture at atmospheric pressure and $t=25°$. Quantities of radon from 2.0×10^{-13} to 4.4×10^{-11} gram were used. These quantities were determined by means of an ionization chamber and electrometer calibrated against a radium standard. Silica gel was used as adsorbent. The quantity of silica gel and the water contained in it were such that below 3.6×10^{-13} gram of radon the adsorption isotherm followed Henry's law and at higher quantities the exponent of isotherm equation became less than unity allowing therefore, the determination in this region of unknown quantities of radon directly from the isotherm. The apparatus and procedure will be described.

F9. The Use of Frequency Modulation in a Sensitive Micrometer. G. M. FOLEY, *Battelle Memorial Institute.* (*Introduced by H. W. Russell.*)—In order to measure the unimpeded displacement of an object, one plate of a small air condenser is attached to the object. The other plate is fixed close to the moving plate, and the condenser is used to tune a radio frequency oscillator. The change in frequency which results from motion of the object is converted into proportional d.c. voltage by a receiver similar to a frequency-modulation radio receiver. Voltages of plus or minus 300 are obtained from small displacements, and a magnification of the motion of 10,000 to 100,000 times can be obtained, permitting detection of displacements of less than 10^{-6} inch. The apparatus is rugged and stable, and requires no electrical connection with the object whose position is being measured. Two such micrometers were placed at right angles to measure the rotation of a precision lathe spindle in its bearings, the outputs of the two micrometers being applied to two axes of a cathode ray oscilloscope. A similar micrometer was used as a high speed recording dilatometer to follow the allotropic transformation of steel on heating and cooling.

F10. Note on the Hydrodynamic Theory of Journal Bearings. J. C. BELL, *Battelle Memorial Institute.* (*Introduced by H. R. Nelson.*)—A type (a) of journal bearing being studied by A. F. Underwood[1] supports a rotating radial load of constant magnitude, but has no rotation of the two surfaces.[2] In order to describe the hydrodynamic lubrication in this bearing, Reynolds' classic equation is generalized to allow for both tangential and normal relative motions of the surfaces. Except for a factor 2, the lubrication in this bearing has the same differential equation as that for either (b) a shaft rotating together with a radial

load of constant magnitude or (c) a rotating shaft with a unidirectional load. Thus, the hydrodynamic lubrication is the same for all these types, except that in Type (a) a given thickness of film can support twice as great a load as in the others. Since the service behavior in Types (b) and (c) is known to depend on film thickness, an alternative explanation is offered for the greater load-carrying capacity of bearings of Type (b) over Type (c).

[1] General Motors Research Laboratories.
[2] Described in preprint for 1944 Annual Meeting of A.S.M.E.

F11. Ponderomotive Forces of Light upon Matter as Shown by Experiments. FELIX EHRENHAFT, *New York City.*—In a vertical beam of light, particles of Cr, Fe, Ni, Mn, CuO_2, etc., of a size of about the order of the wavelength of light, fall vertically, while some of those slightly larger describe, in falling, distinct helical paths in the beam of light. This helical movement, appearing in the horizontal beam of light as sine curves or spirals have already been described and later were found independently by Whytlaw-Gray and Patterson[1] in repeating my experiments in photophoresis.[2] It was determined in experiments made with Richard Whitall that often the bodies made five to ten revolutions per second around the axis of the helix. The radius of this helical path is very large compared with the radius of the body. The path has been observed with linear polarized and natural light and with and without parallel external magnetic fields. These observations added to the light-positive and light-negative movements of photophoresis show that light can exert repulsion, traction, and torsion on matter free to move with three degrees of freedom. New experiments using sunlight will be described. The principle of the conservation of linear and angular momentum of electrodynamics will be generalized.

[1] Whytlaw-Gray and Patterson, *Smoke, A Study of Aerial Disperse Systems* (Edward Arnold and Company, London, 1932), p. 120.
[2] F. Ehrenhaft, Ann. d. Physik 56, 81 (1918); See also J. Frank. Inst. 233, 235 (1942).

T1. The Electric Counterpart of Oersted's Experiment. FELIX EHRENHAFT, *New York City.*—In the sense of Oersted-Ampere, a single magnetic charge rotates around the electric current. An Alnico 5 magnet—60,000 maxwells—was fitted with two circular cylindrical pole pieces ending in truncated cones 5 mm in diameter and 1.5 mm apart. The horizontal opposing pole faces were covered with a thin electrically insulating layer of Picein. The rotation of ferric hydroxide particles suspended in a cylindrical drop of ferrous chloride solution placed in the homogeneous field between these pole-faces-can be observed to be counterclockwise when looking at the South pole and to be independent from the influence of light under the conditions of illumination described.[1] Connecting the poles of the magnet with a piece of soft iron of small cross-section, the rotation of the particles is slower. With a piece of larger cross section the rotation ceases. Upon adding a trace of NH_4OH to the droplet, the rotation diminishes. Adding more the rotation ceases; further additions reverse the rotation. Obviously this phenomenon can-not be explained by Biot-Savart-Lorentz force nor by Faraday, Quincke movements. If we term the magnetic vortex detected by Oersted the magnetic action of electric currents, the above described electric vortex should be termed the electric action of magnetic currents.

[1] F. Ehrenhaft, J. Frank. Inst. 233, 236 (1942).

T2. Polarity of Magnetism. FELIX EHRENHAFT, *New York City.*—In continuing the experiments reported previously[1] a cell was used having separate compartments for the poles. With the electromagnet formed of one piece of iron, and dilute H_2SO_4 in the cell, a greater evolution of gas, often 100 percent more, was observed when the magnetic field was in action than when the gas was evolved by chemical action alone. Whereas in the first experiments reported more oxygen was detected in the gases evolved than could be accounted for by the air dissolved in the water, following the reports of J. T. Kendall[2] and others the earlier experiments were repeated without duplicating the first results. It therefore seems necessary to investigate the whole matter further in order to solve the old Fresnel-Ampère dispute.[3] However, in using a cell with one or two compartments, two kinds of gas bubbles were observed when the magnetic field was in action, one kind circulates counter-clockwise when looking on the south pole, the second kind being repelled or attracted by one of the poles in the homogeneous part of the field. The first kind behave as if they bear an electric charge, the second a magnetic charge. Both reverse with the field. From these observations one must again conclude that magnetism has to be described as a polar vector.

[1] F. Ehrenhaft, Phys. Rev. 63, 461 (1943); 65, 287 (1944); Nature (September 30, 1944).
[2] J. T. Kendall, Nature (February 5, 1944).
[3] Augustin Fresnel, Oeuvres T 2, 676.

Proceedings of the American Physical Society

MEETING AT STANFORD UNIVERSITY, CALIFORNIA, JULY 14, 1945

THE 267th meeting of the American Physical Society was held at Stanford University, California, on Saturday, July 14, 1945. The attendance at the meeting varied from 60 to 65, which is practically a pre-war figure. Almost all of those present came from the San Francisco commuting zone. Over sixty members and guests had luncheon together in the Stanford Union. At the conclusion of the luncheon Professor J. W. McBain gave a most interesting and significant account of his trip to Moscow, as one of the invited delegates to the International Scientific Conference recently held there. Brief remarks were made also by Dr. K. K. Darrow.

The morning session opened at 9:30 A.M. and adjourned just at noon. It was devoted to the first six contributed papers and to the first invited paper. This paper, entitled **Decompression Sickness as a Medical-Physical Problem,** was read by Dr. C. A. Tobias, of the Division of Medical Physics, University of California. Dr. John Lawrence, who is in charge of this newly created division of the department of physics, and who was to read the paper, was unable to be present.

The second invited paper, by Dr. Paul Kirkpatrick, Stanford University, was postponed to the afternoon session, which by agreement was started at 1:45 P.M. The paper was titled **The Continuous X-Ray Spectrum in Theory and Experiment.** It was followed by the remainder of the contributed papers. Only paper No. 8 was read by title. The meeting adjourned at 4:50 P.M., after which tea and cake were served by the wives of staff members.

R. T. BIRGE
Local Secretary for the Pacific Coast

ABSTRACTS OF CONTRIBUTED PAPERS

1. Combination Voltage and Current Regulation of an X-Ray Tube. JAMES F. MCGEE, *Stanford University.*—The voltage regulation section is of the degenerative type while current regulation is accomplished by modulating the r.f. filament supply by the voltage drop across a resistance in series with the anode of the x-ray tube. The regulator is entirely a.c. operated, the usual reference battery being replaced by a highly regulated low voltage d.c. supply. The latter plays several roles in the operation of the combination regulator. It serves as a reference voltage to "detect" voltage fluctuations while at the same time serving as a reference for the emission current fluctuations. It supplies the plate voltage for the d.c. amplifiers located in the voltage and current regulation sections respectively. Finally, it provides plate supply for the modulated r.f. oscillator, the output of which heats the x-ray tube filament. Capacitance voltage division is used to increase the "detected" fraction of any rapid voltage fluctuation. While the range has been restricted to 0–50 kv and 0–3 ma for thin target x-ray studies, higher ranges are possible. The combination regulator has maintained voltages to 0.01 percent and currents to 0.02 percent for periods less than five minutes. Electron microscopy and electron diffraction are obvious additional fields of application.

2. Mechanism of Charge Production in Thunderclouds. SEVILLE CHAPMAN, *Stanford University.*—The well-known conflicting theories of Wilson (charge separation on falling drops by induction in the earth's electric field) and of Simpson (breaking drops) are both quantitatively inadequate. Furthermore, Wilson's theory makes no use of rising air currents characteristic of thunderclouds; Simpson's theory yields the wrong polarity. While early measurements showed positive charge retained on breaking drops and negative charge in the air, either the *net* negative charge in the air was measured, or air blast conditions differed substantially from thundercloud conditions. The author's measurements of *spray* electrification[1] showed negative and positive charges in the air in *nearly equal* numbers, negative predominating, but the charge ratio varied markedly with spraying or bubbling procedure. If the charge ratio approaches unity by the breaking drop mechanism of thunderclouds, another order of magnitude of charge is available. Thus breaking drops may provide the required charges of both signs in the air, which may be separated by the Wilson mechanism in nonturbulent regions of the cloud, yielding, as observed, a positive cloud top and negative cloud center and bottom, except for a localized volume in the updraft region containing positive charge on the breaking drops.

[1] S. Chapman, Phys. Rev. **54**, 520 and 528 (1938).

3. Cosmic-Ray Mesotron Ionization in Helium and Argon Gases. LESTER L. SKOLIL, *University of California.*—Counter-controlled cloud-chamber photographs of cosmic-ray mesotron track have been taken in helium and

argon gases. The chamber was operated as previously described[1] in the case of hydrogen. A triple-coincidence counter telescope was used with sufficient lead above the chamber so that electron tracks could be distinguished from mesotron tracks. The expansion of the chamber was delayed to allow the ions to diffuse sufficiently for drop counting. The clearing field was reduced after sufficient time for the track to be separated into positive and negative ion columns. Studies of condensation efficiencies for a wide range of alcohol-water vapor mixtures indicate that whenever more than 50 percent of the negative ions have formed drops, then all of the positive ions have formed drops. From photographs of tracks taken under these conditions, the average specific ionization has been determined by counting the number of positive ion drops per cm of path.

[1] Lester L. Skolil, Phys. Rev. **66**, 158 (1944).

4. The Intensity of Cosmic-Ray Electrons Relative to Mesotrons at Sea Level. B. LOMBARDO, JR. AND W. E. HAZEN, *University of California.*—Counter measurements in other laboratories have indicated fewer electrons than one expects on the usual assumptions concerning the properties of mesotrons. A suggested explanation has been decay into two neutrinos and one electron. In this laboratory, measurements have been made by direct observation of absorption in lead plates in a cloud chamber. For the lower energies, where the absorber was primarily glass and radiation losses were relatively small, the results should be quite accurate. For the higher energies the results depend on radiation theory and there is a consequent decrease in reliability. Even for the cases of energies >100 Mev, where the energy is estimated from the nature of the cascade shower, the results are more reliable than counter results since the detailed history of the shower is observed. The number of electrons with energy >6.6 Mev was 38 per hundred mesotrons with $H\rho > 4.2 \times 10^5$, the momentum necessary for penetration of all the absorbers. The predicted value is 35, which is within the estimated uncertainty. The shape of the energy distribution and the other absolute values agree reasonably well with theory. Since the assumed decay products are one neutrino and one electron, this experiment favors the usual picture of mesotron decay.

5. Cascade Showers in Lead. SALWA C. NASSAR, *University of California.* (*Introduced by W. E. Hazen.*)—Cascade showers initiated by cosmic-ray electrons of energy less than 700 Mev, have been studied in a cloud chamber placed in a magnetic field of about 1000 gauss. The chamber was counter-controlled with three counters above it so that the entire history of each shower was observed. The absorbing power of the counter telescope was made very small in order to minimize the possibility of starting a shower outside the chamber. The chamber contained four lead plates, each 0.7 cm thick. In each shower the total number of particles of energy greater than 3 Mev was determined. A plot of the total number *versus* the number at the maximum was made. Since all shower curves (average number of particles *versus* depth in shower units) have essentially the same shape, the above plot should be a straight line whose slope depends on the ratio of height to area of the shower curve. Preliminary results from 20 showers indicate that the ratio of height to area of the experimental shower curve is 1.8 times that of the theoretical one. This value may be too large to be accounted for by the 20 to 30 percent uncertainty estimated in the most recent calculations by Bhabha and Chakrabarty.[1]

[1] H. J. Bhabha and S. K. Chakrabarty, Proc. Roy. Soc. **A181**, 267 (1943)

6. Decay Electrons from Neutral Mesotrons of Small Mass. P. GERALD KRUGER AND LYLE W. SMITH, *University of Illinois.*—In an earlier report[1] it was suggested that a new neutral radiation might consist of neutral small mass mesotrons. To test this hypothesis the penetrating radiation has been examined with a cloud chamber, which was surrounded by a ring (19 cm thick) of lead blocks (6″ high) in the horizontal plane. Several hundred stereoscopic pictures were taken with the cloud chamber in a magnetic field of about 1000 oersteds. Three aluminum foils 0.8 mm thick were spaced 5 cm apart in the cloud chamber. Observation of the loss of energy suffered by an electron in passing through the foils makes it possible to determine the direction of motion of the electron. If a neutral mesotron decays into positive and negative electrons, both having the same energy, tracks showing a decrease in energy in opposite directions along the track should be observed. Several such pictures have been obtained. From measurements it appears that the decay electrons have energies between 2.5 and 6 Mev and the rest mass of the neutral mesotron varies between 13 and 24 mc^2.

[1] Groetzinger, Kruger, and Lloyd Smith, Phys. Rev. **67**, 52 (1945).

7. A Simple, High Voltage, Electrostatic Voltmeter. L. MARTON, *Stanford University.*—A very simple and inexpensive electrostatic voltmeter consists of a cylindrical steel container as one electrode and a disk-shaped electrode made of any other metal in its center. This latter is mounted on a bushing passing through a tightly closed cover of the steel container. The container is provided with a cylindrical well at the bottom center, which is filled with mercury. A thin circular steel disk floats on top of the mercury. The well communicates with an inclined glass capillary through which the position of the mercury meniscus can be observed. The upper end of the glass capillary is connected to the top part of the steel container. All the space above the mercury is filled with an insulating liquid. When a field is applied, the mercury-pool level is raised and a corresponding retraction of the meniscus is produced. The range of the instrument can be conveniently changed by altering the distance between the disk-shaped electrode and the mercury pool. A variation of the same principle consists of building in a flexible metallic bellows in the well instead of filling it with mercury, and using two nonmiscible liquids in the capillary.

8. Magnetism as a Polar Vector. FELIX EHRENHAFT, *New York City.*—In previous bulletins,[1] the author presented experimental proof that magnetic ions and consequently magnetic currents exist, and that magnetism should be described not as an axial vector but as a polar vector. That the magnetic cell discovered in the Stefan-Loschmidt laboratory,[2] and later investigated by many workers cannot be interpreted by the axial theory of magnetism has been conceded.[3] The following experiment made with Rhichard Whitall is presented in evidence. Two pole pieces of soft Swedish iron electrically insulated from one another could be attached to either one or two so-called permanent magnets of Alnico Blue Streak alloy, and their opposing pole faces immersed in 4-percent H_2SO_4. The potential differences between the pole pieces were measured by a potentiometer. With two magnets alternating with one magnet in position, the average of the successive readings taken at five minute intervals was 0.0031 volt with two magnets, and 0.0022 volt with one magnet. In both cases north was positive. Thus the potential difference is seen to depend on the pole strength, and the polarity of magnetism is evidenced. It is clear that the polar theory of magnetism will facilitate the understanding of heretofore unclear magnetic phenomena.

[1] F. Ehrenhaft, Phys. Rev. **60**, 169 (1941); **61**, 733 (1942); **63**, 216, 461 (1943); **64**, 43 (1943); **65**, 62, 256, 287, 394 (1944); **66**, 38 (1944); **67**, 63, 201 (1945); and Bulletin 266, Meeting at Columbus, Ohio, June 1945.
[2] Gross, Wiener Akad. Ber. **92**, 1378 (1888).
[3] S. R. Williams, *Magnetic Phenomena* (1931), p. 146.

9. Conditions for Small Grid Current in Types 38 and 954 Pentodes. CARL E. NIELSEN, *University of California.*—The magnitude and constancy of the grid current in a vacuum tube place a lower limit upon the photoelectric or ionization current measurable with that tube. The 38 and 954 pentodes have been so operated[1] as to have grid currents much smaller than usual in common vacuum tubes. Published applications of these tubes have, however, not required the minimum grid current, and other considerations have influenced the operating potentials chosen. A study of grid currents of 6C8G, 38, and 954 tubes with various potentials applied to the elements has led to some understanding of the influence of various factors upon grid current in these tubes. Under proper conditions a grid current as small as 2×10^{-14} ampere (less than one-tenth of the value previously reported) was observed in the 954. This result suggests that the 954 is a suitable substitute for "electrometer tubes" in applications not requiring the maximum possible sensitivity. A balanced circuit may be successfully employed with the 954 tube. Such a circuit is desirable for a photo-cell amplifier, even when only moderately high sensitivity is required, because of its convenience and stability.

[1] Strong, *Procedures in Experimental Physics* (Prentice-Hall Inc., New York, 1938), pp. 427, 428.

10. Advancing and Receding Contact Angles in Glass Capillaries and the Partial Removal of Contamination by Water and Soap Solutions. HARENDRA K. ACHARYA* AND J. W. MCBAIN, *Stanford University.* (*Introduced by Paul Kirkpatrick.*)—If a capillary (0.025–0.05 cm in diameter) freshly drawn from a Pyrex glass tube is dipped in distilled water, the advancing and receding heights are equal at the same depth, indicating a clean capillary surface with zero-contact angle. If the capillary is contaminated with oleic acid, the advancing height is only about one-third as great. Washing of the contaminated capillary with distilled water increases the receding height up to that for a clean tube, while the advancing height remains constant at the first value. Hence water leaves a residual film of oleic acid on glass even though the receding contact angle becomes zero. Washing with 0.03-percent sodium oleate solution has practically the same effect as washing with distilled water. However, the still partially contaminated glass is perfectly wetted by the soap solution, advancing and receding contact angles both being zero. Repeated washing with higher concentrations of sodium oleate solution (0.3 and 3.0 percent) removes the residual oleic acid and equalizes the advancing and receding heights with those for the clean capillary. Aerosol OT solution (0.3 percent) has the same effect as washing with distilled water.

* Bristol-Myers Company Research Fellow in Chemistry.

11. The Application of Stokes' Law to the Electrical Conductivity of Organic Ions. EMANUEL GONICK, *Stanford University.* (*Introduced by Paul Kirkpatrick.*)—The application of Stokes' law to the ionic conductances of univalent ions leads to the following equation for λ, the limiting equivalent conductance of the ions

$$\lambda = (e.96500\times10^{7})/6\pi\eta r. \qquad (1)$$

This equation is shown to be applicable to organic ions, and the effective radius, r, is shown to be proportional to a fractional power of the number of carbon atoms contained in the ions, provided none of these is a substituted carbon, the value of this fractional power depending on the type of ion. From Eq. (1) by appropriate substitutions are developed equations from which the van der Waals radius of the methylene radical and substituted methylenes may be calculated. The calculated value of the methylene radical agrees with that obtained from crystallographic data. An equation is also developed by which the limiting equivalent conductances of organic ions can be calculated when experimental data are lacking. The method applies to ions containing unsaturated linkages and substituted methylenes as well as to saturated, unsubstituted ions. As a check the conductivity of the hexanolammonium ion is calculated and is found to agree exactly with the experimental value found in this laboratory.

12. Silver Plated Constantan Thermopiles for Skin Temperature Measurements. J. E. GULLBERG, C. A. TOBIAS, AND H. WELTIN, *Aero Medical Unit, University of California.*—Thermocouples by electro-deposition were first constructed by Wilson and Epps[1] whose work has been adapted to an instrument, making possible the quick measurement of skin temperatures. If 200 turns per inch of 1.5 mil constantan wire are wrapped around a suitable form of polystyrene and the wires are plated with 50 micrograms per cm of silver by partly submerging the form in

a plating solution, one obtains 400 junctions of very small mass, and hence of low heat capacity. One-half of the junctions are placed in contact with a copper block insulated by a very thin piece of mica; the other half are placed in contact with the surface whose temperature is to be determined. The potential from 200 turns per inch is 6.5 millivolts per °C, which cannot be greatly increased by a heavier deposit of silver. Methods of calibration, linearity, and sensitivity are discussed. A radiometer of similar design has been constructed. Both instruments promise to be of particular interest to the clinician as a diagnostic aid in the evaluation of peripheral vascular diseases. The work was carried out under a contract between the University of California and the Office of Scientific Research and Development on the recommendation of the Committee on Medical Research.

[1] W. Wilson and P. D. Epps, Proc. Phys. Soc. **32**, 326 (1919–20).

13. Rapid Least-Squares Solution of Polynomials. R. T. BIRGE AND J. W. WEINBERG, *University of California.*—When the abscissa values are equally spaced, and the observations are of equal weight, the least-squares solution of a polynomial of any degree becomes greatly simplified and the result can be obtained in a number of forms. The Birge and Shea form involves the evaluation of the coefficients of the usual power series, $f(\epsilon) = \sum_{k=0}^{j} a_{kj}\epsilon^k$, in terms of orthogonal polynomials, expressed explicitly in terms of the observations y_i. The required coefficients a_{kj} are given by $\sum_{t=k}^{j} R_{kt}a_{tt}$ and Birge and Shea gave a general formula for a_{tt}. By means of a useful modification of Tchebycheff's recursion formula, explicit expressions have now been obtained for all R_{kt} functions needed in the case of polynomials of the tenth or lower degree. These check in detail published results of F. E. Allan, who based his work on an entirely different formula. Furthermore, a general expression has been derived for $t!a_{tt}$ in the form of a weighted average of the finite differences $\Delta^t y_i$, for any value of t. Tables of values of the required weight of each $\Delta^t y_i$ have been calculated for $t=1$, 2, 3 and 4, and for n (=number of observations) up to 20.

14. Probable Errors for Least-Squares Solutions of Polynomials. J. W. WEINBERG AND R. T. BIRGE, *University of California.*—Inability to evaluate the probable errors of the coefficients or of the function itself has hitherto constituted a serious defect in all of the proposed special methods, including that of Birge and Shea, for obtaining the least-squares solution of a polynomial (see preceding abstract). A general expression has now been obtained for the weight N_t of the final coefficient a_{tt} of a polynomial of degree t. A set of such coefficients (with $t=k$ to j) is required for the evaluation of each coefficient a_{kj} of the jth-degree polynomial. Due to the orthogonal character of the solution, the various members a_{tt} of such a set act like *independently* observed quantities, and this fact has been explicitly proved. Hence the law of propagation of errors can be applied to any *function* of the a_{tt}, including the expressions for the a_{kj} and for the function itself. Thus an explicit expression for each desired probable error is readily obtained. Finally, the value of Σv^2 (v=residual) for the jth-degree polynomial, needed in the calculation of the various probable errors, is given by the simple formula $\Sigma y^2 - \sum_{t=0}^{j} N_t a_{tt}^2$. Tables of numerical values of N_t have now been calculated, for $t=0$ to 5, and for n up to 20.

15. Short Range Interatomic Forces. W. HORNING, W. O'CONNELL, AND J. WEINBERG. (*Introduced by R. T. Birge.*)—Because of the large momenta involved in the collision of ions with atoms, the corresponding elastic scattering may be analyzed by classical mechanics. In experiments on the collision of argon ions with helium atoms at energies of the order of hundreds of volts,[1] the dependence of cross section upon energy and scattering angle indicates the presence of a repulsive force of exclusion which varies inversely as the cube of the distance. At the distances of approach calculated from this force law, considerable overlapping of the electron clouds of ion and atom takes place; and the average duration of a collision compared to atomic periods is such that the electron distribution has time to become adjusted to the influence of both nuclei. A Fermi-Thomas statistical model of the two-center system should therefore provide a good approximation to the potential energy as a function of nuclear separation. This problem has been solved with the aid of the variational method, for the case of two nuclei of equal atomic number; and the potential energy-function obtained is in satisfactory agreement with the main features of the data. A detailed comparison with experimental results will shortly be possible on the basis of calculations now in progress.

[1] W. J. Hamm, Phys. Rev. **63**, 433 (1943).

16. Absolute Intensity of Cu $K\alpha$ Radiation from a Thick Target. W. L. BRAXTON, A. V. BAEZ, AND PAUL KIRKPATRICK, *Stanford University.*—Copper $K\alpha$ radiation emerging at a grazing angle of 10° from a thick target was isolated by Ross filters of cobalt and nickel and received in a large air-filled ion chamber standardized for absolute energy measurements. After making allowances for continuous radiation, for absorption in the target, the tube and chamber windows, the intervening air and the filters, it is concluded that the $K\alpha$ energy produced in the target by electron bombardment at 15.5 kev is 2×10^{-13} erg per electron. The efficiency of the production of Cu $K\alpha$ radiation in thick targets at this bombardment energy is about 0.01 percent. Slightly less than half of the produced radiation emerges from the target face. Corresponding figures for other tube voltages are easily obtained from *relative* intensity measurements. The observed intensities were approximately predicted on the basis of earlier measurements of the intensity of $K\alpha$ radiation from thin targets of nickel.

17. Some Observations Made Upon the Surface Properties of Solutions of Detergents in Water. JAMES V. ROBINSON, *Stanford University*. (*Introduced by Paul Kirkpatrick.*)—This paper is a discussion of some of the more interesting observations made during the course of an uncompleted study. Peculiarities in the surface behavior of high molecular weight substances in aqueous solutions have been observed. Surface tension-concentration curves obtained from measurements upon detergent solutions show minima or broad horizontal sections as the rule rather than the exception. The absolute surface adsorption of one of these solutions was measured, and found to disagree with that predicted from the adsorption theorem, calculated in the usual way. The surface tension of certain detergent solutions, at the concentration where a minimum in surface tension occurs, may be further lowered by the addition of another surface-active agent. The addition of large amounts of surface-inactive materials to the detergent solutions is shown to produce almost no change in surface tension, in contrast to the large changes in surface tension demonstrated upon the addition of small amounts of surface active material. Some of the detergents apparently hydrolyze. Bubbles rising through solutions of detergents in long tubes accumulate large concentrations of the detergent at their surfaces. The surface concentration on the bubbles may be equivalent to hundreds of molecular layers.

18. Diffraction of X-Rays by Aqueous Solutions of Hexanolamine Oleate. SYDNEY ROSS, *Stanford University*. (*Introduced by Paul Kirkpatrick.*)—A number of papers published in Germany since 1937 by K. Hess, H. Kiessig, and W. Philippoff have reported results on the diffraction of x-rays by soap solutions. This paper presents results on a series of aqueous solutions of hexanolamine oleate, varying in concentration from 92 percent to 25 percent by weight of soap. As the solutions become more dilute, the long spacing increases linearly from a value of 54A at 92 percent to 135A at 30 percent of solute. The value of the side-spacing is about 4.6Å, independent of changes of concentration. Solutions of 60 percent and less show two orders of the long spacing, corresponding to the 002 and 004 diffraction orders. The linear relation pursues its course through a range of concentration in which great changes in viscosity and anisotropy are taking place. It is therefore conclusively shown that changes of viscosity and gel/sol transitions in soap solutions are due to rearrangements of the primary micelles with respect to each other. The internal structure of the micelle itself is meanwhile independently maintained. The presence of lamellar micelles in aqueous solutions of this colloidal electrolyte is proved directly by these results.

19. Foam Volumes and Foam Stabilities. SYDNEY ROSS, *Stanford University*. (*Introduced by Paul Kirkpatrick.*)—Ease of foam formation, foaming volume, and the stability of the foam once formed, do not necessarily bear any relation to each other. Most writers have confined their attention to the measurement of stability. The present paper provides further data to show the relation between foam stability and foaming volume and to determine the conditions under which foaminess may be accounted an intrinsic property of the liquid, independent of the fortuitous mechanical conditions attendant on its production. A method of measuring foam volume is described and investigated to establish the critical factors in its operation. Data on foaming volumes and foam stabilities are given for a series of hydrocarbons and for a range of concentrations of aqueous ethylene glycol solutions. It is shown that the amount of foam formed depends on the machinery of its production as well as on its stability. The stability of the foam produced, within specified mechanical limitations chiefly of a nature that would tend to affect the size of the bubbles in the foam, is primarily a function of the liquid.